VOL. 8 NO. 2 AUGUST 1964
PUBLISHED MONTHLY

Journal of

ELECTROANALYTICAL CHEMISTRY

International Journal Dealing with all Aspects of Electroanalytical Chemistry, Including Fundamental Electrochemistry

ELSEVIER

GENERAL INFORMATION

See also Suggestions and Instructions to Authors which will be sent free, on request to the Publishers.

Types of contributions

(a) Original research work not previously published in other periodicals.
(b) Reviews on recent developments in various fields.
(c) Short communications.
(d) Bibliographical notes and book reviews.

Languages

Papers will be published in English, French or German.

Submission of papers

Papers should be sent to one of the following Editors:

Professor J. O'M. BOCKRIS, John Harrison Laboratory of Chemistry, University of Pennsylvania, Philadelphia 4, Pa., U.S.A.
Dr. R. PARSONS, Department of Chemistry, The University, Bristol 8, England.
Professor C. N. REILLEY, Department of Chemistry, University of North Carolina, Chapel Hill, N.C., U.S.A.

Authors should preferably submit two copies in double-spaced typing on pages of uniform size. Legends for figures should be typed on a separate page. The figures should be in a form suitable for reproduction, drawn in Indian ink on drawing paper or tracing paper, with lettering etc. in thin pencil. The sheets of drawing or tracing paper should preferably be of the same dimensions as those on which the article is typed. Photographs should be submitted as clear black and white prints on glossy paper.
All references should be given at the end of the paper. They should be numbered and the numbers should appear in the text at the appropriate places.
A summary of 50 to 200 words should be included.

Reprints

Twenty-five reprints will be supplied free of charge. Additional reprints can be ordered at quoted prices. They must be ordered on order forms which are sent together with the proofs.

Publication

The *Journal of Electroanalytical Chemistry* appears monthly and has six issues per volume and two volumes per year, each of approx. 500 pages.

Subscription price (post free): £ 10.15.0 or $ 30.00 or Dfl. 108.00 per year; £ 5.7.6 or $ 15.00 or Dfl. 54.00 per volume.
Additional cost for copies by air mail available on request.
For advertising rates apply to the publishers.

Subscriptions

Subscriptions should be sent to

ELSEVIER PUBLISHING COMPANY, P.O. Box 211, Amsterdam, The Netherlands.

SUMMARIES OF PAPERS PUBLISHED IN JOURNAL OF ELECTROANALYTICAL CHEMISTRY

Vol. 8, No. 2, August 1964

THE SIMULTANEOUS DETERMINATION OF HYDRAZINE AND HYDROXYLAMINE

AN ANALYTICAL APPLICATION OF CHRONOPOTENTIOMETRY

Mixtures of hydrazine and hydroxylamine may be analyzed by anodic chronopotentiometry. Hydrazine gives a four-electron wave ($E_{\frac{1}{4}}$ = +0.36 V *vs.* S.C.E.) and hydroxylamine produces a six-electron wave ($E_{\frac{1}{4}}$ = +0.83 V *vs.* S.C.E.) in 0.1 *F* sulfuric acid at a platinum anode. Mixtures having mole ratios as large as 50:1 hydrazine:hydroxylamine and as small as 1:50 have been successfully analyzed. The accuracy is within ±5% for most cases. At high hydrazine concentrations nitrogen bubbles form at the electrode surface and block the approach of hydroxylamine leading to low hydroxylamine results. Chloride ion interferes and must be removed.

M. D. MORRIS AND J. J. LINGANE,

J. Electroanal. Chem., 8 (1964) 85–92.

THE ELECTRICAL VARIABLE AND THE FORM OF THE ISOTHERM FOR THE ADSORPTION OF ORGANIC COMPOUNDS AT ELECTRODES

The criticisms of a recent paper made by FRUMKIN and DAMASKIN are discussed.

R. PARSONS,

J. Electroanal. Chem, 8 (1964) 93–98.

THE REDUCTION AND OXIDATION OF VANADIUM IN ACIDIC AQUEOUS SULFATE SOLUTIONS AT MERCURY ELECTRODES

The rates and mechanisms of electrolytic processes occurring at mercury electrodes in aqueous acidic sulfate solutions of vanadium in its various oxidation states have been studied by polarography, absorption spectroscopy, and controlled-potential amperometry and chronocoulometry. The complex behavior observed is interpreted in terms of polynuclear species containing vanadium and undergoing slow transformation. Both vanadium(II) and vanadium(III) exist in three forms, each of which may be reduced to give hydrogen and a deprotonated species of vanadium; these reductions give rise to kinetic and induced currents the behaviors of which are described in detail.

Y. ISRAEL AND L. MEITES,

J. Electroanal. Chem., 8 (1964) 99–119.

ELECTRODE PROCESSES FOLLOWED BY CHEMICAL REACTIONS INVOLVING ELECTROACTIVE SPECIES

I. THE EFFECT OF ETHYLENEDIAMINETETRAACETATE ON THE POLAROGRAPHIC REDUCTION WAVES OF HEXAQUOCHROMIUM(III) AND HEXAMMINECHROMIUM(III)

The effect of ethylenediaminetetraacetate (EDTA) on the one-electron reduction process of hexamminechromium(III) and hexaquochromium(III) at the dropping mercury electrode has been investigated in acid media. In the presence of EDTA, chromium(II) produced by the reduction reacts with EDTA to form a Cr(II)–EDTA complex. As long as the potential is sufficiently positive, this complex is oxidized at the electrode, and a current dependent on the rate at which chromium(II) combines with EDTA is observed.

N. TANAKA AND K. EBATA,
J. Electroanal. Chem., 8 (1964) 120–126.

ANODIC BEHAVIOR OF PLATINUM ELECTRODES IN OXYGEN-SATURATED ACID SOLUTIONS

The anodic behavior of Pt electrodes in O_2-saturated sulfuric acid solution is shown to be critically dependent on the treatment of the electrode. The open circuit potentials, 1.48, 1.13 and 0.98 V, observed in purified solution, are related to the thermodynamic platinum-oxide potentials. The erratic behavior of Pt electrodes in non-purified solutions is also explained.

The thermodynamic value of 1.23 V for the H_2O–O_2 reaction was obtained when certain conditions were fulfilled. The Tafel (b) parameter for the anodic oxygen evolution reaction was 0.113, and $i_0 = 2.5 \times 10^{-10}$ A/cm^2. Chemisorption of oxygen leads to a dipole potential of 0.98 V. An oxide film is produced by anodic oxidation. This was confirmed by an optical method (thin film ellipsometer) which showed that the growth of a film commences only above 1 V.

Cathodic transient technique was used to measure the oxygen coverage (Q) of the Pt electrode as a function of the applied potentiostatic voltage (V). A linear relationship between Q and V was found. This relationship, $Q = f(V)$, is explained on the basis of a modified Cabrera–Mott model. The evidence suggests that growth takes place on certain sites of the first layer only.

W. VISSCHER AND M. A. V. DEVANATHAN,
J. Electroanal. Chem., 8 (1964) 127–138.

POTENTIOMETRIC ACID–BASE TITRATIONS IN MOLTEN SALTS

THE APPLICATION OF THE PRINCIPLE OF BIMETALLIC ELECTRODES FOR THE DETERMINATION OF EQUIVALENCE POINTS

Silver, nickel, copper, iron and tungsten were successfully applied as indicator electrodes in the titration of the acid $K_2Cr_2O_7$ in molten KNO_3 at 350°. With all electrodes sharp potential drops were recorded at the theoretically calculated equivalence points. Because of differences in E^0 potentials (as oxygen electrodes), the measurement of potential differences between any two indicator electrodes allowed the determination of equivalence points. In this type of titration no reference electrode is needed.

Bimetallic combinations were equally suitable for the determination of equivalence points of acids neutralizing in more than one step, *e.g.*, $NaPO_3$ and NaH_2PO_4

A. M. SHAMS EL DIN AND A. A. EL HOSARY,
J. Electroanal. Chem., 8 (1964) 139–144.

THE CHRONOPOTENTIOMETRIC OXIDATION OF OXALIC ACID AND OXALATE IONS AT PALLADIUM ANODES

An investigation of the anodic chronopotentiometry of oxalic acid and the oxalate anions indicates that the oxidation of these species is not inhibited by coverage of the palladium anode surface with a film of PdO, in contrast to behavior reported elsewhere for platinum anodes. An oxidation mechanism which accounts for the observed behavior is suggested, and quantitative studies indicate that the oxidation is diffusion-controlled at pH 2.45, although subject to slight but significant kinetic hindrance at pH 7.1.

T. R. Blackburn and P. C. Campbell,

J. Electroanal. Chem., 8 (1964) 145–150.

REVIEW

APPLICATION OF ELECTRON PARAMAGNETIC RESONANCE TECHNIQUES IN ELECTROCHEMISTRY

R. N. Adams,

J. Electroanal. Chem., 8 (1964) 151–162.

ANODIC OXIDATION OF *p*-METHOXYPHENOL

(Short Communication)

D. Hawley and R. N. Adams,

J. Electroanal. Chem., 8 (1964) 163–166.

THE EFFECTIVENESS OF *iR* COMPENSATION IN CONTROLLED-POTENTIAL POLAROGRAPHY

(Short Communication)

L. Němec,

J. Electroanal. Chem., 8 (1964) 166–170.

THE SIMULTANEOUS DETERMINATION OF HYDRAZINE AND HYDROXYLAMINE

AN ANALYTICAL APPLICATION OF CHRONOPOTENTIOMETRY

MICHAEL D. MORRIS* AND JAMES J. LINGANE

Department of Chemistry, Harvard University, Cambridge, Mass., 02138 (U.S.A.)

(Received May 7th, 1964)

The analysis of mixtures of hydrazine and hydroxylamine is a problem for which no very satisfactory solution has been found in classical titrimetric analysis. The available titrimetric methods are either cumbersome or depend upon indirect procedures which are insensitive to minor amounts of one or other of the constituents.

SANT[1] proposed an indirect ferricyanide titration which is simple and rapid, but which is useful only when no more than a three-fold excess of either constituent is present. The method of LANG[2], titration of hydrazine with iodate, followed by titration of hydroxylamine with ferric iron is lengthy. Furthermore, hydroxylamine interferes when present above a concentration of 7 mF. In the presence of excess bromate, hydrazine is oxidized to nitrogen and hydroxylamine to nitrate[3]. The unreacted bromate is determined in one aliquot and the nitrogen evolved is measured in another. The procedure is laborious and insensitive to small amounts of hydroxylamine.

GLEU[4] proposed a method which is sensitive to small amounts of either hydrazine or hydroxylamine. The hydroxylamine present is reduced to ammonium ion with excess titanous chloride. The excess titanous ion is titrated with ferric ammonium sulfate to a thiocyanate end point. The solution is neutralized and hydrazine is titrated with iodine. This is the most satisfactory of the classical methods.

The chronopotentiometric technique described in this paper overcomes some of the limitations of the older methods and permits the measurement of as little as 2% hydrazine in the presence of 98% hydroxylamine, and 2% hydroxylamine in the presence of 98% hydrazine. In 0.1 F sulfuric acid hydrazine produces a four-electron wave ($E_{\frac{1}{4}} = +0.36$ V *vs.* S.C.E.) resulting from oxidation to nitrogen. Hydroxylamine produces a six-electron wave ($E_{\frac{1}{4}} = +0.83$ V *vs.* S.C.E.) due to oxidation to nitrate. The present method exploits the non-linearity of the concentration–transition time relationship to attain increased sensitivity to the less easily oxidizable component, hydroxylamine.

BARD[5] reported the chronopotentiometric behavior of hydrazine in 1.44 M sulfuric

* Present address: Department of Chemistry, The Pennsylvania State University, University Park, Pennsylvania (U.S.A.)

acid. He found that the quantity $i_0\tau^{\frac{1}{2}}/C$, a constant for diffusion-controlled reactions under chronopotentiometric conditions, increases linearly with current density in the case of hydrazine. BARD suggested that the inconstancy may be due either to the disproportionation of the oxidation intermediates to yield ammonia, resulting in decreasing current efficiency for the hydrazine to nitrogen reaction as the electrolysis proceeds, or to the surface-catalyzed disproportionation of hydrazine before and during the electrolysis. Either complication would result in $i_0\tau^{\frac{1}{2}}/C$ decreasing with decreasing current density.

DAVIS[6] studied the chronopotentiometry of hydroxylamine on a platinum anode. He observed a single anodic wave in acid solutions, the transition time of which corresponds to a six-electron oxidation to nitrate. As the pH of the solution is increased, multiple waves appear and the total transition time becomes shorter. This implies oxidation to some lower oxidation state, but the exact mechanism and the nature of the products remain uncertain. In any medium the oxidation is inhibited on an oxidized electrode.

PRINCIPLES OF THE CHRONOPOTENTIOMETRIC ANALYSIS OF MIXTURES

The chronopotentiometric analysis of mixtures was first employed by JULIARD AND GIERST[7] for the determination of cadmium and zinc. Although the method is rapid and simple, it has been little used since then. The present paper appears to be the first published example of the analysis of a mixture by anodic chronopotentiometry.

If the current density is held constant and linear diffusion is the sole mode of transport of the electroactive substance to the electrode, then for the oxidation of a single substance, the well-known Sand equation (1) is obeyed.

$$\frac{i_0\tau^{\frac{1}{2}}}{C} = \frac{n\pi^{\frac{1}{2}}D^{\frac{1}{2}}F}{2} \tag{1}$$

where i_0 is the current density, τ the transition time, C the bulk concentration of the electroactive substance, D its diffusion coefficient, n the number of electrons in the electrode reaction and F the Faraday constant.

If the solution contains two electroactive substances with sufficiently different oxidation potentials, a wave with two inflections is obtained. In general, the potentials must be at least 0.1 V apart for two clearly developed waves to be visible. BERZINS AND DELAHAY[8] have shown that for this case the Sand equation holds for the first transition time (corresponding to the reaction of the more easily oxidized substance) while eqn. (2) relates the second transition time to the concentration of the less easily oxidizable substance.

$$i_0(\tau_1 + \tau_2)^{\frac{1}{2}} = \frac{n_2\pi^{\frac{1}{2}}D_2^{\frac{1}{2}}FC_2}{2} + \frac{n_1\pi^{\frac{1}{2}}D_1^{\frac{1}{2}}FC_1}{2} \tag{2}$$

The subscripts 1 and 2 refer to the first and second waves and to the substances causing them. The second transition time is measured from the first; $\tau_1 + \tau_2$ is the transition time for the entire wave.

Equation (2) shows that τ_2 depends upon both C_1 and C_2. In fact, τ_2 is always longer than the transition time for substance 2 alone under the same conditions. In the case

of hydrazine ($n_1 = 4$) and hydroxylamine ($n_2 = 6$) the second wave is substantially enhanced. If, as is approximately true, hydrazine and hydroxylamine have equal diffusion coefficients, the second transition time (hydroxylamine oxidation) for an equimolar mixture of hydrazine and hydroxylamine should be 84% of the total. When a fifty-fold excess of hydrazine is present, the hydroxylamine wave should still be almost 6% of the total.

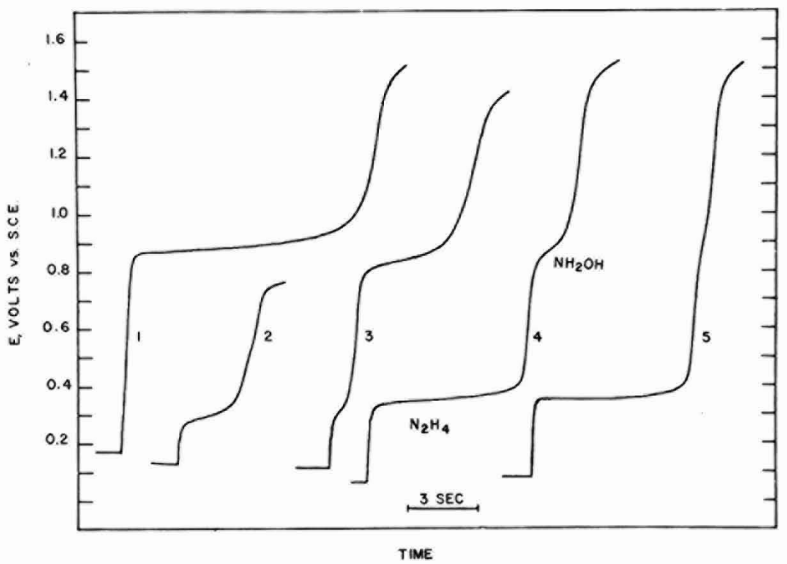

Fig. 1. Anodic chronopotentiometry of hydrazine–hydroxylamine solutions at a platinum electrode, 0.1 F sulfuric acid solution.

Curve	N_2H_4 *(mF)*	NH_2OH *(mF)*	i_0 *(μA/cm²)*
1	1.02	4.99	2970
2	1.02	4.99	668
3	1.02	1.00	2350
4	10.2	1.00	4560
5	10.2	0.199	4560

This enhancement is demonstrated by Fig. 1, which shows chronopotentiograms for various mixtures of hydrazine and hydroxylamine in 0.1 F sulfuric acid. The current densities were chosen to make the waves of convenient length for graphical presentation and otherwise bear no special relationship to one another. Curve 3 of this figure, for example, shows the behavior of approximately equimolar quantities of hydrazine and hydroxylamine. When, as in curve 1, the hydroxylamine concentration is only five times the hydrazine concentration, the hydrazine wave ($E_{\frac{1}{4}} = +0.36$ V *vs.* S.C.E.) is barely detectable with a recording potentiometer when the total transition time is below 30 sec. When, as in curve 5, a fifty-fold excess of hydrazine over hydroxylamine is present, the hydroxylamine wave is still clearly visible.

CORRECTION FOR ELECTRODE OXIDATION IN MULTI-STEP CHRONOPOTENTIOMETRIC PROCESSES

In anodic chronopotentiometry observed transition times deviate more or less from the Sand equation (or the analogous equations for geometries other than linear) and are longer than predicted. LINGANE[9] pointed out that the discrepancy is due mainly to electrode oxidation and he demonstrated that the observed current density could be corrected for this effect by the empirical relation

$$i_{corr} = i_0 - \frac{Q_{ox}}{\tau} \tag{3}$$

where i_{corr} is the current density corrected for the oxide formation and Q_{ox} is the amount of oxide film formed on the electrode when it is polarized to the transition potential. The current density to be used in the Sand equation or other appropriate current–transition time function is i_{corr}, that is

$$\frac{i_{corr}\tau^{\frac{1}{2}}}{C} = \frac{n\pi^{\frac{1}{2}}D^{\frac{1}{2}}F}{2} \tag{4}$$

If the experimental data are treated according to eqn. (4) or its analogue for other geometries, good agreement is obtained.

BARD[10] extended this approach to include the effect of double-layer charging and adsorption as well as the effect of electrode oxidation. BARD prefers to plot $i_0\tau$ against $\tau^{\frac{1}{2}}$, since the effect of double-layer charging, electrode oxidation and adsorption may be represented by

$$i_0\tau = \frac{n\pi^{\frac{1}{2}}D^{\frac{1}{2}}FC\tau^{\frac{1}{2}}}{2} + B \tag{5}$$

where

$$B = C_{dl}\Delta E + Q_{ox} + nF\Gamma \tag{6}$$

C_{dl} is the average double-layer capacity in the voltage interval ΔE of the chronopotentiogram and Γ is the amount of electroactive species adsorbed on the electrode. The slope of the linear $i_0\tau$ *vs.* $\tau^{\frac{1}{2}}$ plot is just the right-hand side of eqn. (4). It is obvious that the corrections of BARD AND LINGANE are equivalent.

The approach of LINGANE AND BARD may be extended to the oxidation or reduction of two-component mixtures. We shall consider the contributions due to electrode filming and double-layer charging. The arguments can easily be extended to mixtures containing a greater number of components or to other complicating processes.

Equations (3) and (5) are deduced from the assumptions that the fractions of the current resulting from electrode oxidation, double-layer charging and the diffusion-controlled oxidation remain unchanged during the electrolysis. We retain these assumptions with the modification that the total of the contributions of both diffusion-controlled electrode reaction is a constant fraction of the observed current density.

For the successive oxidation of two substances, denoted here by subscripts 1 and 2, the transition time in the absence of complications is related to the observed current density by eqn. (2). From this equation and from the assumption of constant contributions to the observed current density from the combined diffusion-controlled

electrode processes, electrode filming and double-layer charging, we may write, after BARD[11]

$$i_0 = \frac{[n_1\pi^{\frac{1}{2}} D_1^{\frac{1}{2}} FC_1 + n_2\pi^{\frac{1}{2}} D_2^{\frac{1}{2}} FC_2]}{2(\tau_1 + \tau_2)^{\frac{1}{2}}} + \frac{C_{dl}\Delta E}{\tau_1 + \tau_2} + \frac{Q_{ox}}{\tau_1 + \tau_2} \tag{7}$$

Equation (7) may be rearranged into the form proposed by LINGANE[9] or the form suggested by BARD[10]. Letting $B = C_{dl}\Delta E + Q_{ox}$, we may write

$$\left(i_0 - \frac{B}{\tau_1 + \tau_2}\right)(\tau_1 + \tau_2)^{\frac{1}{2}} = \frac{n_1\pi^{\frac{1}{2}} D_1^{\frac{1}{2}} FC_1}{2} + \frac{n_2\pi^{\frac{1}{2}} D_2^{\frac{1}{2}} FC_2}{2} \tag{8}$$

or an equivalent formulation

$$i_0(\tau_1 + \tau_2) = \left[\frac{n_1\pi^{\frac{1}{2}} D_1^{\frac{1}{2}} FC_1 + n_2\pi^{\frac{1}{2}} D_2^{\frac{1}{2}} FC_2}{2}\right](\tau_1 + \tau_2)^{\frac{1}{2}} + B \tag{9}$$

B is a function of the transition potential, since C_{dl}, ΔE, and Q_{ox} are all dependent upon the electrode potential. B may be obtained as the intercept of an appropriate $i_0\tau$ *vs.* $\tau^{\frac{1}{2}}$ plot. Since B depends upon transition potential, we designate the corrections made to the first portion of the wave and to the total wave by B_1 and B_2.

The concentration of the less easily oxidizable substance may be obtained from chronopotentiometric data *via* eqn. (10) below, which is obtained by combining eqns. (4) and (8). The same information may be obtained from the slopes of $i_0\tau$ *vs.* $\tau^{\frac{1}{2}}$ plots for the first transition time and the total transition time.

$$\left(i_0 - \frac{B_2}{\tau_1 + \tau_2}\right)(\tau_1 + \tau_2)^{\frac{1}{2}} - \left(i_0 - \frac{B_1}{\tau_1}\right)\tau_1^{\frac{1}{2}} = \frac{n_2\pi^{\frac{1}{2}} D_2^{\frac{1}{2}} FC_2}{2} \tag{10}$$

Independent confirmation of the validity of this correction for oxide filming to multiple waves is presented elsewhere[12].

EXPERIMENTAL PROCEDURE

Hydroxylamine sulfate (Eastman, White Label) and hydrazine sulfate (Fisher, Reagent-grade), recrystallized from 80% ethanol were used as hydrazine and hydroxylamine sources. Eastman White Label hydroquinone was used without further purification. Stock solutions of hydroxylamine sulfate and hydrazine sulfate were deaerated with nitrogen and stored under nitrogen. Solutions stored in this way showed a change of titer of less than 0.3% per month.

The constancy of the titer of hydrazine solutions was checked against potassium iodate[13]. Hydroxylamine titer was checked by oxidation with ferric ammonium sulfate according to BRAY *et al.*[14]. The ferrous ion generated was titrated with standard potassium dichromate.

The current supply and electrolysis cell have been described in a previous communication[15]. The auxiliary cathode, a piece of platinum wire or foil, was isolated from the working electrode by a sintered-glass disc. The nylon-shielded working electrode had an area of 0.201 $\pm$ 0.002 cm^2. In later experiments the nylon plug was replaced with a Teflon plug of the same design. Since some distortion of Teflon occurs when it is under pressure, the area of the Teflon-shielded electrode was determined empirically

by measurement of transition times for the reduction of solutions of ferric chloride in 1 F hydrochloric acid and thallous sulfate in 0.25 F potassium sulfate. By this method the area was found to be 0.145 $\pm$ 0.001 cm^2.

The saturated calomel reference electrode was located in a separate compartment behind a cracked-glass seal. All potentials in this paper are quoted relative to the S.C.E.

For most experiments, air stirring, effected manually with a rubber bulb, was used instead of nitrogen stirring. All measurements were made at 25.0 $\pm$ 0.1°.

Complete potential–time curves were recorded with a Sargent Model MR recorder, whose full-scale response time was less than one second. Transition times were measured directly from the recordings. The currents were adjusted to give transition times in the range 2–30 sec. Currents were corrected for electrode oxidation by means of eqn. (8). The corrections were applied to the currents in the measurement of $\tau_1 + \tau_2$ only. The hydrazine transition time occurs at a potential below that at which significant electrode oxidation occurs.

Solutions containing from 0.2 mF to 50 mF hydroxylamine and hydrazine and 0.1 F sulfuric acid were prepared from the stock solutions. Transition times were measured over a two to three-fold range of current densities and concentrations were found *via* eqns. (1) and (10) with B_1 taken to be zero. The chronopotentiometric constants, *i.e.*, $n_1\pi^{\frac{1}{2}}D_1^{\frac{1}{2}}F/2$ and $n_2\pi^{\frac{1}{2}}D_2^{\frac{1}{2}}F/2$ were evaluated experimentally from transition time measurements on hydrazine and hydroxylamine solutions. The chronopotentiometric constant for hydrazine oxidation was found to be 1141 $\pm$ 28 A sec$^{\frac{1}{2}}$ cm/mol from measurements of the first transition time of a solution 1.015 mF in hydrazine and 9.98 mF in hydroxylamine. The chronopotentiometric constant for hydroxylamine was found to be 1709 $\pm$ 38 A sec$^{\frac{1}{2}}$ cm/mole from measurements of the transition times of a solution 4.95 mF in hydroxylamine. The complete data for this and all other chronopotentiometric data summarized in this paper are presented elsewhere[12]. In all experiments the electrode was anodized to oxygen evolution and then cathodized to hydrogen evolution before the measurement of a chronopotentiogram. This pre-treatment results in the formation of finely divided platinum on the platinum surface. Electrodes not pre-treated in this fashion gave results which were not reproducible.

CHRONOPOTENTIOMETRY OF HYDRAZINE–HYDROXYLAMINE MIXTURES IN 0.1 F SULFURIC ACID

Typical analytical results are given in Table 1. Each entry in this table is derived from two measurements at each of three or more current densities.

In general, the amounts of hydrazine and hydroxylamine found are within a few percent of the amounts taken. Thus the strength of the chronopotentiometric method lies in the analysis of mixtures of hydrazine and hydroxylamine in which the mole ratio of the two substances is far from unity. For nearly equimolar mixtures of hydrazine and hydroxylamine the classical methods offer superior accuracy and precision. However, since the chronopotentiometric method is much faster and simpler than any of the published titrimetric methods it may be used to advantage for rough estimates of hydrazine and hydroxylamine concentrations even in situations where titrimetry offers higher accuracy.

At hydrazine concentrations well below 0.5 mF, the hydrazine wave is too poorly

developed to permit its use for analytical purposes. When more than 50 mF hydroxylamine is present, the wave for 1 mF hydrazine is poorly developed. At hydroxylamine concentrations above 200 mF the hydrazine wave is not observed. This phenomenon is quite unusual, and its cause is unknown.

When the hydrazine concentration is 5 mF or more, low results are obtained for hydroxylamine. Very probably this stems from the decrease of the electrode area by adherent bubbles of nitrogen which are produced in the prior oxidation of hydrazine. Although the equilibrium solubility of nitrogen in the electrolysis solution is about 0.5 mF, bubble formation is not observed until the extant nitrogen concentration is much higher, because of supersaturation.

TABLE 1

THE CHRONOPOTENTIOMETRIC ANALYSIS OF MIXTURES OF HYDRAZINE AND HYDROXYLAMINE

Taken (mmoles/l)		*Found (mmoles/l)*		*Error (% relative)*	
N_2H_4	NH_2OH	N_2H_4	NH_2OH	N_2H_4	NH_2OH
1.015	0.998	0.959 ± 0.016	1.020 ± 0.036	+1.5%	+1.2%
1.94	1.98	2.02 ± 0.16	2.00 ± 0.19	+4.0%	+1.0%
4.84	4.95	5.00 ± 0.10	4.21 ± 0.11	+3.2%	− 15%
1.94	0.198	1.90 ± 0.10	0.191 ± 0.036	−2.0%	−3.5%
9.68	0.989	9.78 ± 0.19	0.878 ± 0.33	+1.0%	− 11%
10.15	0.199	10.15 ± 0.02	0.202 ± 0.032	0.0%	+2.0%
1.015	4.99	1.005 ± 0.030	5.14 ± 0.16	−1.0%	+3.0%
1.015	9.98	1.015 ± 0.018	9.62 ± 0.25	0.0%	−3.0%
0.484	9.89	0.516 ± 0.029	10.08 ± 0.10	+6.2%	+1.9%
1.02	50.7	1.04 ± 0.06	not sought	+2.0%	—

Inspection of Table 1 shows that the error does not depend on the ratio of the bulk concentrations of hydrazine and hydroxylamine, but upon the absolute magnitude of the hydrazine concentration. This rules out kinetic interactions as the source of the error. The prior oxidation of a substance which does not produce gas bubbles, hydroquinone, does not lead to an error in the apparent amount of hydroxylamine found regardless of the absolute amounts of hydroquinone and hydroxylamine present[12]. Removal of nitrogen by saturation of the hydrazine–hydroxylamine solutions with carbon dioxide does not change the results.

The precision of the hydroxylamine measurements in the solution containing 10.15 mF hydrazine and 0.199 mF hydroxylamine, a mole ratio of 50:1, is sufficiently poor (±16% relative), that it is impossible to attach much significance to the fact that the amount of hydroxylamine found happens to coincide with the amount of hydroxylamine taken to well within experimental error. It is a sufficient testimony to the value of the chronopotentiometric method that it is able to detect a two percent component in a mixture of compounds as chemically similar and as close in molecular weight as hydrazine and hydroxylamine.

Chloride interferes in this analysis. In a solution containing approximately $1 \cdot 10^{-3}$ F each hydrazine and hydroxylamine, 2 mF potassium chloride and 0.1 F sulfuric acid, the quantity $i_0\tau_1^{\frac{1}{2}}$ decreases from 1528 to 1130 A sec$^{\frac{1}{2}}$/cm^2 as the current is decreased from 189 μA to 31.5 μA. Some decrease of $i\tau_1^{\frac{1}{2}}$ is usually observed, but the magnitude is approximately 10–15% over this range of currents in solutions contain-

ing no chloride ion, as compared to over 30% in the presence of chloride. KARP AND MEITES[16] studying the anodic behavior of hydrazine suggest that the side reactions of N_2H_2, the first oxidation product of hydrazine, leading to the production of ammonium ion are catalyzed by chloride ion. If these side reactions are slower than the anodic oxidation of N_2H_2, their importance will increase as the current density decreases, thus accounting for the observed behavior. The length of the total wave, moreover, is much shorter than that found in chloride-free solutions of the same hydrazine and hydroxylamine concentrations.

Furthermore, we observe that no hydroxylamine wave at all is found in solutions 0.2 *F* in hydrochloric acid, indicating that the chloride ion has an inhibiting effect on the oxidation of hydroxylamine. We have not investigated the phenomenon extensively and cannot say whether the inhibition is due to the formation of an oxychloride film[17] on the electrode or to some chemical inhibiting action of chloride ion upon the intermediates of hydroxylamine oxidation.

ACKNOWLEDGEMENTS

We wish to thank the National Institutes of Health, Division of General Medical Sciences, for a Fellowship held by one of us (M.D.M.).

SUMMARY

Mixtures of hydrazine and hydroxylamine may be analyzed by anodic chronopotentiometry. Hydrazine gives a four-electron wave ($E_{\frac{1}{4}} = +0.36$ V *vs.* S.C.E.) and hydroxylamine produces a six-electron wave ($E_{\frac{1}{4}} = +0.83$ V *vs.* S.C.E.) in 0.1 *F* sulfuric acid at a platinum anode. Mixtures having mole ratios as large as 50:1 hydrazine:hydroxylamine and as small as 1:50 have been successfully analyzed. The accuracy is within $\pm 5\%$ for most cases. At high hydrazine concentrations nitrogen bubbles form at the electrode surface and block the approach of hydroxylamine leading to low hydroxylamine results. Chloride ion interferes and must be removed.

REFERENCES

1 B. R. SANT, *Anal. Chim. Acta*, 20 (1959) 371.
2 R. LANG, *Z. Anorg. Allgem. Chem.*, 142 (1925) 280.
3 R. LANG, *Newer Methods of Volumetric Analysis*, edited by W. BÖTTGER, D. Van Nostrand Company Inc., New York, 1938, p. 69.
4 K. GLEU, *Ber.*, 61 (1928) 702.
5 A. J. BARD, *Anal. Chem.*, 35 (1963) 1602.
6 D. G. DAVIS, *Anal. Chem.*, 35 (1963) 764.
7 A. L. JULIARD AND L. GIERST, *Proc. Intern. Comm. Electrochem. Thermodyn. and Kinet.*, 2nd Meeting, Tamburini, Milan, 1951, p. 179.
8 T. BERZINS AND P. DELAHAY, *J. Am. Chem. Soc.*, 75 (1953) 4205.
9 J. J. LINGANE, *J. Electroanal. Chem.*, 1 (1960) 379.
10 A. J. BARD, *Anal. Chem.*, 35 (1963) 340.
11 A. J. BARD, *Anal. Chem.*, 33 (1961) 11.
12 M. D. MORRIS, Ph. D. thesis, Harvard University, (1964).
13 L. F. AUDRIETH AND B. A. OGG, *Hydrazine*, John Wiley and Sons Inc., New York, 1951, p. 158.
14 W. C. BRAY, M. E. SIMPSON AND A. A. MACKENZIE, *J. Am. Chem. Soc.*, 41 (1919) 1363.
15 M. D. MORRIS AND J. J. LINGANE, *J. Electroanal. Chem.*, 6 (1963) 300.
16 S. KARP AND L. MEITES, *J. Am. Chem. Soc.*, 84 (1962) 906.
17 D. G. PETERS AND J. J. LINGANE, *J. Electroanal. Chem.*, 4 (1962) 193.

THE ELECTRICAL VARIABLE AND THE FORM OF THE ISOTHERM FOR THE ADSORPTION OF ORGANIC COMPOUNDS AT ELECTRODES

ROGER PARSONS

Department of Physical Chemistry, University of Bristol (England)

(Received April 20th, 1964)

In a recent paper[1] adsorption at electrodes and its dependence upon the electrical state of the interphase was discussed. The suggestion was made that it might be useful to consider two limiting forms of adsorption isotherm based on Langmuir's isotherm and on a two-dimensional hard sphere equation of state (HFL) and further that the charge should be taken as the primary electrical variable. These suggestions have been criticized by FRUMKIN[2] and by DAMASKIN[3].

I. THE ADSORPTION ISOTHERM

FRUMKIN[2] has demonstrated clearly that the adsorption of a solute in an ideal solution with a solvent having molecules of the same size is accurately described by Langmuir's equation. It must then be considered to what extent a real system can be described by the modification of Langmuir's equation introduced by FRUMKIN[4] in 1925. A method by which this may be assessed has already been described[1]. This involves the plotting of the change in reciprocal capacity resulting from adsorption, as a function of the logarithm of the bulk activity of the adsorbate at constant charge. This test is valid for systems where the free energy of adsorption is linear in the charge but a similar test was described for system where it is quadratic in the charge. Equivalent plots can be made, if the potential is assumed to be the primary electrical variable. It has been demonstrated[1] that asymmetric plots are obtained for some systems, whereas the Langmuir equation and the Frumkin modification predict symmetrical plots. Hence it is necessary to consider in what respect this modification of Langmuir's equation is inadequate. It was originally proposed as a useful way of introducing into Langmuir's equation an expression for the interaction between adsorbed particles which would be correct to a first approximation. However, as FRUMKIN's remarks show, it is likely to be correct only for a system in which the particles of solute and solvent are of equal size. Deviations as a result of the charge in size ratio can be taken up by the interaction coefficient only as far as the second virial coefficient; the higher terms are of great importance for the region of surface coverage accessible to experiment.

For a solution in which the solute molecules occupy r times the surface area occu-

pied by the solvent molecules, a simple lattice model (*cf.* ref. 5) leads to the isotherm for non-interacting particles:

$$\beta a = \frac{\theta}{r(1-\theta)^r} \tag{1}$$

where θ is still defined as Γ/Γ_s where Γ_s is the saturation value of the surface concentration, Γ, of the solute. Thus a more general isotherm allowing for interaction is

$$\beta a = \frac{\theta}{r(1-\theta)^r} e^{A\theta} \tag{2}$$

It is easy to show that for this isotherm $\partial\theta/\partial \ln \beta$ has a maximum when $\theta = (1 + 1/r)^{-1}$. Thus this isotherm allows the possibility of an asymmetric curve of the change of reciprocal capacity against log a. Further the asymmetry should increase as the solute particle size increases. There is as yet insufficient experimental evidence to confirm the existence of this effect.

The disadvantage of eqn. (2) is that it contains one more adjustable parameter than the isotherms previously suggested. Nevertheless, if the values of the parameters Γ_s, r and A can be obtained by a combination of the methods previously described, it seems likely that their physical interpretation should be more meaningful. In particular there should be a close parallel between Γ_s and r in a given solvent. At the same time the interpretation of r does not appear to be simple in terms of molecular size. It has already been shown[1] that thiourea adsorbed on mercury in aqueous KNO_3 solution gives symmetrical reciprocal capacity – log concentration curves. Similarly DAMASKIN's data on *tert.*-amyl alcohol seem to give symmetrical peaks when analysed by the methods of ref. 1. (This confirms that DAMASKIN is correct in using FRUMKIN's isotherm for this system.) The molecular area of thiourea on a mercury surface is probably about 29 Å^2, while that of *tert.* amyl alcohol is somewhat larger. DAMASKIN's data give a limiting slope corresponding to 45 Å^2. The area of a water molecule is probably about 6 Å^2 so that one would expect to find r values of 5–7 for these systems and hence very asymmetric curves. This discrepancy between the simple theory and experiment may mean that the former is inadequate or it could mean that the water molecules on the surface are not independent, but are sufficiently strongly linked in small clusters of an area of the order of 30 or 40 Å^2. The latter suggestion receives some support from the fact that the peak in the benzene disulphonate curve (Fig. 8 of ref. 1) occurs close to $\theta \simeq 1/3$, which corresponds to $r = 4$. The experimental area for this ion[6] was found to be 125 A^2 or about four times the area of the thiourea molecule.

It might be expected that the HFL equation would provide a limiting isotherm for the case when the solvent molecule is large in comparison with the solute molecule. This however, is not in agreement with the Florey–Huggins model (eqn. 1) which leads to a value for the reduced nth virial coefficient of r/n to be compared with a value of n from the HFL equation. Thus the question remains open as to which equation provides the more accurate limiting isotherm for this case.

2. THE ELECTRICAL VARIABLE

It is not easy to provide unequivocal reasons for the choice of the electrical variable,

nor is conclusive experimental evidence available. FRUMKIN[7] originally suggested the equation

$$q = q_0(1 - \theta) + q'\theta \tag{3}$$

as the simplest assumption. He showed that this equation, together with the isotherm (2) with $r = 1$ could be fitted to experimental results on *tert.* amyl alcohol if A and the saturation area were allowed some variation with potential and coverage respectively. This has been confirmed by DAMASKIN using capacity measurements.

More recently, DAMASKIN[3] has attempted to show that the use of a constant q isotherm for this system leads to an unreasonable variation of the interaction constant, A, with charge. However, this conclusion is based on the assumption that eqn. (3) is exact; in other words that a constant E isotherm is obeyed. This argument could be inverted by assuming initially that a constant q isotherm was obeyed and fitting the θ value obtained to a constant E expression. Presumably similar anomalies would result. It seems therefore essential that a comparison should be carried out as far as possible without making any non-thermodynamic assumptions in the derivation of the data from experiment. This can be done by calculating surface pressure curves at constant E ($\pi = \gamma^b - \gamma$) and at constant q($\phi = \xi^b - \xi$). Figure 1 shows a comparison of composite curves with composite ϕ curves for the adsorption of n-butanol from aqueous 0.1 M NaF. These are calculated from electrocapillary measurements made

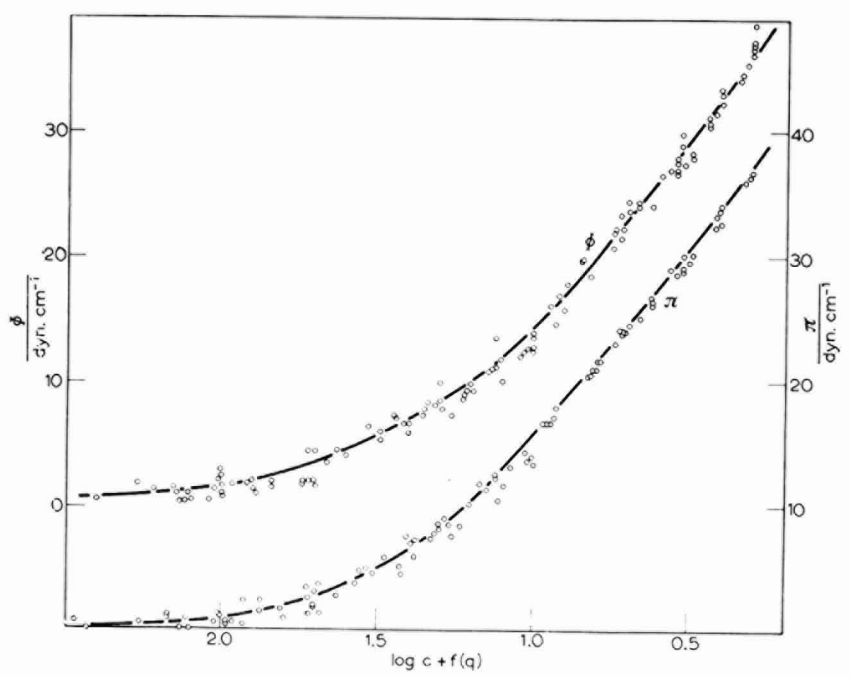

Fig. 1. Composite surface pressure curves calculated from electrocapillary data for the adsorption of n-butanol from aqueous 0.1 M KF. ϕ is the surface pressure at constant charge ($\phi = \xi^b - \xi$). π is the surface pressure at constant potential ($\pi = \gamma^b - \gamma$).

by Dr. E. DUTKIEWITZ in this laboratory. Similar results may be obtained from Damaskin's capacity measurements for the adsorption of *tert.*-amyl alcohol. It is evident that there is very little difference between these two plots, so that this method of analysis does not permit a distinction between the two electrical variables.

A more conclusive result is obtained by a comparison of these results with those obtained by KRYUKOVA AND FRUMKIN[8] for the same alcohol in aqueous 3 *N* KCl. In Fig. 2 the lowering of interfacial tension is plotted against the potential for both

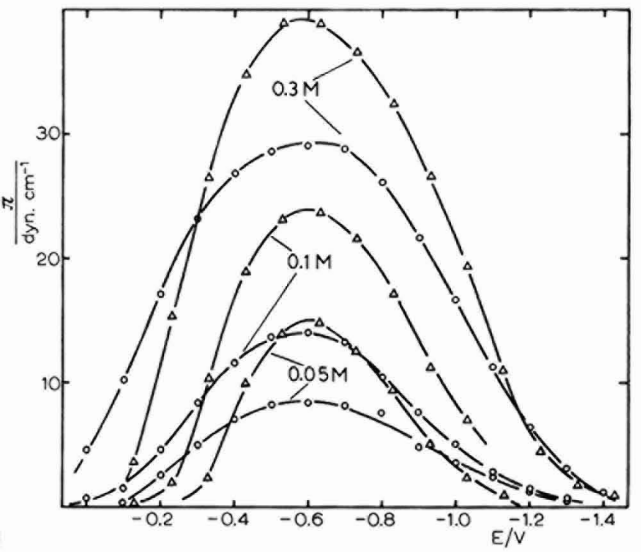

Fig. 2. Surface pressure (π) at constant potential plotted as a function of potential for three concns. of *n*-butanol. ○, base solution: 0.1 *M* KF; △, base solution: 3 *M* KCl.

systems. It is evident that these curves are approximately symmetrical for the measurements in NaF whereas in KCl the anodic branch is very much steeper than the cathodic branch. (Surface pressures are higher in 3 *N* KCl for the same concentration of butanol owing to the effect of the salt on the activity coefficient of the butanol). This is due to the specific adsorption of the chloride ion which causes a marked rise in the capacity of the electrode on the anodic branch, *i.e.*, a more rapid change of the charge with the potential. If, on the other hand, the results are plotted as a lowering of ξ as a function of q as in Fig. 3, the shape of the curves is essentially unchanged when the base electrolyte is changed. This suggests strongly that the charge is the more satisfactory electrical variable.

From the theoretical point of view, DAMASKIN[3] suggests that the field in the inner layer is not constant at constant charge. This is certainly correct if one considers the total field. However, it seems reasonable to adopt a simple model in which the molecules of solvent and solute interact with the constant field $4\pi q$ due to the electrode producing a dipolar field $4\pi\Sigma n_i\mu_i$ which is superimposed on it. The energy of the adsorbed molecule can then be obtained as the sum of the electrode–molecule interaction and the intermolecular interaction. The alternative of focussing attention on

the total average potential drop across the inner layer suffers from the disadvantage that the total average field is constant only when the thickness of the inner layer is constant. Further, at constant E, the quantity which is held constant includes contributions from both electrode–molecule interactions and intermolecular interactions; thus only part of the latter must be included in the interaction A of the adsorption isotherm. The experimental findings, shown in Fig. 1, that the shape of the isotherm does not depend on the choice of the electrical variable is probably due to the fact that the adsorbate in this example has its non-polar part in the inner layer. It should also be noted that at constant E the potential across the diffuse layer changes with the amount of neutral substance adsorbed; correction for this should be made even in 1 M solutions.

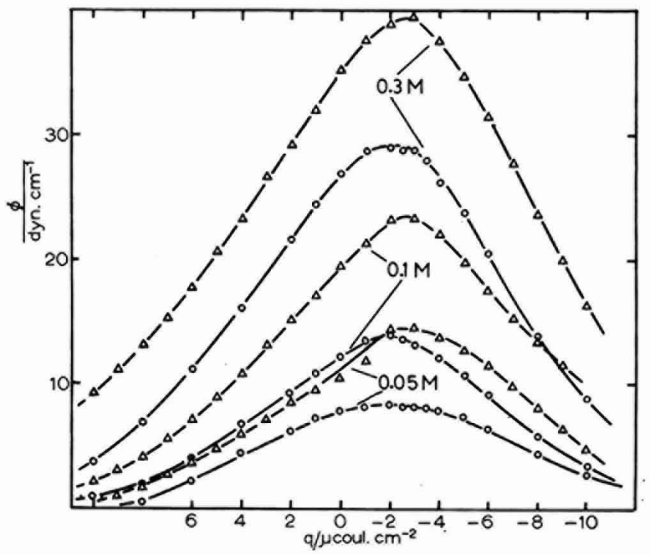

Fig. 3. Surface pressure (ϕ) at constant charge plotted as a function of charge for three concns. of n-butanol. ○, base solution: 0.1 M KF; △, base solution: 3 M KCl.

It has already been mentioned in ref. 1 that adsorption from the gas phase is always studied at constant charge on the adsorbent and not at constant potential, even though double layers are frequently formed in such systems. It is also relevant to recall the important correlation pointed out by FRUMKIN[9] between adsorption at the air–water interface and at the uncharged mercury–water interface. This correlation could only be obtained by using the correct, constant charge, isotherm for both interfaces.

The fact that the determination of the charge of a solid metal is at present inaccurate does not support the argument that the potential is the correct electrical variable, but only the fact that it is more convenient to use.

ACKNOWLEDGEMENTS

I am very pleased to acknowledge helpful discussions with Professor FRUMKIN and

Dr. DAMASKIN and thank them particularly for their sending me a table of Dr. DAMASKIN's results on the capacity of the mercury electrode in aqueous sodium fluoride containing *tert.*-amyl alcohol.

SUMMARY

The criticisms of a recent paper[1] made by FRUMKIN[2] and DAMASKIN[3] are discussed.

REFERENCES

1 R. PARSONS, *J. Electroanal. Chem.*, 7 (1964) 136.
2 A. N. FRUMKIN, *J. Electroanal. Chem.*, 7 (1964) 152.
3 B. B. DAMASKIN, *J. Electroanal. Chem.*, 7 (1964) 155.
4 A. N. FRUMKIN, *Z. Physik. Chem.*, 116 (1925) 466.
5 E. A. GUGGENHEIM, *Mixtures*, Oxford, 1952.
6 J. M. PARRY AND R. PARSONS, *Trans. Faraday Soc.*, 59 (1963) 241.
7 A. N. FRUMKIN, *Z. Physik*, 35 (1926) 792.
8 T. A. KRYUKOVA AND A. N. FRUMKIN, *Zh. Fiz. Khim.*, 23 (1949) 819.
9 A. N. FRUMKIN, *Ergeb. Exakt. Naturw.*, 7 (1928) 235.

THE REDUCTION AND OXIDATION OF VANADIUM IN ACIDIC AQUEOUS SULFATE SOLUTIONS AT MERCURY ELECTRODES

YECHESKEL ISRAEL*† AND LOUIS MEITES**

Department of Chemistry, Polytechnic Institute of Brooklyn, Brooklyn, N.Y. (U.S.A.)

(Received April 11th, 1964)

The polarographic characteristics of vanadium in its various oxidation states in acidic aqueous media free from strong complexing agents have been investigated by many authors[1-4]. It is generally agreed that, at least in strongly acidic media, the standard heterogeneous electron-transfer rate constant for the vanadium(III)–(II) couple is so high—RANDLES AND SOMERTON[5] give its value as $4 \cdot 10^{-3}$ cm/sec in 1 F perchloric acid—that the couple behaves reversibly at mercury electrodes. There is much evidence for the existence of appreciable concentrations of hydroxovanadium(III) complexes at higher pH values[3,6-8], but there is no known complication in the behavior of the couple if the pH does not exceed about 1.

The vanadium(IV)–(III) couple, however, despite its potentiometric reversibility[9], involves a large activation energy, and potentials sufficiently negative to bring about the reduction of vanadium(IV) at a polarographically detectable rate therefore cause the reduction to proceed all the way to vanadium(II). Vanadium(V) gives a wave rising from zero applied e.m.f., which reflects reduction to vanadium(IV), and also gives a second wave at more negative potentials, which is identical with the single wave obtained with vanadium(IV).

Despite this apparent simplicity, MEITES AND MOROS[10] found that the controlled-potential electrolytic reduction of vanadium(IV) in an acidic supporting electrolyte consumed much more than the expected quantity of electricity for reduction to vanadium(II), even after correction for a large current that was produced by the presence of the vanadium(II). This was the first example of the existence of the induced quantity of electricity, of which several other cases have since been found[11,12].

This investigation was originally directed toward a detailed elucidation of the kinetic and induced currents that accompany the reduction of vanadium(IV) to vanadium(II). It was found, however, that all four of the oxidation states of vanadium behave in fashions considerably more complex than the literature indicated, and a detailed re-investigation of the subject was therefore undertaken.

* This paper is based on a thesis submitted by YECHESKEL ISRAEL to the Faculty of the Polytechnic Institute of Brooklyn in partial fulfillment of the requirements for the Ph.D. degree in June, 1964.

† Present address: Israel Mining Industries Laboraories, P.O. Box 313, Haifa, Israel.

** To whom correspondence and requests for reprints should be addressed.

EXPERIMENTAL

Polarograms were obtained with a conventional pen-and-ink recording instrument. The precautions used in obtaining them, and the manner in which electron-transfer kinetic parameters were obtained from them, have been described previously[13]. Most polarograms were obtained in the controlled-potential electrolysis cell, but a few (especially of vanadium(V)) were obtained in a modified H-cell[14].

The potentiostat and integrator were obtained from Analytical Instruments, Inc., Wolcott, Conn. The integrator had previously been equipped with a 10-mA range[15]; in the course of the present work, provision was added for the injection of a small d.c. bias voltage at the chopper input to overcome the decrease of sensitivity that had previously[15,16] been observed at input currents small compared to the rated maximum for the input resistor in use. The voltage required for this purpose is independent of the range being used, and could be selected by straightforward comparison of the integrator readings with the quantities of electricity represented by the flow of steady input currents for accurately measured intervals. Appropriate adjustment of the bias voltage resulted in a sensitivity that was the same, within better than 0.1% over a 1000-fold range of input currents on each of the four ranges of the instrument.

Vanadium(II) is very sensitive to air-oxidation, and some of the electrolyses had to be so prolonged that it was necessary to construct a modified double-diaphragm controlled-potential electrolysis cell designed to exclude atmospheric oxygen as completely as possible. The working-electrode compartment was fabricated from the male member of a ST 71/60 ground joint. It was fitted with a sintered-glass gas-dispersion cylinder for rapid de-aeration and with a 3-way stopcock having a Teflon plug. The stopcock served for draining the mercury from the cell, and also for making electrical connection to the potentiostat *via* a platinum or tantalum wire dipping into the mercury column extending through the Teflon plug and into a vertical tube. This served to eliminate any possible contact between the solution and the wire leading to the potentiostat, where the rates of electron-transfer processes might differ from those at the mercury surface. In use, this compartment was sealed with a cap made from the female member of the joint, a Teflon sleeve being used to achieve a tight grease-free seal. One hole in this cap was fitted with a Teflon bearing machined to fit the rod of the propeller-type stirrer as closely as possible; another carried a glass tube, extending to just above the surface of the solution, which usually served for the escape of nitrogen through a water trap, but which was also used to pass nitrogen over the surface of the solution while a polarogram was being recorded; and a third, terminating above the cell in the male member of a ST 19/38 joint, was usually capped with the sealed female member of the joint and a Teflon sleeve, but could also be used for the addition of a sample, for the insertion of a dropping electrode, or for the withdrawal of part of the solution into an absorption cell. The essential features of this cell are shown in Fig. 1. The area of the working electrode was always 40 cm^2 in the experiments described in this paper.

A silver–silver chloride electrode, of the type previously described[10], was employed and is also shown in Fig. 1. The presence of chloride ion in the solutions being electrolyzed was found to be undesirable, and saturated potassium bisulfate was therefore used in the bridge compartment of this electrode. This solution was always placed in the bridge just before an electrolysis was begun, and discarded as soon as it was com-

pleted. The solution in the electrode compartment was saturated with both potassium chloride and potassium bisulfate and contained an excess of each. Between electrolyses it was stored in contact with a similar solution. The potentials of such electrodes were checked repeatedly against both saturated calomel and ordinary (bisulfate-free) silver–silver chloride electrodes, and were found to be -58.5 ± 1.0 mV *vs.* S.C.E. All potentials are referred to the customary saturated calomel electrode.

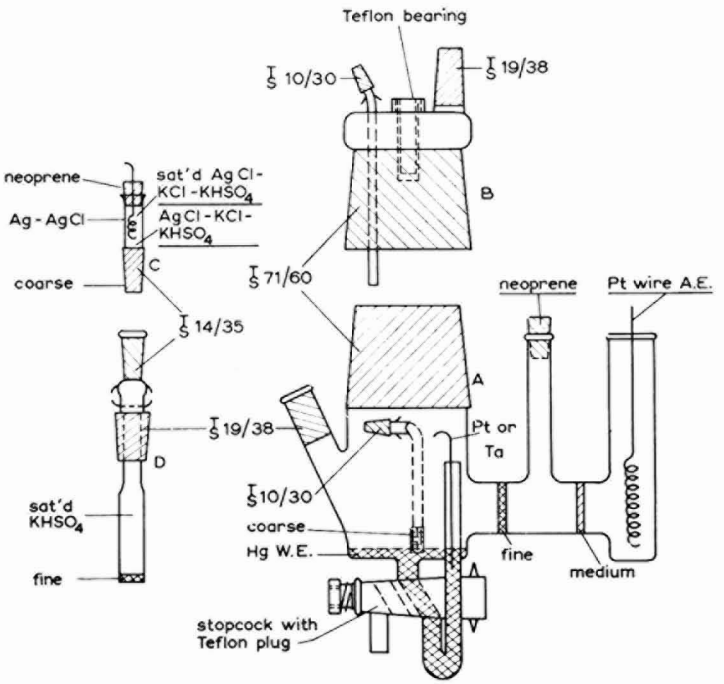

Fig. 1. Cell and reference electrode for controlled-potential electrolysis.

In all polarographic and electrolytic work, the cell employed was immersed in a water thermostat maintained at $25.00 \pm 0.05°$. De-aeration was effected by a stream of pre-purified nitrogen from which the last traces of oxygen were removed, and which was equilibrated with the supporting electrolyte, by passage through a gas-washing train that included several efficient scrubbers filled with a chromous solution and containing excess amalgamated zinc.

Ammonium metavanadate was obtained in C.P. quality from two sources: the Fisher Scientific Co. and E. H. Sargent and Co. Nujol mulls of these materials gave infrared spectra that were essentially identical with each other and with the spectrum given by FREDERICKSON AND HANSEN[17], differing only in that the doublet at 940–930 cm^{-1} was distorted for the Fisher reagent. X-ray powder diffraction patterns of these materials were identical with each other and with the data given on A.S.T.M. card no. 9-411. Ultraviolet spectra of freshly prepared solutions of the two reagents, in either 1 *F* perchloric or 3 *F* sulfuric acid, were identical. After the solutions in sulphuric acid

had been standing, however, the spectra became appreciably different, as shown by curves (b) and (c) of Fig. 2. This is probably due to the slow formation of a heteropoly sulfatovanadate(V) complex; it is not surprising that such a species should exist nor that it should form slowly*, but the difference in rate indicates that there is a difference between the samples despite the evidence of their identity. Recrystallization of either material by the procedure of LINGANE AND MEITES[3] had no discernible effect

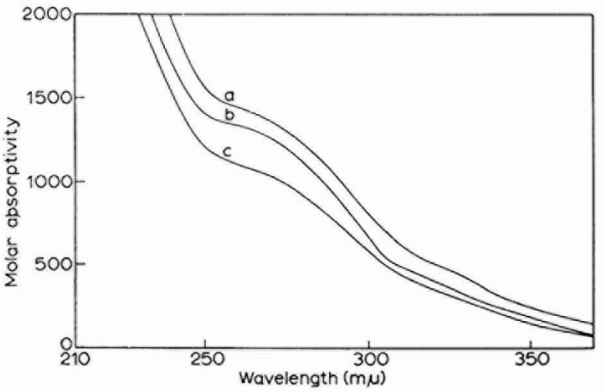

Fig. 2. Ultraviolet spectra of solutions of ammonium metavanadate in 3 *F* sulfuric acid: (a), Fisher or Sargent reagent, freshly prepared; (b), Fisher reagent, 8 days old; (c), Sargent, 8 days old.

on its behavior. The vanadium(V) solutions used in this work were prepared by prolonged boiling of a sample of ammonium metavanadate with a small excess of sodium hydroxide, followed by neutralization to pH 7 with sulfuric acid. They were standardized by the conventional sulfur dioxide–permanganate method.

Vanadium(IV) was prepared in three ways: (i) by reducing a sodium metavanadate solution with sulfur dioxide in the presence of enough sulfuric acid to prevent precipitation, then expelling the excess sulfur dioxide and diluting to the desired composition; (ii) by similarly reducing a suspension of ammonium metavanadate in sulfuric acid; (iii) by controlled-potential electro-reduction of vanadium(V) at about 0 V until a constant current was reached. Although the ionic state of vanadium(IV) in acidic solutions is always taken to be VO^{2+}, Fig. 3 indicates that matters are not as simple as this: the ultraviolet spectrum varies significantly with the source of the vanadium (curves a and c) and with the acid employed (curve d). Evaporation almost to dryness during the removal of sulfur dioxide, followed by dissolution of the residue in 3 *F* sulfuric acid, appeared to yield solutions containing some of the vanadium in colloidal form (curve b), and these gave higher background currents in the controlled-potential experiments than any other solutions.

Vanadium(II) was prepared by the controlled-potential reduction of vanadium(IV) or (III). In 3 *F* sulfuric acid its solutions gave three absorption bands, at 368 mμ ($\varepsilon_{max} = 2.3$), 562 mμ ($\varepsilon_{max} = 4.5$), and 852 mμ ($\varepsilon_{max} = 3.3$). Almost identical visible spectra were obtained in 1 *F* perchloric acid, except that a shoulder replaced the max-

* BAUMGARTEN[19] found that polarograms of tungsten(VI) in phosphoric acid media continued to change even after six months.

imum at 368 mμ. In the ultraviolet there was a shoulder at about 255 mμ ($\varepsilon = 80$), but the most prominent and important feature of the ultraviolet spectra was the dependence of the absorptivities throughout the ultraviolet on the length of time for which the solution had been electrolyzed. A solution prepared by controlled-potential electrolysis for 11,000 sec at −0.9 V gave absorptivities about 10% lower than one prepared by electrolysis for only 4000 sec. This was not due to any difference in the total

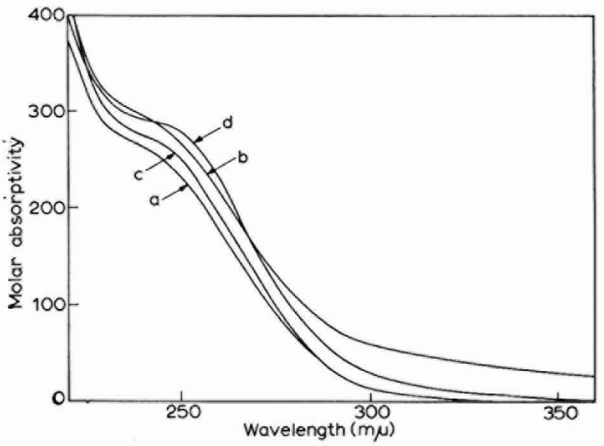

Fig. 3. Ultraviolet spectra of solutions of vanadium(IV): (a), fresh or 5-month-old solutions in 3 *F* sulfuric acid, prepared by reducing Sargent ammonium metavanadate with sulfur dioxide in such a way that no solid residue separated; (b), fresh solution in 3 *F* sulfuric acid, prepared as (a) but with evaporation nearly to dryness; (c), fresh or very old solutions in 3 *F* sulfuric acid, prepared by reducing Fisher ammonium metavanadate, either electrolytically or with sulfur dioxide; (d), very old solution in 1 *F* perchloric acid, prepared by electrolytic reduction of Fisher ammonium metavanadate.

concentration of vanadium(II), because measurements of the quantity of electricity required to effect reoxidation to vanadium(III) showed that this did not vary with the length of the reduction step, and therefore it must reflect a slow transformation of a strongly absorbing species into one or more less strongly absorbing species. This slow chemical transformation is responsible for large variations of the kinetic current.

Vanadium(III) was obtained by controlled-potential oxidation of vanadium(II) at potentials around −0.25 V. Its spectra in perchloric and sulfuric acid media were in good agreement with those described by other authors[19,20].

Mercury was purified by a procedure similar to that used by MEITES AND MOROS[10]. Potassium bisulfate was recrystallized twice from distilled water. Other chemicals were ordinary reagent-grade and were used without further purification. Calibrated glassware was used throughout.

RESULTS AND DISCUSSION

The continuous faradaic current.

The effect of working-electrode potential on the continuous faradaic current corresponding to the rate of formation of hydrogen gas in a typical acidic sulfate solution is shown in Fig. 4. The curve may be divided for convenience into three parts: one at

potentials more negative than about −0.8 V, another at potentials more positive than about −0.5 V, and the transition region between them. In the first of these regions, varying the concentration of hydrogen ion but keeping that of bisulfate nearly constant (*e.g.*, by using 3 *F* potassium bisulfate) displaces the line shown in Fig. 4 but does not affect its slope. The current in this region is proportional to the concentration of hydrogen ion, calculated by successive approximations based on extrapolating litera-

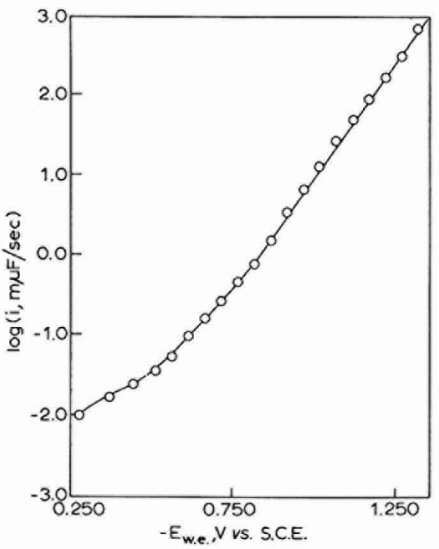

Fig. 4. Effect of working-electrode potential on the continuous faradaic current in 1 *F* sulfuric acid–2 *F* potassium bisulfate.

ture values[21] of pK_2 for sulfuric acid to the appropriate ionic strength, within the rather large (±20%) uncertainty involved in this extrapolation. It may therefore be concluded that this linear portion of the curve corresponds to the direct reduction of hydrogen ion.

In the most positive region, the current is greatly increased by the addition of multivalent cations, and is also increased, though to a much smaller extent, by the addition of sodium ion. These are conditions known to increase the rates of reduction of anions *via* changes in the potential ψ_1 of the double layer[22–24]. Accordingly this branch of the curve may be attributed to the half-reaction $HSO_4^- + e \rightarrow \frac{1}{2} H_2 + SO_4^{2-}$. In 3 *F* potassium bisulfate, where the currents due to this process are largest and those due to the reduction of hydrogen ion are smallest, so that the values are most reliable, this is characterized by $\alpha n_a = 0.155$. De Bethune and Kimball[25] considered this process to be unlikely at a negatively charged electrode, but reductions of anions under such conditions are far too well known to render this view acceptable. However, it does appear possible that the low value of αn_a is attributable to increasing repulsion of bisulfate ions at more negative potentials.

The reduction of vanadium(V)

Although vanadium(V) reacts readily with metallic mercury in acidic sulfate media, yielding solid mercurous sulfate, useful coulometric data can be obtained at potentials where it is reduced to vanadium(IV) if stirring is avoided until the mercurous salt has been quantitatively re-reduced. Thus, in 1 *F* sulfuric acid–3 *F* potassium bisulfate, 12 reductions at +0.1 V of quantities of vanadium(V) ranging from 0.078 to 1.0 mmole (in 80 ml of solution) gave a mean error of ±0.23%, with no detectable bias. At this potential no correction is necessary except for the continuous faradaic current. At more negative potentials, however, the rate of the further reduction to vanadium(III) becomes appreciable. For example, at −0.06 V this gives rise to a steady current of 3.5 *n*F/sec in excess of the continuous faradaic current observed when no vanadium is present. Correction for this is difficult; the formation of vanadium(III) causes no error as long as an appreciable concentration of vanadium(V) remains unreduced, because of the reaction that occurs between these in the bulk of the solution. Neglecting this reaction would lead to an over-correction, and the equations that would be needed to take it into account would be too complex for convenience.

In 0.1–0.2 *F* perchloric acid, reductions at 0 V gave results that were quite concordant but 5.3% high. This error is far in excess of what could reasonably be attributed to reduction of vanadium below the +4 state; it must reflect an induced reduction of perchlorate.

The oxidation of vanadium(II)

Provided that the solution is very strongly acidic ($[H^+] \geqslant 0.1$), this process is unique among all those considered here in being apparently completely straightforward. The anomalies observed in less acidic solutions are described below. In sulfuric acid–bisulfate solutions the vanadium(III)–(II) couple obeys the reversible equations to well within the experimental error. Experiments in which oxidations of vanadium(II) solutions, previously prepared by the reduction of vanadium(IV), were allowed to proceed to equilibrium at various potentials between −0.4 and −0.6 V, and in which the fraction of the vanadium remaining in the +2 state was then determined coulometrically at −0.25 V, gave the formal potential as $-0.536_7 \pm 0.001_4$ V (*vs.* S.C.E.) in 3 *F* sulfuric acid, while $dE/d(\log [V^{II}]/[V^{III}])$ was −0.0598 V. Unexpectedly long times, however, were required for these equilibria to be reached. This is because of the slow chemical transformations involved in the approach to equilibrium. The formal potential, which is nearly 30 mV more negative than in 1 *F* sulfuric acid, reflects not only the difference between the stabilities of the sulfato or bisulfato complexes of vanadium(II) and (III), but also a sizable liquid-junction potential.

When vanadium(II), produced as specified above, is oxidized at −0.25 V, the plot of log *i* *vs.* *t* is strictly linear after correction is made for the continuous faradaic current. The value of β, which is the electrolytic rate constant defined by the equation

$$-\frac{dC}{dt} = \beta C \qquad (1)$$

where *C* is the concentration of vanadium(II), was $(5.37 \pm 0.11) \cdot 10^{-3}$ sec^{-1} in four

replicate experiments in 1 F sulfuric acid–3 F potassium bisulfate, the variation being due to variations in stirring efficiency. The accuracy and precision obtained in 25 determinations of quantities of vanadium(II) varying from 0.08 to 1.0 mmole in various supporting electrolytes (sulfuric acid alone or with potassium bisulfate, or potassium bisulfate–sodium sulfate buffers, at various concentrations from 0.1 to 3 F) were $\pm 0.22\%$. The process should prove useful in analytical applications.

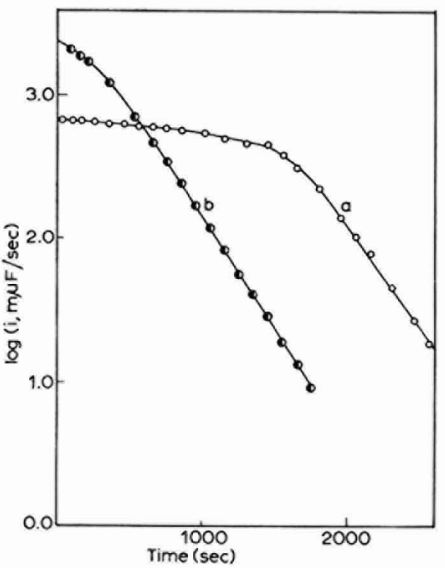

Fig. 5. Plots of log i against t for oxidations of vanadium(II) in 0.3 F potassium bisulfate–1.5 F sodium sulfate, pH 1.55, at a working-electrode potential of -0.250 V *vs.* S.C.E.: (a), oxidation of the vanadium(II) obtained by reducing 1 mmole of vanadium(IV) at -1.200 V *vs.* S.C.E.; (b), oxidation of the vanadium(II) produced by re-reducing the vanadium(III) formed in (a) at -1.200 V *vs.* S.C.E.

In sulfate–bisulfate media, however, striking complexities are observed in plots of log i *vs.* t, as illustrated by Fig. 5. Curve (a) in this figure shows the data obtained in oxidizing vanadium(II) obtained from the reduction of vanadium(IV); curve (b) shows the data obtained under identical conditions but using vanadium(II) obtained from the reduction of vanadium(III). The shapes of these curves cannot correspond to oxidations of mixtures of vanadium(II) species, for in that case the curves would have to be concave upward. Various mechanisms that lead to curves of the observed shape have been devised[26–29]; of these, the only one that appears reasonable in this case is of the form

$$V_n^{II} - p\,e \overset{\beta_1}{\rightarrow} (V_{n-p}^{II}V_p^{III}) \overset{k_2}{\rightarrow} V_{n-p}^{II} + V_p^{III} - (n-p)\,e \overset{\beta_3}{\rightarrow} V_{n-p}^{III} + V_p^{III} \qquad (2)$$

in which the oxidation of an n-meric vanadium(II) species is assumed to occur in two steps. If k_2 is assumed to be so high that it is chronocoulometrically invisible, and if

A represents the n-mer and C represents the $(n-p)$-mer, one may write approximately

$$\beta_A/\beta_C = D_A/D_C \quad (3)$$

where the D's are the appropriate diffusion coefficients. Invoking Jander's rule and assuming that the formula weights are proportional to the degrees of polymerization, one obtains eventually

$$i_A^0/i_C^0 = p(n-p)^{\frac{1}{3}}/n^{\frac{1}{3}} \quad (4)$$

where i_A^0 is the initial current due to the oxidation of A, obtained by extrapolating the measured currents to zero time, and i_C^0 is the hypothetical initial current that would have been obtained from the oxidation of C if all of the vanadium(II) had been in that form initially, calculated from the equation

$$i_C^0 = \beta_C Q_\infty \quad (5)$$

where Q_∞ is the total number of mg-atoms of vanadium(II) present or the total number of mF consumed, and β_C is the final slope of a plot of ln i *vs.* t. Various combinations of values of n and p can be envisioned. For example, the combination $n = 4$, $p = 1$ yields a calculated ratio ($i_A^0/i_C^0 = 0.216$) that is in good agreement with the lowest value (0.208) obtained experimentally. No other combination with $n \leqslant 6$ is as satisfactory.

Of course this is not certain evidence for the existence of a tetrameric species of vanadium(II). The experimental values varied over about a two-fold range; they increased with increasing ionic strength and with increasingly negative potential during the prior reduction of vanadium(IV) to vanadium(II), and also varied with the acidity. The cited ratio of 0.208 is the lowest found under a wide variety of conditions, but it is very possibly higher than the limiting value. Moreover, it is hard to believe that only a single polymeric species would exist under conditions like these: a mixture of several different n-mers seems at least as probable.

There can, however, be little doubt of the existence of polymeric species. It is clear from eqn. (2) that a mechanism of the type envisioned here will involve some depolymerization of the n-mer; for $n = 4$ and $p = 1$ the oxidation would yield a mixture of monomeric and trimeric vanadium(III). If the polymerization equilibria are slow, which is not an unreasonable supposition, the reduction of this mixture back to vanadium(II) would yield a mixture of species in which the average polymerization number was considerably smaller than in the solution resulting from the original reduction of vanadium(IV). This mixture would give a value of i_A^0/i_C^0 more nearly equal to 1 (*i.e.*, a more nearly linear plot of log i *vs.* t), and this is exactly the behavior shown by curve (b) of Fig. 5. Oxidizing the mixture of monomer and trimer obtained from the above cycle should further increase the fraction of the vanadium present in the monomeric form; if the resulting solution is again reduced to vanadium(II) and again re-oxidized, the plot of log i *vs.* t should be still more nearly linear than before. In fact, such a plot does become more and more nearly linear on repeated oxidation and reduction.

The formation of polymeric vanadium(II) in the reduction of vanadium(IV) implies that the latter is also polymeric under these conditions. This is not improbable *a priori*, and if vanadium(II) polymerized when it was formed from monomeric vanadium(IV) it would also be expected to do so when formed from vanadium(III), which is not in agreement with the observed effect of oxidizing the vanadium(II) and then reducing it again.

The reduction of vanadium(III)

A plot of log i *vs.* t for the reduction of vanadium(III) in 1 F sulfuric acid-2 F potassium bisulfate is concave upward and it decays to a finite value that is much larger than the continuous faradaic current at the same potential. This excess current, which has been termed the "kinetic current"[10], i_k, is proportional to the concentration of vanadium(II); under typical conditions the kinetic current constant, a, defined by the equation

$$i_k = a[V^{II}] \tag{6}$$

was equal to 3.19 ± 0.14 nF/sec/mmole/l, and thus constant to about ±5%, over the range of vanadium(II) concentrations from 2.5 to 12 mM.

If this kinetic current were due to the reduction of vanadium(III) resulting from oxidation of vanadium(II) by the supporting electrolyte, it should be independent of potential over the region corresponding to the plateau of the vanadium(III) wave, and in addition there should be a finite steady-state concentration of vanadium(III) present at the end of the electrolysis, whose rate of increase on disconnecting the potentiostat from the cell should be possible to correlate with the steady-state kinetic current. All these phenomena, which may be regarded as defining a "chemical kinetic" current, have been observed in a case in which a chemical reaction is responsible for the kinetic current[11], but none of them is observed here. On the contrary, changing the potential from −0.80 to −0.95 V, for example, in 1 F sulfuric acid–2 F potassium bisulfate causes a to increase from 0.6 to 1.7 nF/sec/mmole/l; no detectable concentration of vanadium(III) is present at the end of an electrolysis even under conditions where the value of a would correspond to a concentration of vanadium(III) 80% as high as at the start; and although vanadium(II) solutions are known not to be perfectly stable their rate of decomposition under these conditions is negligibly small.

The kinetic current must therefore be attributed to a rate-determining reduction of vanadium(II), followed by a chemical process that regenerates the original species. It is improbable that the reduction should be $V^{2+} + 2\,e \rightarrow V$, as was suggested previously[10], for two reasons: the standard potential (*ca.* −1.42 V[30]) of this half-reaction is far too negative, and it leads to the expectation that a will vary little if at all with solution composition. In fact, under otherwise identical conditions Table 1 shows that

TABLE 1

EFFECT OF SOLUTION COMPOSITION ON THE KINETIC CURRENT CONSTANT

The data were obtained by reducing aged solutions of Fisher's ammonium metavanadate to vanadium(II) at −0.95 V, oxidizing this to vanadium(III) at −0.25 V, re-reducing this to vanadium(II) at −0.95 V, and measuring the essentially steady current after electrolysis for 3000 sec at the last of these potentials, when the reduction was judged to be complete.The concentration of vanadium varied from 2.5 to 12 mM.

$[H_2SO_4]$ (F)	$[KHSO_4]$ (F)	a (nF/sec/mmole/l)
3	0	12.9
2.87	0.13	10.5
1	3	3.19 ± 0.14
1	2	1.71 ± 0.20
0	1.1 (+ 1.9 F Na_2SO_4)	0.6

a varies with the concentrations of both sulfuric acid and bisulfate. Activity coefficients are impossible to estimate with any confidence in solutions like these, and the value of pK_2 for sulfuric acid is not known with certainty at these ionic strengths. It is therefore hardly possible to deduce the mechanism. But if, as appears to be the case, a increases with increasing concentrations of both hydrogen and bisulfate ions, one may envision a bisulfato complex of vanadium(II) that accepts an electron through a hydronium ion serving as a bridge between it and the electrode, as in the mechanism envisioned for the reduction of α-furildioxime in acidic media[31]. As the addition of an electron to the vanadium orbitals is virtually impossible under these conditions, however, the structure can retain the electron only by decomposing to yield hydrogen gas.

Complicating this simple picture of an electrochemical kinetic current is the fact that the kinetic currents observed become dependent in an intricate fashion on the potential, the duration of electrolysis, and the previous history of the solution if the working-electrode potential becomes more negative than about −0.95 V. The phenomena then observed are summarized in Fig. 6.

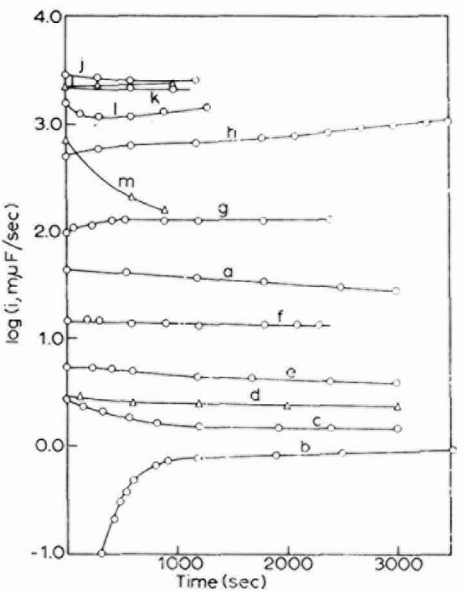

Fig. 6. Effects of working-electrode potential and time on the kinetic current of vanadium(II). A solution containing 2.027 mmoles of vanadium(IV) in 70 ml of 1 F sulfuric acid–2 F potassium bisulfate was reduced at −0.950 V *vs.* S.C.E. for 3600 sec; then the kinetic currents were measured at the following potentials in the following order: (a), −0.950; (b), −0.750; (c), −0.800; (d), −0.850; (e), −0.900; (f), −0.950; (g), −1.000; (h), −1.050; (i), −1.100; (j), −1.150; (k), −1.200; (l), −1.250; (m), −1.350 V *vs.* S.C.E. All currents are corrected for the continuous faradaic currents obtained with the supporting electrolyte alone under identical conditions.

Curve (a) in this figure begins 3600 sec after the start of a reduction of vanadium(IV) to (II) in 1 F sulfuric acid–2 F potassium bisulfate; this time was judged to be well in excess of that necessary for quantitative reduction, but a slow decay of current was still observed. This is attributed to the slow transformation of the vanadium(II)

species first formed, into another yielding a smaller kinetic current; the previously mentioned change of absorptivity on prolonged electrolysis provides support for the occurrence of such a transformation. On changing the potential to −0.75 V (curve b), an anodic current flowed at first; the quantity of electricity corresponding to the anodic current during the first 1000 sec or so can be quantitatively correlated with the extent of oxidation to vanadium(II) demanded by the Nernst equation. Most of this is re-reduced during the first portion of a subsequent electrolysis at −0.80 V (curve c), where a nearly steady current is again reached, but this is higher than the current at −0.75 V, as mentioned above. The remaining curves show that the kinetic current increases on standing if the potential is between about −1.0 and −1.1 V (curves g–i) but decreases on standing at still more negative potentials. The steady-state value is clearly much smaller at −1.35 V (curve m) than at −1.10 to −1.15 V (curves i–j).

If the initial currents at these potentials are measured as rapidly as possible, one obtains the data shown in Fig. 7, which could be regarded as an ordinary voltammetric

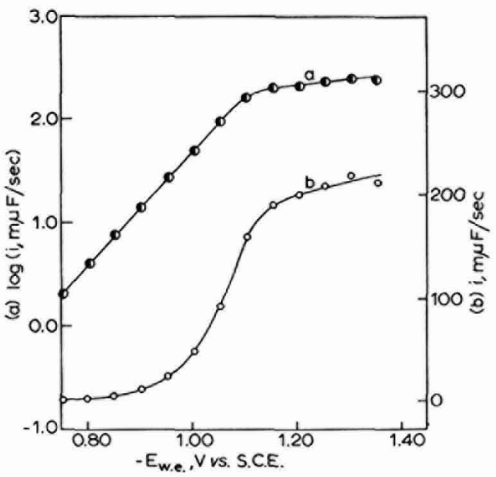

Fig. 7. Effect of working-electrode potential on the initial kinetic current of vanadium(II). A solution of vanadium(IV) in 1 *F* sulfuric acid–2 *F* potassium bisulfate was reduced to vanadium(II) at −0.950 V *vs.* S.C.E.; when the reduction was complete, the current was rapidly measured at each of the potentials shown, beginning with the most positive potential and proceeding toward more negative ones. All currents are corrected for the continuous faradaic currents obtained with the supporting electrolyte alone under the same conditions. (a), Plot of log i_k *vs.* $E_{w.e.}$ (left-hand ordinate scale); (b), plot of i_k *vs.* $E_{w.e.}$ (right-hand ordinate scale).

wave except for the fact that the limiting current is far too small to correspond to the transfer of an electron to each vanadium atom at the electrode surface (which would give a current nearly a hundred times as large as the value on this plateau). If the current is due to electron addition to the hydronium-ion-bridged structure postulated above, this is easily explained. Because the bisulfate ion is only very weakly basic, the probability of bridge formation is low, and the limiting current reflects, not the rate of mass transfer of vanadium(II) to the electrode surface, but rather the rate of bond

formation between hydronium ions in contact with the electrode and bisulfate ions co-ordinated to vanadium(II). The plateau then simply corresponds to the region in which electron addition is much more rapid than bond formation.

To explain the effects of potential and time on the kinetic current, it seems necessary to assume that three species of vanadium(II) and (III) can exist in strongly acidic sulfate solutions. It may be recalled that monomeric, trimeric, and tetrameric species had to be postulated to explain the behavior of the current–time curves obtained in the oxidation of vanadium(II). For convenience in discussion we shall denote these species by the symbols A_2, B_2, C_2, A_3, B_3, and C_3, where the subscript represents the oxidation state of the vanadium. The necessary assumptions regarding the current–potential curves of these species are portrayed by Fig. 8; although this shows the

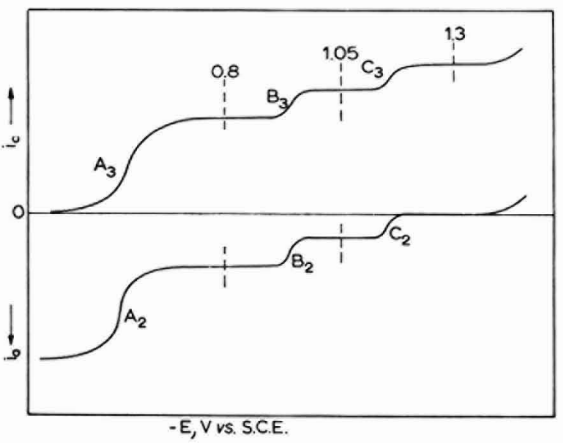

Fig. 8. Assumed current–potential curves for the species of vanadium(II) and (III) in sulfuric acid–bisulfate solutions.

B_3–B_2 and C_3–C_2 couples as reversible, overpotentials of the order of tens of millivolts are not excluded by the data. The different species of vanadium(II) have different kinetic current constants, that for B_2 being the largest and that for C_2 the smallest.

Whereas the kinetic current is attributed to the reduction of vanadium(II) in such a way as to yield hydrogen, evidence similar to that previously adduced[11] in the reduction of manganese(II) in cyanide media shows that an induced current also flows during the reduction of vanadium(III), and this must be similarly attributed to a side reaction that leads to the formation of a deprotonated vanadium(III) species and hydrogen instead of the expected vanadium(II). This induced current (or, experimentally, its integral, the induced quantity of electricity) also varies with solution composition, working-electrode potential, and other experimental conditions. To each of the vanadium(III) species there belongs an induced current constant (b in our previous notation[10]) the value of which under any given conditions reflects the probability of obtaining hydrogen rather than vanadium(II) from the electron-transfer process. Other factors being constant, the values of b for the vanadium(III) species parallel those of a for the corresponding vanadium(II) species: B_3 gives the highest, and C_3 the smallest, induced quantities of electricity.

If, for example, vanadium(III) is reduced at a potential no more negative than about −0.95 V, A_3 is the only reducible species, while A_2 is the only stable product. The current decreases slowly at the end of the reduction (Fig. 6, curve a) as the last of the B_3 is transformed into A_3 and then reduced to A_2. Around −1.1 V, however, both B_3 and A_3 can be reduced; because B_3 is reducible, the induced quantity of electricity is higher than at the less negative potential, and because B_2 is stable at this potential the kinetic current is also higher. The upward drift of the current at the end of the electrolysis means that the steady-state concentration of B_2 is higher than the original concentration of B_3, so that A_2 is slowly transformed into B_2. At still more negative potentials, such as −1.35 V, the induced quantity of electricity is still high because B_3 is still reducible, but now C_2 is stable toward oxidation and its accumulation leads to kinetic currents that are smaller than at −1.1 V (Fig. 6, curves i and m) and that decrease with time as A_2 and B_2 are transformed into C_2.

The phenomena observed when the potential is changed after the completion of an electrolysis can be explained similarly. For example, B_2 cannot exist at appreciable concentrations at −0.9 V, because it is oxidized to B_3 as rapidly as it is formed from A_2. But if the potential is changed to −1.1 V B_2 can accumulate, and because its kinetic current constant is larger than that of A_2, the current drifts upward as the transformation of A_2 into B_2 proceeds.

Species A_3 and A_2 are surely the monomeric species involved in the reversible couple whose formal potential is around −0.53 V in these media. Partly because of the slowness of the transformations that occur, and partly because of the manner in which the currents vary with solution composition, it seems necessary to assume that B_3 and B_2 are polynuclear and include co-ordinated bisulfate, the acidity of which is responsible for the relatively high rates of formation of hydrogen by the induced and kinetic processes. The species C_3 and C_2 are also doubtless polynuclear but probably do not contain bisulfate; as the transformations involving them are not grossly different in rate from those involving B_3 and B_2, it is not possible to say whether the B and C species differ only in the ligands they contain or whether there is also a difference between their degrees of polymerization. It is interesting to note that the half-wave potentials that must be assigned to the B and C couples are in approximate agreement with those of two waves observed[3] in weakly acidic solutions of vanadium(III) and previously assigned to hydrolysis products of vanadic ion.

To evaluate the induced current constant b, it is convenient to adopt the following chronocoulometric approach. The current (in mF/sec) at any instant is given by

$$i = i_O + i_k + i_i \tag{7}$$

where i_O is the current corresponding to the n-electron reduction of O to R (vanadium(III) to vanadium(II)), i_k is the kinetic current, and i_i is the induced current. Writing

$$i_k = aC_R \tag{8}$$

$$i_i = bC_O \tag{9}$$

and

$$i_O = \beta nVC_O = -nV\frac{dC_O}{dt} = nV\frac{dC_R}{dt} \tag{10}$$

where the concentrations C_O and C_R are given in mmoles/l, the volume V in l, and the

mass-transfer constant β in sec^{-1}, one has

$$i = (\beta V + b - a)C_O + aC_O^0 \tag{11}$$

where C_O^0 is the initial concentration of O. Hence the quantity of electricity Q_t (in mF) accumulated up to any time t is

$$Q_t = [Q_O + \frac{b - a}{\beta} C_O^0](1 - e^{-\beta t}) + aC_O^0 t \tag{12}$$

where Q_O is the quantity of electricity that would correspond to the quantitative reduction of O to R in the absence of any other reaction. At a time t^* so long that the exponential term is negligible,

$$Q_{t^*} = Q_O + \frac{b - a}{\beta} C_O^0 + aC_O^0 t^* \tag{13}$$

whence the difference[29] Q_R becomes

$$Q_R = \left[Q_O + \frac{b - a}{\beta} C_O^0\right] e^{-\beta t} + aC_O^0(t^* - t) \tag{14}$$

This is necessary because the quantity Q_∞ used in the definition of Q_R in the absence of induced and kinetic processes is meaningless in their presence. One has

$$Q_O = nVC_O^0 \tag{15}$$

and the current flowing when $t = t^*$ is given by

$$i_{t^*} = aC_O^0 \tag{16}$$

since C_R then equals C_O^0. Hence eqn. (14) becomes

$$\ln [Q_R - i_{t^*}(t^* - t)] = \ln \left[Q_O\left(1 + \frac{b - a}{\beta V}\right)\right] - \beta t \tag{17}$$

from which the value of β is readily obtained. An alternative approach consists of writing eqn. (11) for $t = 0$:

$$b = \frac{i^0}{C_O^0} - \beta V \tag{18}$$

Combining eqns. (11), (16), and (18) yields ultimately

$$\beta = \frac{1}{t} \ln \frac{i^0 - i_{t^*}}{i - i_{t^*}} \tag{19}$$

After β has been evaluated in either of these ways, and after a has been calculated from eqn. (16), the value of b is easily obtained by combining the intercept of a plot of eqn. (17) with the theoretical value of Q_O from eqn. (15).

Because the definition of b according to eqn. (9) includes the rate of mass transfer of O to the electrode surface, it is appropriate to consider the ratio $b/\beta V$, which should be independent of such experimental variables as the stirring rate. In 1 F sulfuric acid–2 F potassium bisulfate this ratio was 0.046 $\pm$ 0.003 in experiments with 0.4–1.0 mmole of vanadium(III); in 1 F sulfuric acid–3 F potassium bisulfate it was 0.104 $\pm$ 0.004 with 0.2–0.6 mmole of vanadium(III); and in 2.87 F sulfuric

acid–0.13 F potassium bisulfate it was 0.20 in a single experiment with 1 mmole of vanadium(III). All these reductions were performed at −0.95 V; in others at potentials between −0.75 and −0.95 V in 1 F sulfuric acid–2 F potassium bisulfate, the variation with potential corresponded to $\alpha n_a = 0.34$ for the electron-transfer step that determines the rate of reduction of protons from the vanadium(III) species termed A_3 above. A similar treatment could not be applied to data obtained at more negative potentials because the drifts of the final current with time, due to the slow equilibration of the different species capable of existence there, were so severe that the necessary values of a could not be obtained.

The reduction of vanadium(IV)

Figure 9 is a plot of the logarithm of the maximum current during the life of a drop at a dropping electrode in a solution of vanadium(IV) in 3 F sulfuric acid against the potential of the drop, appropriate corrections having been applied for the residual

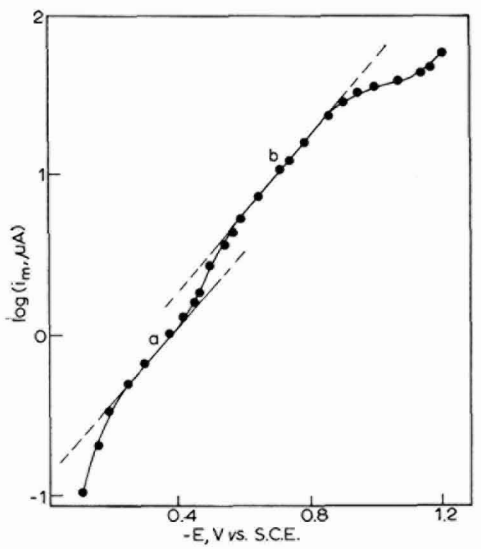

Fig. 9. Effect of dropping-electrode potential on the maximum current during the life of a drop in a 5.72 mM solution of vanadium (IV) in 3 F sulfuric acid. Currents are corrected for the residual current at the end of the drop life.

current. If the plateau of the wave at about −1.0 V and the subsequent onset of rapid reduction of hydrogen ion are neglected, the plot consists of two parallel linear segments, each having $\alpha n_a = 0.14$, and differing by a factor of almost exactly 2 in the current. At potentials less negative than about −0.4 V the reduction proceeds only to the +3 state, but at potentials more negative than about −0.6 V it proceeds practically completely to the +2 state, and this change of the overall n-value is responsible for the unusual shape of the curve.

Even if vanadium(IV) is reduced at potentials negative enough to ensure quan-

titative reduction to vanadium(II), this voltammetric behavior gives rise to relatively complex current–time curves, as shown in Fig. 10. The vanadium(II) first formed reacts with unreduced vanadium(IV) in the bulk of the solution; if the potential is less negative than about −1.0 V it is on the plateau of the wave of the resulting vanadium-(III) even though it is not on the plateau of the wave of the vanadium(IV) present originally, and consequently the current increases, passes through a maximum, and

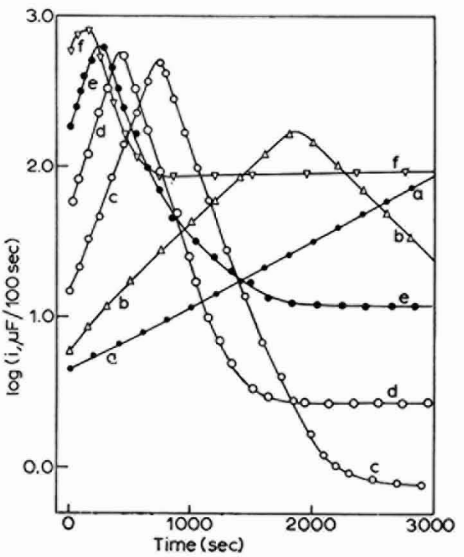

Fig. 10. Plots of log i *vs.* electrolysis time for controlled-potential electro-reductions of solutions containing 1.004 mmole of vanadium(IV) in 70 ml of 1 F sulfuric acid–2 F potassium bisulfate at working-electrode potentials of: (a), −0.630; (b), −0.720; (c), −0.850; (d), −0.950; (e), −1.050; (f), −1.200 V *vs.* S.C.E.

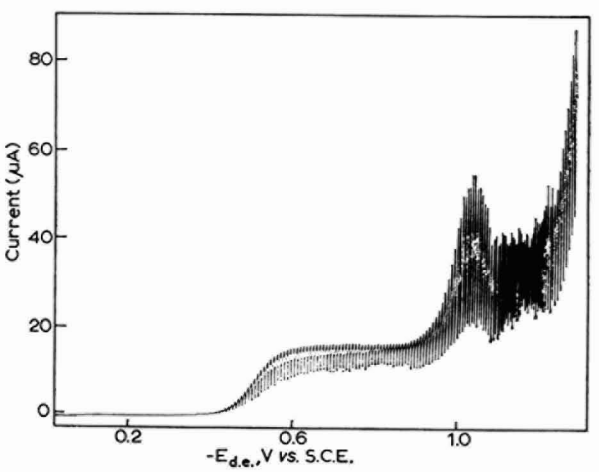

Fig. 11. Polarogram of 5.72 mM vanadium(III) in 3 F sulfuric acid. The vanadium(III) was obtained by reducing vanadium(IV) at −1.150 V *vs.* S.C.E., then reoxidizing the resulting vanadium-(II) at −0.250 V, and the polarogram was obtained *in situ* in the controlled-potential electrolysis cell.

finally decreases again as the reduction of the vanadium(III) proceeds toward completion. A maximum is also observed, however, even if the potential is so negative that it lies on the plateau of the vanadium(IV) wave. This is because the polarogram of vanadium(III) shows a second wave at very negative potentials, as shown in Fig. 11, which corresponds to proton reduction (*i.e.*, to the induced currents discussed above) and which has not yet been mentioned in the literature. Hence the current obtained from the reduction of vanadium(III) always exceeds that obtained from the reduction of vanadium(IV) at the same concentration. It is clear that both the induced and the kinetic currents observed in reductions of vanadium(III) affect reductions of vanadium(IV) as well.

Plotting the logarithm of the initial current against the potential for the reduction of vanadium(IV) gives the curve shown in Fig. 12. There is some scatter because of

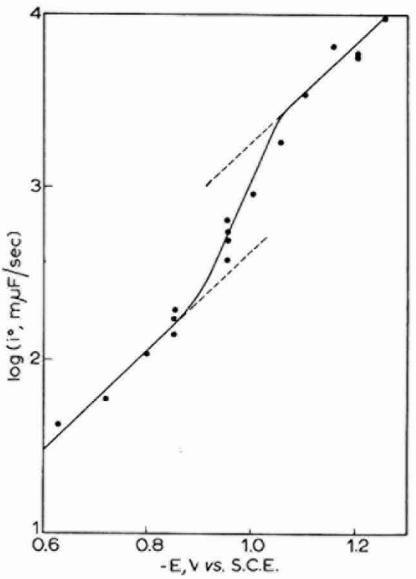

Fig. 12. Initial currents obtained in controlled-potential electro-reductions of vanadium(IV) at various potentials. Each solution contained 1.004 mmole of vanadium(IV) in 70 ml of 1 *F* sulfuric acid–2 *F* potassium bisulfate. Corrections for the continuous faradaic current are negligible on the scale shown.

the difficulty of reproducing mass-transfer coefficients in replicate experiments, but the general shape is unmistakably similar to that of Fig. 9. (Note, however, that these two figures pertain to different media.) The vertical distance between the two parallel segments of Fig. 12 represents a factor of almost exactly 4 in the overall n-values; since n is certainly 2 at potentials between −0.6 and −0.8 V, it is apparently 8 at potentials between −1.0 and −1.2 V. The latter value would correspond to a 2-electron reduction of each of the vanadium atoms in a tetrameric species. It is appropriate to recall the evidence for the existence of tetrameric vanadium(II) that has already been described in connection with Fig. 5.

Although solutions prepared from Sargent and Fisher ammonium metavanadate

gave strikingly different kinetic currents (those obtained with the Sargent reagent were lower, the difference being sometimes as large as a factor of 10), solutions of vanadium(II) derived from the Fisher reagent by reduction at potentials no more negative than about −0.95 V gave essentially the same current when they were prepared by reducing vanadium(IV) as when they were prepared by reducing vanadium(III). Values of the kinetic current constant a obtained in the latter fashion are listed in Table 1. When vanadium(IV) prepared from the Fisher reagent was reduced at −0.95 V, the essentially steady currents obtained after 4000 sec gave $a = 1.56 \pm 0.11$ (nF/sec/mmole/l) in 1 F sulfuric acid–2 F potassium bisulfate, 2.91 ± 0.12 in 1 F sulfuric acid–3 F potassium bisulfate, and 0.71 in 1.1 F potassium bisulfate–1.9 F sodium sulfate. These are all in excellent agreement with the values in Table 1. In more acidic solutions, however, substantial discrepancies appeared: in 2.87 F sulfuric acid–0.13 F potassium bisulfate, for example, the kinetic current constant was 2.85 nF/sec/mmole/l for vanadium(II) obtained by reducing vanadium(IV) at −0.95 V, whereas the operations described in Table 1 gave a value nearly 4 times as large. This must reflect a considerable difference between the rates of depolymerization of vanadium(II) and (III) under these conditions.

At potentials sufficiently positive to permit the kinetic and induced currents (both of which increase exponentially as the potential becomes more negative) to be neglected, one can in principle evaluate the rate constant for the reaction between vanadium(IV) and (II) from chronocoulometric data. Such an application of chronocoulometry has not been described before, and it may therefore be of interest to outline the argument here. If one assumes[32] that the reaction in question is first-order with respect to both vanadium(IV) and (II), one has

$$\frac{dC_4}{dt} = -\beta_4 C_4 - kC_2C_4 \tag{20a}$$

$$\frac{dC_3}{dt} = 2kC_2C_4 - \beta_3 C_3 \tag{20b}$$

$$\frac{dC_2}{dt} = \beta_4 C_4 + \beta_3 C_3 - kC_2C_4 \tag{20c}$$

The total current (which is assumed to contain no contribution from proton reduction) is

$$i = i_4 + i_3 = V(2\beta_4 C_4 + \beta_3 C_3) \tag{21}$$

Combining eqns. (20a), (20c), and (21) gives

$$i = V\left(\frac{dC_2}{dt} - \frac{dC_4}{dt}\right) \tag{22}$$

which may be integrated and combined with appropriate conservation equations to give a description of Q_t, the quantity of electricity consumed during the first t seconds of electrolysis:

$$Q_t = V(2C_2 + C_3) \tag{23}$$

whence, by further use of the conservation equations,

$$C_3 = 2(C_4^0 - C_4) - \frac{Q_t}{V} \tag{24}$$

and

$$C_4 = \frac{\beta_3(2VC_4^0 - Q_t) - i}{2V(\beta_3 - \beta_4)} \tag{25}$$

Differentiating this with respect to time and combining it wih eqn. (20a) gives

$$k = \frac{\beta_3 i + (\mathrm{d}i/\mathrm{d}t)}{2V(\beta_3 - \beta_4)C_2C_4} \tag{26}$$

Equations (23)–(26), together with data on Q_t and i at various times and experimental values of β_3 (obtained, for example, by applying eqn. (19) to data obtained in a reduction of vanadium(III) under the same conditions) and β_4 (obtained, for example, from the initial current), permit the evaluation of k, the pseudo-second-order rate constant of the vanadium(II)–(IV) reaction. This is most conveniently done at the point where i has its maximum value, both because $\mathrm{d}i/\mathrm{d}t = 0$ at that point and because the relative error in the product C_2C_4 can be expected to be smaller there than anywhere else. A number of experiments with 5–15 mM vanadium in 3 F sulfuric acid gave, in mean, $k = (15 \pm 3)$ l/mole/sec, which is not very different from values previously obtained in other media containing sulfate by both OLIVER AND ROSS[32] and NEWTON AND BAKER[33], who gave 10 and 12.2 l/mole/sec, respectively, in 0.4 F sulfuric acid–0.15 F sodium bisulfate. Extrapolation of the data of NEWTON AND BAKER to the considerably higher ionic strengths used here seems somewhat dangerous but would tend to bring the values into better accord.

SUMMARY

The rates and mechanisms of electrolytic processes occurring at mercury electrodes in aqueous acidic sulfate solutions of vanadium in its various oxidation states have been studied by polarography, absorption spectroscopy, and controlled-potential amperometry and chronocoulometry. The complex behavior observed is interpreted in terms of polynuclear species containing vanadium and undergoing slow transformations. Both vanadium(II) and vanadium(III) exist in three forms, each of which may be reduced to give hydrogen and a deprotonated species of vanadium; these reductions give rise to kinetic and induced currents the behaviors of which are described in detail.

REFERENCES

1 S. ZELTZER, *Collection Czech. Chem. Commun.*, 4 (1932) 319.
2 J. J. LINGANE, *J. Am. Chem. Soc.*, 67 (1945) 1916.
3 J. J. LINGANE AND L. MEITES, *J. Am. Chem. Soc.*, 70 (1948) 2525.
4 I. FILIPOVIČ, Z. HAHL, Z. GAŠPARAC AND V. KLEMENČIĆ, *J. Am. Chem. Soc.*, 76 (1954) 2074.
5 J. E. B. RANDLES AND K. W. SOMERTON, *Trans. Faraday Soc.*, 48 (1951) 937.
6 G. JONES AND W. A. RAY, *J. Am. Chem. Soc.*, 66 (1944) 1571.
7 L. MEITES, *J. Am. Chem. Soc.*, 75 (1953) 6059.
8 S. C. FURMAN AND C. S. GARNER, *J. Am. Chem. Soc.*, 72 (1950) 1785.
9 G. JONES AND J. H. COLVIN, *J. Am. Chem. Soc.*, 66 (1944) 1563.
10 L. MEITES AND S. A. MOROS, *Anal. Chem.*, 31 (1959) 23.

11 S. A. MOROS AND L. MEITES, *J. Electroanal. Chem.*, 5 (1963) 103.
12 M. SPRITZER AND L. MEITES, *Anal. Chim. Acta*, 26 (1962) 58.
13 L. MEITES AND Y. ISRAEL, *J. Am. Chem. Soc.*, 83 (1961) 4903.
14 L. MEITES AND T. MEITES, *Anal. Chem.*, 23 (1951) 1194.
15 S. A. MOROS, Ph.D. Thesis, Polytechnic Institute of Brooklyn, 1962.
16 L. MEITES, *Anal. Chem.*, 27 (1955) 1116.
17 L. D. FREDERICKSON, JR. AND D. M. HANSEN, *Anal. Chem.*, 35 (1963) 818, 1167.
18 S. A. BAUMGARTEN, unpublished experiments at the Polytechnic Institute of Brooklyn.
19 S. C. FURMAN, personal communication; *cf.* also ref. 8.
20 E. L. MARTIN AND K. E. BENTLEY, *Anal. Chem.*, 34 (1962) 354.
21 N. BJERRUM, G. SCHWARZENBACH AND L. SILLEN, *Stability Constants*, Part II, The Chemical Society, London, 1958, p. 79.
22 A. N. FRUMKIN, *Advances in Electrochemistry and Electrochemical Engineering*, Vol. I, edited by P. DELAHAY, Interscience Publishers Inc., New York, 1961, pp. 65–121.
23 A. N. FRUMKIN, *Trans. Faraday Soc.*, 55 (1959) 156.
24 P. HERASYMENKO AND I. SLENDYK, *Z. Phys. Chem.*, A149 (1930) 123.
25 A. J. DE BETHUNE AND G. KIMBALL, *J. Chem. Phys.*, 13 (1945) 53.
26 S. KARP AND L. MEITES, *J. Am. Chem. Soc.*, 84 (1962) 906.
27 A. J. BARD AND J. S. MAYELL, *J. Phys. Chem.*, 66 (1962) 2173.
28 L. MEITES, *J. Electroanal. Chem.*, 5 (1963) 270.
29 R. I. GELB AND L. MEITES, *J. Phys. Chem.*, 68 (1964) 630.
30 W. M. LATIMER, *Oxidation States of the Elements and their Potentials in Aqueous Solution*, Prentice-Hall Inc., New York 2nd ed., 1952.
31 R. I. GELB AND L. MEITES, *J. Phys. Chem.*, in press.
32 J. W. OLIVER AND J. W. ROSS, *J. Phys. Chem.*, 66 (1962) 1699.
33 T. W. NEWTON AND F. B. BAKER, *J. Phys. Chem.*, 68 (1964) 228; *Inorg. Chem.*, 3 (1964) 569.

ELECTRODE PROCESSES FOLLOWED BY CHEMICAL REACTIONS INVOLVING ELECTROACTIVE SPECIES

I. THE EFFECT OF ETHYLENEDIAMINETETRAACETATE ON THE POLAROGRAPHIC REDUCTION WAVES OF HEXAQUOCHROMIUM(III) AND HEXAMMINECHROMIUM(III)

NOBUYUKI TANAKA AND KAZUKO EBATA

Department of Chemistry, Faculty of Science, Tokohu University, Sendai (Japan)

(Received March 26th, 1964)

It has been reported that the one-electron reduction wave of hexamminechromium-(III) is not well-defined in neutral media, but that it is nearly complete when an approximately equivalent amount of disodium ethylenediaminetetraacetate (EDTA) is added to the solution[1,2]. This was interpreted as that the rapid complex formation reaction between EDTA and chromium(II) produced by the reduction of hexammine-chromium(III) prevented chromium(II) from precipitating as an insoluble film on the electrode surface. Recently, it was observed that the presence of EDTA also affected the well-defined waves of hexamminechromium(III) that were obtained in acid solutions. When a small amount of EDTA was added, the one-electron reduction wave split into two steps; the position of the first step was almost the same as that of the reduction of hexamminechromium(III), while the position of the second step was more negative than that of the first by some tenths of a volt. The height of the first step decreased with increase in EDTA concentration. When the concentration of EDTA exceeded an appropriate value, only a single step was observed at the potential corresponding to that of the second step. In this paper, a more detailed investigation on the mechanisms of these phenomena is presented.

EXPERIMENTAL

Reagents

Hexamminechromium(III) chloride was prepared according to the method of MORI[3]. The acidic solution of hexaquochromium(III) was obtained by the reduction of sodium dichromate in perchloric acid with hydrogen peroxide. The chromium content of the solution was determined polarographically[4] after oxidation to chromate with hydrogen peroxide in alkaline solution. The preparation and standardization of the EDTA solution was carried out as described previously[5]. All other chemicals used were of guaranteed reagent-grade.

Apparatus

Polarographic measurements were carried out with a Yanagimoto PB-4 pen-

recording polarograph at 25°. In most cases, the current–time curves during the life of a mercury drop were recorded using a Rikadenki ER-J1 recorder (pen speed: full scale, 0.5 sec; maximum chart speed: 16 mm/sec) with an RLDC-201 preamplifier. In the following sections, the word "current," denoted by i, means the maximum current observed just before the mercury drops, unless otherwise stated. The dropping mercury electrode used had an m-value of 2.11 mg/sec and a drop time, t_d, of 4.22 sec in de-aerated 0.2 M potassium nitrate solution at −0.5 V *vs.* S.C.E. and at 59 cm mercury height. A saturated calomel electrode (S.C.E.) with a large surface area served as an anode.

Electrolysis at constant potential was carried out using a Yanagimoto automatic potentiostat VE-3 at room temperature. Mercury pools were used for both the anode and cathode, and the anode and the cathode compartments were connected with a potassium chloride salt bridge. The change in the visible and the ultraviolet absorption spectra of the solution in the cathode compartment was measured with a Hitachi EPU-2 spectrophotometer.

RESULTS

In 0.1 M acetate buffer solutions without EDTA, the half-wave potential of hexamminechromium(III) was −0.89 V *vs.* S.C.E.; this shifted to −1.23 V when excess EDTA was added to the solution. This potential was identical with the half-wave potential of the one-electron reduction wave of ethylenediaminetetraacetatochromate-(III), which gave a reversible log-plot under the same condition.

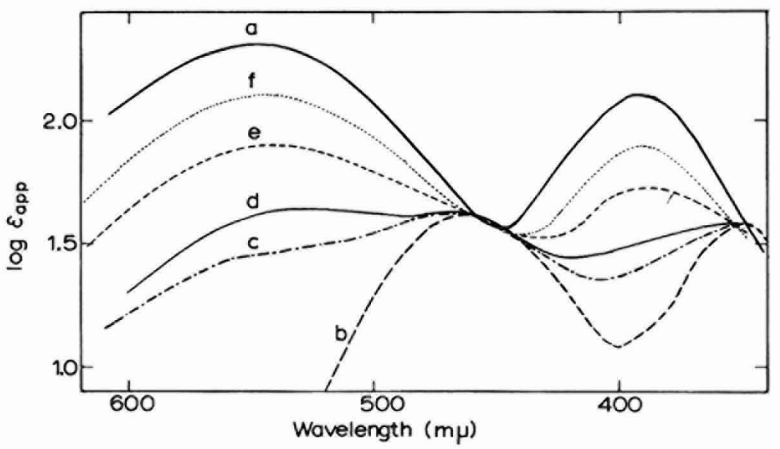

Fig. 1. The absorption spectra of $[CrY(H_2O)]^-$, (a), and those of the solns. subjected to the controlled-potential electrolysis at −1.0 V *vs.* S.C.E. for 0 (b), 25 (c), 50 (d), 105 (e) and 210 min (f). The initial composition of the soln. (pH 4.5) is 3 mM $[Cr(NH_3)_6]Cl_3$, 0.014 M EDTA and 0.1 M acetate buffer. ε_{app} is the apparent extinction coeff. obtained by dividing the optical density by the total chromium concn. and the thickness of the cell.

Electrolysis was carried out in a de-aerated solution containing 3 mM $[Cr(NH_3)_6]Cl_3$, 0.014 M EDTA and 0.1 M acetate buffer solution (pH 4.5) with the mercury pool cathode, the potential of which was set at −1.0 V *vs.* S.C.E. When the circuit was open, the solution did not show any change in the absorption spectra for several hours. During the electrolysis a stream of nitrogen gas was bubbled continuously

through the solution to provide stirring and to exclude atmospheric oxygen. Portions of the solution were taken out at appropriate intervals and the changes in the absorption spectra measured. The spectra obtained 0, 25, 50, 105 and 210 min after the beginning of electrolysis are given in Fig. 1. The spectra of ethylenediaminetetraacetatoaquochromate(III) are also given in Fig. 1.

The effect of EDTA on the one-electron reduction waves of hexaquochromium(III) and hexamminechromium(III) was investigated in acid media. Fig. 2 shows the

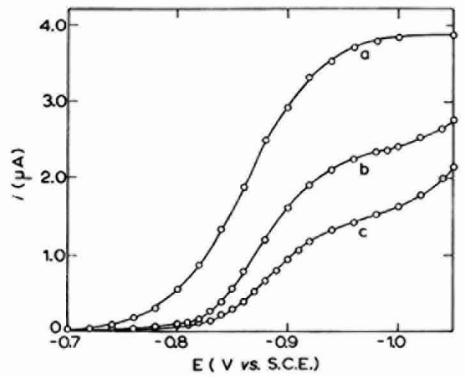

Fig. 2. Current–potential curves of 1.115 mM $[Cr(H_2O)_6]^{3+}$ in the absence (a), and in the presence of 0.48 mM (b), and 0.80 mM (c), EDTA in a soln. containing 0.0115 N $HClO_4$, 0.0885 M $NaClO_4$ and 0.005% gelatin.

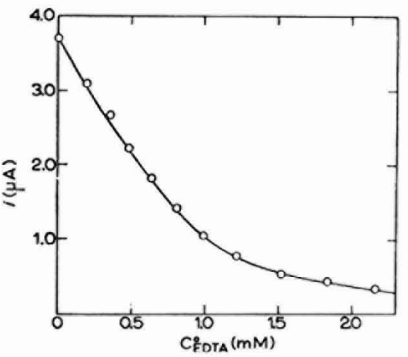

Fig. 3. The effect of EDTA on the current at −0.96 V in a soln. containing 1.115 mM $[Cr(H_2O)_6]^{3+}$, 0.0115 N $HClO_4$, 0.0885 M $NaClO_4$ and 0.005% gelatin.

current–potential curves of 1.115 mM hexaquochromium(III) in solutions containing 0.0115 N $HClO_4$, 0.0885 N $NaClO_4$, 0.005% gelatin and various concentrations of EDTA. As the half-wave potential of the second step was about −1.11 V under these conditions*, a well-defined limiting plateau of the first step was not observed. In Fig. 3 the currents at −0.96 V were plotted against the EDTA concentration. A similar plot was obtained with 0.943 mM hexamminechromium(III) at −0.97 V.

DISCUSSION

Recently PECSOK, SHIELDS AND SCHAEFER[6] reported that the electrode process,

$$[CrY(H_2O)]^{2-} = [CrY(H_2O)]^{-} + e, \qquad (1)$$

where Y^{4-} represents a tetravalent EDTA anion, was reversible and that the redox potential of reaction (1) was −1.227 V *vs.* S.C.E. at ionic strength 0.1 and at 20°. These results agree with those observed in this study.

The spectra given in Fig. 1 show that the apparent extinction coefficients at about 395 mμ and 545 mμ, which correspond to the two absorption maxima of ethylenediaminetetraacetatoaquochromate(III), $[CrY(H_2O)]^{-}$, increase with time. It can also be seen from the spectra in Fig. 1 that all the curves pass near the isosbestic point

* In acid media, the total height of the first and the second steps increased as the EDTA concentration increased; the dependence of the instantaneous current on time and the relation between the mean current and the mercury height showed that the current was kinetic in nature. This effect was more pronounced as the pH of the solution was decreased.

of hexamminechromium(III) and ethylenediaminetetraacetatoaquochromate(III). These observations indicate that the overall reaction occurring during the electrolysis is

$$[Cr(NH_3)_6]^{3+} + Y^{4-} + H_2O \rightarrow [CrY(H_2O)]^- + 6\ NH_3, \qquad (2)$$

namely, that a ligand exchange of hexamminechromium(III) (being a substitution-inert complex) takes place catalytically on the surface of the mercury pool cathode of -1.0 V *vs.* S.C.E.

From this phenomenon and the fact that the presence of excess EDTA shifts the half-wave potential of hexamminechromium(III) to the oxidation–reduction potential of reaction (1), the electrode process of hexamminechromium(III) in solutions containing EDTA can be assumed to be a process similar to that described by LAITINEN AND KIVALO in the case of the reduction of hexamminecobalt(III) in the presence of ethylenediamine[7]. The presence of EDTA does not affect the reduction potential of hexamminechromium(III). The hexamminechromium(II) thus produced, being a labile complex, will undergo substitution with EDTA:

$$[Cr(NH_3)_6]^{2+} + Y^{4-} + H_2O \rightarrow [Cr\,Y(H_2O)]^{2-} + 6\ NH_3 \qquad (3)$$

As long as the potential is sufficiently positive, oxidation of the chromium(II)–EDTA complex takes place, resulting in a net current equal to zero. As the potential becomes negative, oxidation ceases, and a wave with a half-wave potential equal to that of ethylenediaminetetraacetatochromate(III) appears.

The change of current observed upon the addition of EDTA to hexaquochromium-(III) and hexamminechromium(III) in solutions containing 0.0115 *N* acid has been interpreted according to the scheme mentioned above; this can be expressed as

$$O + e \overset{k_c}{\rightarrow} R \qquad (4a)$$

$$R + X \underset{\sigma_b}{\overset{\sigma_f}{\rightleftharpoons}} RX \qquad (4b)$$

$$RX \overset{k_a}{\rightarrow} OX + e \qquad (4c)$$

Here, O, R and X correspond to a tervalent-aquo or -ammine complex, its reduced form and some species of EDTA, respectively. RX and OX correspond to the EDTA complexes of chromium(II) and chromium(III), respectively. In the present case, it may be assumed that the backward rates of electron-transfer reactions (4a) and (4c) are slower than the rate of diffusion, *i.e.*, (4a) and (4c) are irreversible. To derive the quantitative relationship involved in the above processes, a treatment based on the concept of the diffusion layer and the reaction layer[8] is employed. In this treatment, the diffusion and the chemical reactions are dealt with as heterogeneous processes; the parameters such as σ_f and σ_b, which are related to the rates of the chemical reactions, can be considered as products of the usual rate constants for homogeneous chemical reactions and the thickness of the reaction layer. The parameters which are related to the rate of the diffusion, $\mathscr{D}_j$, can be expressed as

$$\mathscr{D}_j = \frac{D_j}{\delta_j} \qquad (5)$$

where D_j and δ_j are the diffusion coefficient and the thickness of the diffusion layer

of the jth species, respectively. In the present case, the amount of a substance that reaches the electrode surface and the amount that leaves it may be considered to be equal, hence the following equations are obtained:

$$\mathscr{D}_O(C_O^0 - C_O) - k_c C_O = 0 \tag{6a}$$
$$(\mathscr{D}_R + \sigma_f C_X)C_R - k_c C_O - \sigma_b C_{RX} = 0 \tag{6b}$$
$$\mathscr{D}_X(C_X^0 - C_X) + \sigma_b C_{RX} - \sigma_f C_X C_R = 0 \tag{6c}$$
$$(\mathscr{D}_{RX} + k_a + \sigma_b)C_{RX} - \sigma_f C_R C_X = 0 \tag{6d}$$

where C_j and C_j^0 denote the concentrations of the jth species at the electrode surface and in the bulk of the solution, respectively. For simplicity, it is assumed that the bulk concentrations of R and RX are negligible.

The current which accompanies the electrode processes (4a)–(4c) is given by

$$i = Fq(k_c C_O - k_a C_{RX}) \tag{7}$$

where q is the surface area of the electrode. From eqns. (6a)–(6d) and (7), the relation

$$\frac{C_X^0 i}{[k_c/(k_c + \mathscr{D}_O)](i_d - i)} = \frac{\mathscr{D}_R}{\sigma_b}\,\frac{k_a + \sigma_b + \mathscr{D}_{RX}}{k_a} + \frac{i}{\mathscr{D}_X Fq} \tag{8}$$

is derived. Here

$$i_d = Fq\mathscr{D}_O C_O^0 \tag{9}$$

If the potential is sufficiently negative so that the rate of the reduction process (4a) is much faster than that of the diffusion process, *i.e.*, $k_c \gg \mathscr{D}_O$, eqn. (8) becomes

$$\frac{C_X^0 i}{i_d - i} = \frac{\mathscr{D}_R}{\sigma_f}\,\frac{k_a + \sigma_b + \mathscr{D}_{RX}}{k_a} + \frac{i}{\mathscr{D}_X Fq} \tag{10}$$

When the left-hand side of eqn. (10) is plotted against i, it is anticipated that a straight line with a slope equal to $1/(Fq\mathscr{D}_X)$ will be obtained. This procedure was performed with the data given in Fig. 3, and the plots of $iC^0_{EDTA}/(i_d - i)$ against i are shown in Fig. 4. Although data for both hexaquochromium(III) and hexammine-

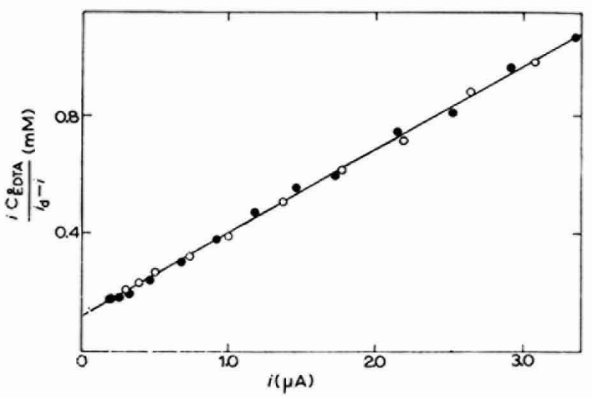

Fig. 4. The dependence of the left-hand side of eqn. (10) against i in a soln. containing 0.0115 N $HClO_4$, 0.0885 M $NaClO_4$, 0.005% gelatin, various EDTA concns. and 1.115 mM $[Cr(H_2O)_6]^{3+}$ (○, at −0.96 V) or 0.943 mM $[Cr(NH_3)_6]^{3+}$ (●, at −0.97 V).

chromium(III) are given in the same figure, most of the points lie close to a single straight line. According to a treatment for more generalized systems[9], this result may be explained by the assumption that, under the present experimental condition, the aquation of hexamminechromium(II) is more rapid than the direct substitution such as reaction (3), and the reaction of chromium(II) with EDTA takes place *via* an aquo-complex.

In the case of a dropping mercury electrode, the thickness of the diffusion layer can be written as

$$\delta_j = \sqrt{\frac{3}{7}\pi D_j t} \tag{11}$$

Taking eqns. (5) and (11) into consideration, the diffusion coefficient of EDTA, D_{EDTA}, obtained from the slope of the straight line in Fig. 4 was 0.66×10^{-5} cm^2 sec^{-1}. In solutions containing 0.0115 N acid, the dissolution wave of mercury accompanied by the formation of a mercury(II)–EDTA complex is not well-defined, while in a 0.1 M acetate buffer solution the wave is well-defined giving the diffusion coefficient of EDTA as 0.67×10^{-5} cm^2 sec^{-1}. The diffusion coefficient of EDTA may depend upon the pH of the solution, but the dependency is not considered to be very great; the value obtained from Fig. 4 seems reasonable.

If the rate of the oxidation reaction (4c) is much faster than the rates of the backward reaction of (4b) and the diffusion, *i.e.*, $k_a \gg \sigma_b$, and $k_a \gg \mathscr{D}_{RX}$, eqn. (8) can be written in the form,

$$\frac{k_c}{k_c + \mathscr{D}_O} = \frac{i}{i_d} + A - \frac{AB}{B + (i/i_d)} \tag{12}$$

where

$$A = Fq\mathscr{D}_X \frac{C_X^0}{i_d} \tag{13a}$$

$$B = Fq \frac{\mathscr{D}_X}{i_d} \frac{\mathscr{D}_R}{\sigma_f} \tag{13b}$$

A comparison of the expressions (13a) and (13b) with eqn. (8) shows that the values of A and B can be obtained from the slope and the intercept of the plot of the left-hand side of eqn. (8) against i. Equation (12) indicates that the relation between $k_c/(k_c+\mathscr{D}_O)$ and i/i_d is hyperbolic with

$$i/i_d = -B \tag{14a}$$

and

$$k_c/(k_c + \mathscr{D}_O) = i/i_d + A \tag{14b}$$

as the two asymptotes. In the absence of EDTA, the value of $k_c/(k_c+\mathscr{D}_O)$ at any potential equals i/i_d. From the current–potential curves shown in Fig. 2, plots of i/i_d against $k_c/(k_c+\mathscr{D}_O)$ were made (see Fig. 5). Solid curves in Fig. 5 are theoretical curves calculated from eqn. (12) using the values of A and B obtained from the straight line in Fig. 4, which is a result of measurements at a constant potential with various concentrations of EDTA. The experimental results obtained at a constant EDTA concentration at various potentials are in a good agreement with these solid curves.

It can be concluded from this that, in the presence of EDTA, the current given by the tervalent-aquo or -ammine complex in the potential region between its reduction potential and the oxidation–reduction potential of chromium(II)- and chromium(III)-EDTA complexes is dependent upon the rate at which chromium(II) combines with EDTA.

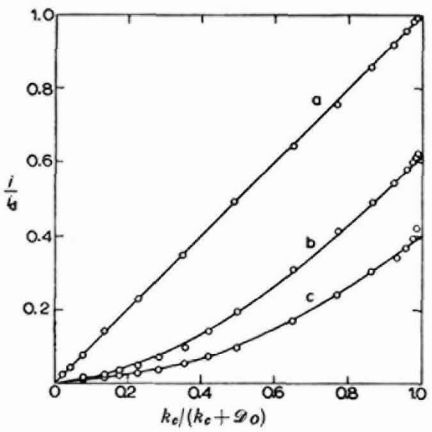

Fig. 5. The variation of i/i_d with $k_c/(k_c+\mathcal{Q}_O)$ in the absence (a), and in the presence of 0.48 mM (b), and 0.80 mM (c), EDTA. Solid curves are theoretical curves obtained from eqn. (12).

ACKNOWLEDGEMENTS

We thank Dr. R. TAMAMUSHI and Dr. G. SATÔ for their helpful advice.

SUMMARY

The effect of ethylenediaminetetraacetate (EDTA) on the one-electron reduction process of hexamminechromium(III) and hexaquochromium(III) at the dropping mercury electrode has been investigated in acid media. In the presence of EDTA, chromium(II) produced by the reduction reacts with EDTA to form a Cr(II)–EDTA complex. As long as the potential is sufficiently positive, this complex is oxidized at the electrode, and a current dependent on the rate at which chromium(II) combines with EDTA is observed.

REFERENCES

1 N. TANAKA AND G. SATÔ, *Nature*, 197 (1963) 176.
2 N. TANAKA, K. EBATA AND G. SATÔ, *Bull. Chem. Soc. Japan*, 36 (1963) 912.
3 M. MORI, *J. Chem. Soc. Japan, Pure Chem. Sect.* (*Nippon Kagaku Zasshi*), 74 (1953) 253.
4 I. M. KOLTHOFF AND J. J. LINGANE, *Polarography*, Interscience Publishers, New York, 1952, p. 455.
5 N. TANAKA, K. KATO AND R. TAMAMUSHI, *Bull. Chem. Soc. Japan*, 31 (1958) 283.
6 R. L. PECSOK, L. D. SHIELDS AND W. P. SCHAEFER, *Inorg. Chem.*, 3 (1964) 114.
7 H. A. LAITINEN AND P. KIVALO, *J. Am. Chem. Soc.*, 75 (1953) 2198.
8 N. TANAKA AND R. TAMAMUSHI, *Proceedings of the 1st International Polarographic Congress, Prague, Part I*, 1951, p. 486.
9 K. EBATA, unpublished.

ANODIC BEHAVIOR OF PLATINUM ELECTRODES IN OXYGEN-SATURATED ACID SOLUTIONS

W. VISSCHER* AND M. A. V. DEVANATHAN

The Electrochemistry Laboratory, The University of Pennsylvania, Philadelphia 4, Pennsylvania (U.S.A.)

(Received May 1st, 1964)

INTRODUCTION

Platinum is known to exhibit a wide variety of anodic potentials; the kinds of potentials depend on whether or not the Pt metal is actively involved in the electrode reaction. This permits a classification into three groups. (1) Dipole potential; in O_2-saturated acid solutions a Pt electrode behaves as a perfectly polarizable electrode. (2) Oxide potential; an electrode reaction is set up which involves Pt and Pt oxides and its behavior is essentially that of a non-polarizable electrode. (3) Redox potential; the treated Pt electrode can also behave as a non-polarizable electrode where Pt and Pt oxides act as catalysts, *e.g.*, in the anodic oxidation of H_2O.

The anodic behavior of Pt is strongly influenced by the pre-treatment of the electrode. By varying the conditions of the pre-treatment it is possible to separate the individual electrode reactions. For example it is possible to establish the reversible O_2 electrode, on a Pt oxide surface.

Because of the apparent importance of the type of oxide surface, the oxygen content of a Pt electrode in the presence of O_2 was measured by cathodic transients, as a function of the anodic potential.

EXPERIMENTAL

Experimental technique

The experiments were carried out in a cell consisting of three compartments; a detailed description of this cell and the technique used is given by BOCKRIS AND HUQ[1] and by WATANABE AND DEVANATHAN[2].

The preparation of the electrodes (Pt) and the solution (0.1 *N* H_2SO_4) was as follows:

1. *Electrodes.* Smooth Pt foils of area 2 cm^2, were spot-welded to Pt wire which was sealed in pyrex-glass supports. They were cleaned by successive washings with hot chromic sulfuric acid, concentrated sulfuric acid, dilute nitric acid and then thoroughly rinsed with conductivity water.

The electrodes were adjusted in the cap of the cell, washed again with conductivity

* Present address: Technische Hogeschool, Eindhoven, The Netherlands.

water and then anodically oxidized for 30–60 min at a current density of 1 mA/cm².

2. *Sulfuric acid.* Analytical reagent-grade sulfuric acid was introduced in the cell, containing redistilled conductivity water. The required concentration was measured with a conductivity bridge. Anodic pre-electrolysis was carried out for 20 h. This solution was used for the measurement of the open circuit potentials.

For polarization measurements (Tafel line) the following procedure was followed. A few drops of hydrogen peroxide were added to 25 ml of analytical reagent-grade sulphuric acid. The solution was then warmed gently to decompose excess H_2O_2. This acid was used to prepare 0.1 N H_2SO_4 as described above. Anodic pre-electrolysis was then carried out in some cases, but this did not appreciably alter the polarization behavior. All experiments were carried out in an atmosphere of purified oxygen.

Electrical measurements

1. *Reference electrode.* All potentials were measured against the hydrogen electrode in the same solution.

2. *Tafel measurements.* The set-up used for the polarization measurements was the usual type of galvanostatic circuit; the potentials were measured with a Doran valve potentiometer (± 0.001 V).

3. *Open circuit potential.* The open circuit potential of Pt electrodes was measured in 0.1 N H_2SO_4 solutions which were purified only by anodic pre-electrolysis, without H_2O_2-treatment of the sulfuric acid.

4. *Oxygen coverage transients.* For the determination of the coverage with oxygen, the following electrical circuit was used (Fig. 1). The electrode potential was kept

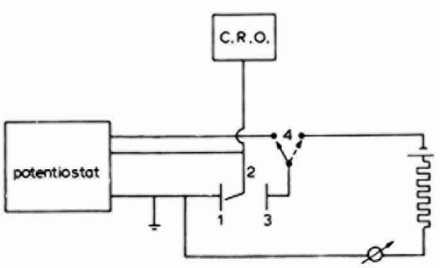

Fig. 1. Electrical circuit: (1), test electrode; (2), reference electrode; (3), counter electrode; (4), switch.

at the required anodic value with a Wenking potentiostat for 10–15 min in order to ensure the attainment of steady state. By means of a high-speed mercury relay device[3], the potentiostatic control was cut off and a cathodic galvanostatic current was imposed within 10 μsec on the electrode. The potential–time behavior was followed on a Tektronix oscilloscope (Type 531A). Photographic records were made of the oscilloscope screen with a Polaroid camera. Several cathodic current densities in the range 10–500 mA were examined[4,5]. A current of 100 mA/cm² was selected as the most suitable current density, for all subsequent transients.

5. *Capacity measurements.* To measure the true area, the capacity of the Pt electrode was determined in 0.5 M Na_2SO_4 in a helium atmosphere by two methods. (I) Galva-

nostatic pulse method: after the electrode had reached its rest potential, a cathodic or anodic pulse was applied; the initial slope of the transient was used to calculate the capacity. (2) A.c. bridge method: a Wayne-Kerr Universal impedance bridge was used to measure the capacity directly at a frequency of 1592 c/sec.

RESULTS AND CALCULATIONS

1. *Tafel line*

The slope of the potential–log current density line was 0.113 ($\pm$ 0.004) V, the exchange current, i_0, being equal to $(2.5 \pm 1.4) \cdot 10^{-10}$ A/cm² (Fig. 2). Two kinds of anomalous behavior were observed (Figs. 2 and 3):

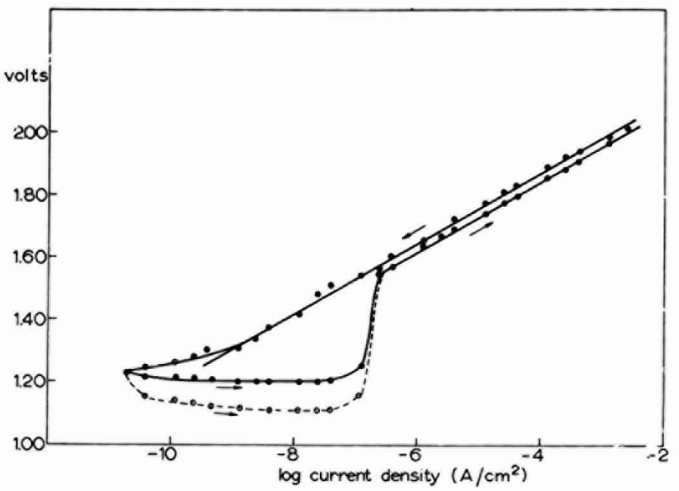

Fig. 2. Tafel line: slope, 0.115; $i_0 = 2.5 \times 10^{-10}$ A/cm².

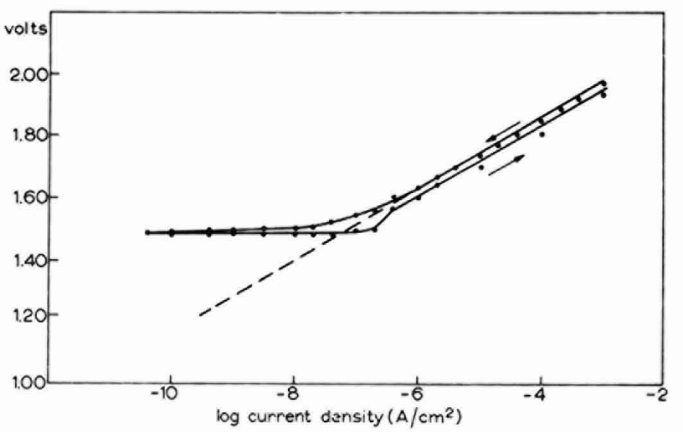

Fig. 3. Tafel line: slope, 0.115.

(a) When measuring the "up" Tafel line with increasing current, the potential did not change between 10^{-10} A/cm^2 and about 10^{-6} A/cm^2; with further increase in current density it rapidly attained the Tafel value. In this lower current density region the potential tends to decrease with time.

(b) With some electrodes the descending Tafel line sometimes flattens out at a potential of 1.48 V.

2. Open circuit potential

The following open circuit potentials were observed depending on the pre-treatment of the electrode:

Pre-treatment	*Potential (V)*	*Solution*
None	0.8 — 1.0	No purification
None	0.98 ± 0.03	Purified by anodic pre-electrolysis.
Anodically oxidized	1.13 ± 0.05	Purified by anodic pre-electrolysis.
	1.48 ± 0.04	Purified by anodic pre-electrolysis.
Anodically oxidized, then raised above the solution in O_2 atmosphere (20 h) (WATANABE AND DEVANATHAN[2])	1.243 ± 0.016	Purified by anodic pre-electrolysis.
As above with platinized platinum	1.235 ± 0.014	Purified by anodic pre-electrolysis.

3. Time dependence

The open circuit behavior was followed after the electrode was kept at a constant potential of 1.8 and 1.6 V respectively. In Fig. 4 V is plotted as function of log t. The initial slope is 0.1 V.

4. Cathodic transient measurements

A typical cathodic transient is shown in Fig. 5. After a steep drop of the potential

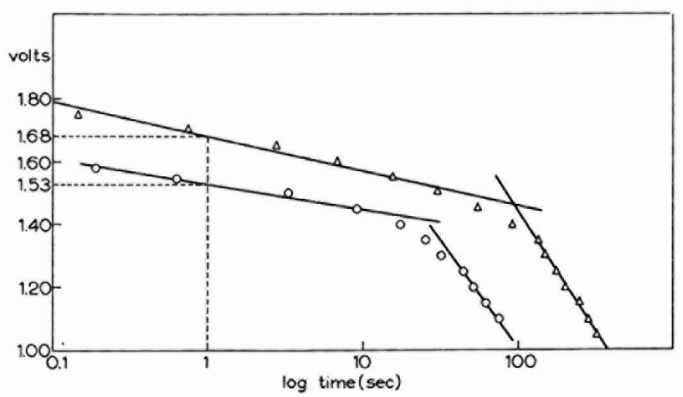

Fig. 4. Decay curve: △, starting at 1.8 V; ○, starting at 1.6 V.

A-B, to around 0.8 V, a gently sloping section, B-C, is observed, the length of which depends on the initial potential. An inflection is perceptible at D corresponding to a potential of 0.3 V after which the potential drops to hydrogen evolution. This value of 0.3 V is identical with the potential at which hydrogen adsorption starts. This is

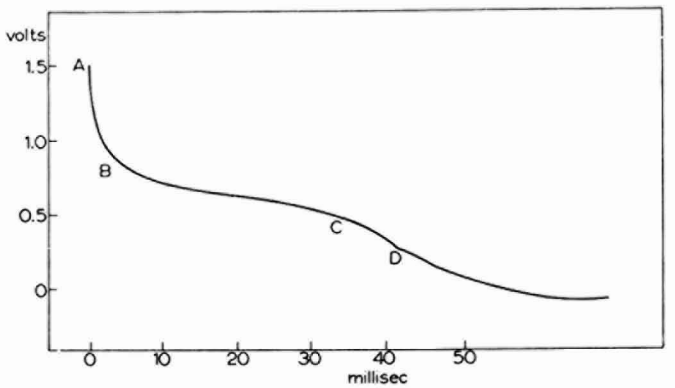

Fig. 5. Typical cathodic transient, i_{cath} = 100 mA/cm².

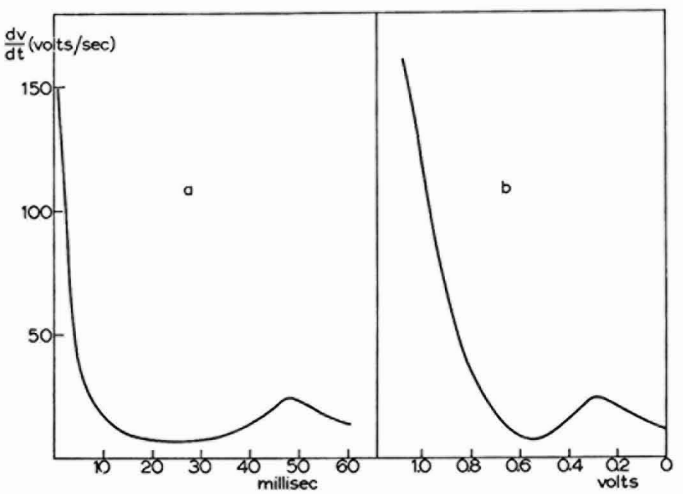

Fig. 6. (a), dV/dt as a function of time; (b), dV/dt as a function of voltage, $V_{t=0}$ = 1.6 V; i_c = 100 mA/cm².

clearly shown in Fig. 6 in which dV/dt is plotted as a function of time and as a function of voltage. The inflection point of the V–t curve appears in this graph as a maximum at 0.3 V.

Q was calculated by taking dV/dt at different values of V. The initial slope of the V–t curve gives $C_{\text{Double Layer}}$. The double-layer charging current was calculated ac-

cording to

$$i_{(DL)_V} = C_{(DL)_V} \times \left(\frac{dV}{dt}\right)_V \tag{1}$$

Assuming C_{DL} is independent of V, the contribution of the double layer for each point on the V–t curve was obtained. Thus

$$i_F = i_{total} - i_{Double\ Layer} \tag{2}$$

Below 0.3 V:

$$i_F = i_{total} - i_{DL} - i_{H_{ads}} \tag{3}$$

$i_{H_{ads}}$ was obtained in an analogous manner from the anodic transient. The area under the curve i_F *vs.* t, Q, was then computed. Since $Q_{DL} \ll Q_F$, this rather elaborate method was unnecessary. It was sufficient to take $Q = i \times t$, with t = time required to reach

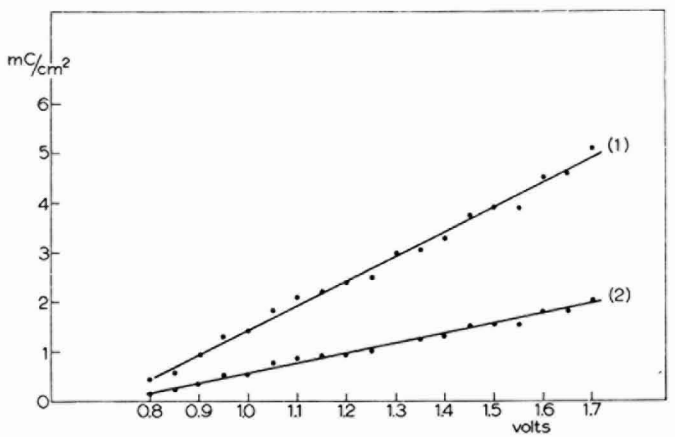

Fig. 7. The number of coulombs required for the dissolution of the oxide film as a function of the steady state applied potential: (1), calculated without roughness factor; (2), calculated with roughness factor (2.5).

0.3 V. A precision of 5% was achieved. The number of coulombs required for the dissolution of the oxide film is plotted as a function of the steady-state applied potential and is shown in Fig. 7. A linear relationship appears to exist between Q and V. The reproducibility was 10%.

5. Roughness factor

A value of 39 μF/cm² was obtained for the capacity at 0.45 V with both anodic or cathodic pulses of 10 mA/cm². The capacity measured in the same solution with the Wayne Kerr universal A-C bridge gave $C = 39.5\ \mu$F/cm².

Taking 16 μF/cm² as the capacity of the double layer, the roughness factor of our electrode was therefore 2.5.

DISCUSSION

1. *Open circuit behavior*

The oxygen evolution reaction is essentially a redox process in which the substrate plays the role of a catalyst. However, as the table given below shows, there are several thermodynamic potentials for the Pt–Pt oxide couple which lie in the vicinity of the H_2O–O_2 potential.

	Volts		*Ref.*
(a) $H_2O_2 \rightleftharpoons O_2 + 2\,H^+ + 2\,e$	0.682		(6)
(b)	0.84	$Pt + H_2O \rightleftharpoons PtOH + H^+ + e$	(7)
(c)	0.98	$Pt + 2\,H_2O \rightleftharpoons Pt(OH)_2 + 2\,H^+ + 2\,e$	(6)
(d)	1.1	$Pt(OH)_2 \rightleftharpoons PtO_2 + 2H^+ + 2\,e$	(6)
(e) $2\,H_2O \rightleftharpoons O_2 + 4\,H^+ + 4\,e$	1.229		(6)
(f)	1.5	$PtO_2 + H_2O \rightleftharpoons PtO_3 + 2\,H^+ + 2\,e$	(8)
(g) $2\,H_2O \rightleftharpoons H_2O_2 + 2\,H^+ + 2\,e$	1.77		(6)

These reactions of the Pt oxides can have appreciable exchange currents.

In order to observe the H_2O–O_2 potential (reaction (e)) it is necessary to suppress the exchange currents of these reactions to below the exchange current of the H_2O–O_2 reaction. Thus the potentials which can be observed are critically dependent on the nature of the oxide surface. The variety of potentials reported in the literature is an indication of the difficulty of reproducing electrode surfaces in a suitable, catalytically active form. This is also clearly shown by the fact that only a slight change in the treatment (prolonged exposure to O_2 gas after anodic oxidation) results in the attainment of the reversible O_2–H_2O potential. An explanation can now be given for the behavior of Pt electrodes in acid solution.

Platinum chemisorbs oxygen to an extent depending on the O_2 partial pressure in the solution. This film of chemisorbed oxygen however can subsequently hydrolyze according to

$$Pt\text{–}O + H_2O \rightarrow Pt(OH)_2.$$

In a purified solution a potential of 0.98 V corresponding to reaction (c) is thus found. Only anodic oxidation results in a higher oxide (reaction (d), and sometimes reaction (f)).

In the presence of reducing impurities (*e.g.*, SO_2, H_2), the potential decays from 0.98 V to 0.84 V. The mechanism appears to be oxidation of the impurities coupled with the reduction of $Pt(OH)_2$ *e.g.*,

$$SO_3^{2-} + H_2O \rightleftharpoons SO_4^{2-} + 2\,H^+ + 2\,e$$

$$Pt(OH)_2 + H^+ + e \rightleftharpoons Pt(OH) + H_2O$$

This mechanism gives an explanation for the erratic time dependence and stirring effects. The PtOH/Pt sets up a potential according to reaction (b). It is noted that the anodic oxidation of platinum likewise starts around 0.8 V even at high current densities, both in O_2-containing and O_2-free solutions. VETTER AND BERNDT[9] found that the potential at which the anodic oxidation starts, depends on the pH (59 mV/pH)

as predicted by eqn. (b). BOCKRIS AND OLDFIELD[7] have shown reaction (b) to be independent of O_2 partial pressure. These facts are consistent with eqn. (b) being the first step in the anodic oxidation process with a high exchange current.

2. Tafel line

The Tafel-(b)-parameter is in good agreement with the theoretically expected value. The degree of purification of the solution does not seem to be so critically important for the slope of the Tafel line (see also CONWAY[10]) as the pre-treatment of the electrode. Heat treatment as used by BOCKRIS AND HUQ[1] (heating in O_2 at 500°) resulted in a lower value (0.097 ± 0.009). The efficacy of cathodic pre-electrolysis as reported by BOCKRIS AND HUQ appears to be connected with the formation of H_2O_2 which oxidizes SO_2 and other reducing substances. Cathodic pre-electrolysis was eliminated by oxidation with H_2O_2.

The flattening out at the high value of 1.48 V, observed in some cases in the polarization measurements, is most probably due to potential control by platinum oxide, PtO_3, (reaction (f); compare levelling off of Tafel lines in hydrogen evolution reaction on corroding metals).

The anomalous behavior of the upward polarization curve could also be attributed to a determination of the potential by reaction (d) or (c). This interference is very likely as the i_0 of the oxygen evolution is about 10^{-10} A/cm^2. A current density of 10^{-10}–10^{-8} A/cm^2 does not differ greatly from open circuit conditions.

3. Decay curves

ARMSTRONG AND BUTLER[11] derived the following expression for the discharge of the double-layer capacity

$$\frac{\mathrm{d}V}{\mathrm{d}\log t} = \frac{RT}{\alpha n F} = 0.1 \qquad (4)$$

The observed slope is in agreement with eqn. (4).

The interesting fact in Fig. 4 is that this relationship does not hold below a potential of 1.4 V. It is at this potential that the Pt oxide reaction (f) starts to interfere. (Compare anomalous behavior observed in Tafel line.)

Beyond 1.45 V the slope of $\mathrm{d}V/\mathrm{d}\log t$ will therefore greatly depend on the nature of the surface.

4. Oxygen coverage

For the oxygen evolution reaction it is known[1] that the rate-determining step is discharge of H_2O (or OH^- in alkaline solution). To evaluate the subsequent step, it is necessary to know the coverage with oxygen. The apparent amount of "oxide" measured in a cathodic transient consists of oxygen attached to the electrode and oxygen diffusing to the electrode from the solution. In order to reduce errors due to the latter it was necessary to use a current density as high as possible. The amount of oxygen was found to be practically constant beyond 50 mA[12]. The high values below 50 mA indicate re-adsorption of oxygen. An oxygen concentration of 10^{-4} mole/l would correspond to a diffusion-current of $i_D = nFD\,(C/\delta)$. With $D = 10^{-5}$ cm^2 sec^{-1}

this corresponds to a diffusion current of the order 10^{-4} A/cm^2. As our values indicate a coverage which goes beyond a mono-layer (1 mono-layer of oxygen corresponds to about 500 μC/cm^2) it is not possible to draw any conclusions concerning a subsequent course in the evolution reaction.

A linear dependence of the coverage with voltage was also found by BECKER AND BREITER[13] and by LAITINEN AND ENKE[14]. The values in this paper are, however, considerably higher. The experiments of BECKER AND BREITER were carried out in hydrogen atmosphere. It is known that molecular hydrogen is capable of reducing oxides or inhibiting the formation of oxides, which could account for the difference. LAITINEN AND ENKE obtained their values in N_2 atmosphere, but they allowed only one minute to elapse before switching on the cathodic current.

There are two different points of view regarding the coverage with oxygen. One is that the oxygen forms a chemisorbed layer. BECKER AND BREITER[13] conclude that at 1.4 V a "mono-atomic" layer exists. More "layers" are assumed to grow continuously at higher potentials. The other idea is that definite phase oxide formation takes place. Evidence for this is (a) the slight inflection in the anodic transients observed at low current densities by EL WAKKAD AND EMARA[15]; (b) the chemical detection of PtO_2 and PtO by ANSON AND LINGANE[16]. The high values that we have obtained are consistent with the hypothesis that phase-oxide formation takes place.

5. *Phase oxide growth*

A growth of phase oxide on platinum can only take place by anodic polarization. Chemisorption of oxygen leads to $Pt(OH)_2$ as shown above. The potential therefore does not exceed 0.98 V. In a galvanostatic charging experiment (current density 100 μA/cm^2) the potential, after a nearly linear rise, flattens out at a potential approximately 100 mV below the final steady-state value (1.8 V). A long time was required to cover the last 100 mV (3 h). However, under potentiostatic conditions, 10–15 min was considered long enough to attain steady state. During this last 100 mV change, most of the current goes for O_2 evolution; only a small fraction is used for oxide growth as a parallel reaction.

The amount of electricity measured in the cathodic transient gives the oxide present per unit area. This however does not necessarily mean that this oxide uniformly covers the total electrode area. It is far more likely that only on certain area of the first layer the oxide growth starts. The oxygen evolution reaction will take place mostly on those sites which are not involved in the oxide growth. In other words, if this model is assumed, the thickness of the oxide must then exceed several monolayers. A similar explanation was put forward by HOAR[17] for the slow attainment of the reversible H_2O–O_2 potential under potentiostatic conditions.

6. *Mechanism of oxide growth*

The growth of oxide films can be rate-controlled at the metal–film interface or within the oxide itself. For very thin films CABRERA AND MOTT[18] consider the rate of entry of metal ions into the film as the rate-determining step.

Under the influence of an electric field, E, this process is accelerated.

Thus:

$$\vec{i} \sim \frac{dX}{dt} = n\nu(Z' - n') \exp - [(W_1 - zaE)/kT] \tag{5}$$

where n = number of metal ions per cm^2;
$Z' - n'$ = available sites for the metal ion in the oxide per cm^2;
ν = frequency factor;
W_1 = activation energy metal–film;
z = valency;
a = activation distance;
k = Boltzmann constant;
T = absolute temperature;
E = electric field = V/X;
X = thickness.

In a strong electric field the movement of the ions will be in one direction only (CABRERA AND MOTT). A limiting thickness was then derived by assuming the growth rate is virtually zero if

$$\frac{dX}{dt} = 10^{-13} \text{ cm sec}^{-1}$$

A diagram of the energy barriers is shown in Fig. 8.

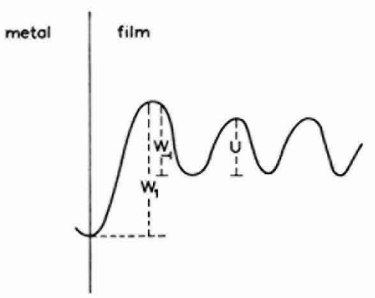

Fig. 8. Diagram of the energy barriers: W, activation energy metal–film; U, diffusion activation energy.

Whether the reverse current can be neglected or not, will depend on the energy level in the metal and the energy level in the metal oxide.

The Pt oxide film will be both ion- and electron-conducting so that the field here can be taken to be small. Therefore the reverse current should also be taken into account, for which we write

$$\overleftarrow{i} \sim n'\nu'(Z - n) \exp - [(W_{-1} + zaE)/kT] \tag{6}$$

where n' = number of mobile metal ions per cm^2;
$Z - n$ = sites available in the metal per cm^2.

The steady state at any fixed value of V is thus reached when

$$\vec{i} = \overleftarrow{i} \tag{7}$$

Hence

$$n\nu(Z' - n') \exp - \frac{(W_1 - zaE)}{kT} = n'\nu'(Z - n) \exp - \frac{(W_{-1} + zaE)}{kT} \tag{8}$$

and thus with $E = V/X$, a limiting thickness is given by

$$\frac{X}{V} = \frac{2\,za}{W_1 - W_{-1} - kT \cdot \log \dfrac{n\nu(Z' - n')}{n'\nu'(Z - n')}} \tag{9}$$

Substituting in formula (9) for the migrating Pt ions, $z = 2$, and taking $a = 2.5 \times 10^{-8}$ cm (a plausible value)

$$\frac{X}{V} = \frac{10 \cdot 10^{-8}}{W_1 - W_{-1} - kT \log \dfrac{n\nu(Z' - n')}{n'\nu'(Z - n)}} \frac{\text{cm}}{\text{volt}} \tag{10}$$

It was found experimentally

$$\frac{Q}{V} = 5 \text{ mC/V} \tag{11}$$

or taking into account the roughness factor of 2.5

$$\frac{Q}{V} = 2 \text{ mC/V} \tag{12}$$

For the conversion of Q into thickness, a value of 500 μC/cm^2 is taken for a monolayer of oxygen, with a thickness of 2.8×10^{-8} cm (radius $O^{2-} = 1.40 \times 10^{-8}$ cm). It follows that,

$$\frac{X}{V} = 11.10^{-8} \text{ cm/V} \tag{13}$$

Neglecting the log term in eqn. (10), would give a value of the order of 10×10^{-8} cm/V for X/V if $(W_1 - W_{-1})$ is taken as 1 eV which is a very probable value. The fair agreement with the experimental value shows that this model of oxide growth is not unreasonable. In this derivation it is assumed that the oxide does not chemically dissolve to any appreciable extent.

Whether or not definite oxide formation and growth occurs, is a question which cannot be unequivocally decided by chronopotentiometric measurements, as this technique cannot discriminate between oxide and chemisorbed (or adsorbed) oxygen.

The presence of an oxide film and its thickness can also be determined by studying *in situ* the polarization state of reflected light[19,20] with a thin-film ellipsometer. In outline the method was as follows.

The potential of a Pt mirror was maintained with a potentiostat. It was observed that the polarization state of the reflected light up to a potential of 1.0 V remained

the same as that at 0.3 V at which potential there is no surface film. The change observed above this potential showed independently that a film was formed above 0.98 V, as discussed earlier.

ACKNOWLEDGEMENTS

We thank Professor J. O'M. BOCKRIS, Dr. A. K. N. REDDY, Dr. N. WATANABE and Dr. BHASKARA RAO for valuable discussions. One of us (W. V.) wishes to thank the Council of the Technische Hogeschool of Eindhoven for leave of absence. This project was supported by the United States Air Force under Contract No. AF 33(616)-8150.

SUMMARY

The anodic behavior of Pt electrodes in O_2-saturated sulfuric acid solution is shown to be critically dependent on the treatment of the electrode. The open circuit potentials, 1.48, 1.13 and 0.98 V, observed in purified solution, are related to the thermodynamic platinum-oxide potentials. The erratic behavior of Pt electrodes in non-purified solutions is also explained.

The thermodynamic value of 1.23 V for the H_2O–O_2 reaction was obtained when certain conditions were fulfilled. The Tafel (b) parameter for the anodic oxygen evolution reaction was 0.113, and $i_0 = 2.5 \times 10^{-10}$ A/cm^2. Chemisorption of oxygen leads to a dipole potential of 0.98 V. An oxide film is produced by anodic oxidation. This was confirmed by an optical method (thin film ellipsometer) which showed that the growth of a film commences only above 1 V.

Cathodic transient technique was used to measure the oxygen coverage (Q) of the Pt electrode as a function of the applied potentiostatic voltage (V). A linear relationship between Q and V was found. This relationship, $Q = f(V)$, is explained on the basis of a modified Cabrera–Mott model. The evidence suggests that growth takes place on certain sites of the first layer only.

REFERENCES

1 J. O'M. BOCKRIS AND A. K. M. S. HUQ, *Proc. Roy. Soc. London, Ser. A*, 237 (1956) 277.
2 N. WATANABE AND M. A. V. DEVANATHAN, *J. Electrochem. Soc.*, 111 (1964) 615.
3 W. MEHL, M. A. V. DEVANATHAN AND J. O'M. BOCKRIS, *Rev. Sci. Instr.*, 29 (1958) 180.
4 M. A. V. DEVANATHAN AND M. SELVARATNAM, *Trans. Faraday Soc.*, 56 (1960) 1820.
5 M. A. V. DEVANATHAN, J. O'M. BOCKRIS AND W. MEHL, *J. Electroanal. Chem.*, 1 (1959/1960) 143.
6 W. M. LATIMER, *The Oxidation States of the Elements and their Potentials in Aqueous Solution*, 2nd ed., Prentice-Hall, New York, 1956.
7 J. O'M. BOCKRIS AND L. F. OLDFIELD, *Trans. Faraday Soc.*, 51 (1955) 249.
8 J. GINER, *Z. Electrochem.*, 63 (1959) 386.
9 K. J. VETTER AND D. BERNDT, *Z. Electrochem.*, 62 (1958) 378.
10 J. J. MACDONALD AND B. E. CONWAY, *Proc. Roy. Soc. London, Ser. A*, 269 (1962) 419.
11 G. ARMSTRONG AND J. A. V. BUTLER, *Trans. Faraday Soc.*, 29 (1933) 1261.
12 BHASKARA RAO AND M. A. V. DEVANATHAN, to be published.
13 M. BECKER AND M. BREITER, *Z. Electrochem.*, 60 (1956) 1080.
14 H. A. LAITINEN AND G. C. ENKE, *J. Electrochem. Soc.*, 107 (1960) 773.
15 S. E. S. EL WAKKAD AND S. H. EMARA, *J. Chem. Soc.*, (1952) 461.
16 F. C. ANSON AND J. J. LINGANE, *J. Am. Chem. Soc.*, 79 (1957) 4901.
17 T. P. HOAR, *Proc. Roy. Soc. London, Ser. A*, 142 (1933) 628.
18 N. CABRERA AND N. F. MOTT, *Rep. Progr. Phys.*, 12 (1948–1949) 163.
19. A. B. WINTERBOTTOM, *Z. Electrochem.*, 61 (1958) 811.
20 A. K. N. REDDY AND M. A. V. DEVANATHAN, to be published.

POTENTIOMETRIC ACID–BASE TITRATIONS IN MOLTEN SALTS

THE APPLICATION OF THE PRINCIPLE OF BIMETALLIC ELECTRODES FOR THE DETERMINATION OF EQUIVALENCE POINTS

A. M. SHAMS EL DIN AND A. A. EL HOSARY

Laboratory of Electrochemistry and Corrosion, National Research Centre, Dokki, Cairo (U.A.R.)

Dedicated to Prof. I. M. KOLTHOFF on the occasion of his 70th birthday

(Received March 23rd, 1964)

INTRODUCTION

The tracing of a potentiometric titration curve is based upon the measurement of the variation of the potential of a suitable indicator electrode relative to that of a reference electrode. The realization of such an arrangement in melts operated at relatively low temperatures has been recently established[1–5]. At temperatures higher than 900°, and/or in glass or refractory corroding melts, the development of reference electrodes offers considerable technical difficulties.

Recently we applied the Cu/CuO electrode as indicator electrode in the potentiometric determination of the acid $K_2Cr_2O_7$ in molten KNO_3[6]. At the theoretically calculated equivalence points, sharp potential drops of *ca.* 600 mV were measured relative to a Ag/Ag(I) reference electrode. Comparison of the titration curves obtained with the Cu/CuO electrode with those traced with an oxygen (Pt) electrode under the same experimental conditions[6,7] showed that the former type of electrode registered potentials which were *ca.* 35 mV more negative than those obtained with the oxygen electrode. This was related to differences in the E^0 values of the two electrodes. This fact aroused our interest and we were encouraged to try other metallic electrodes as indicator electrodes in potentiometric acid–base titrations in melts and to investigate the possibility of applying the principle of bimetallic electrodes for the determination of equivalence points. Different metals would be expected to function as oxygen electrodes of different E^0 values. Also, the potential drop at an equivalence point would vary from one particular indicator electrode to the other. Thus, when the potential difference between two such indicator electrodes is measured, potentiometric titration curves could be constructed which would exhibit distinct inflexions at the equivalence points. The apparent advantage of this technique is that no reference electrode is needed for tracing these titration curves. The principle of potentiometric titrations with bimetallic electrodes has been developed for redox titrations in aqueous media, but, as far as we are aware, it has not been applied to acid–base titrations.

EXPERIMENTAL

Potentiometric titrations were conducted in molten KNO_3 at 350°. The salt was dehydrated by bubbling pure dry oxygen through the melt for 1 h[7]. The titration

assembly has been described previously in detail [4,7-10]. The titration vessel contained two indicator electrodes, one of which, unless otherwise stated, was an oxygen (Pt) electrode. The potential of both electrodes was measured, alternatively, relative to that of a Ag/Ag(I)/glass reference electrode[8]. The potential difference between the two indicator electrodes was noted on a second potentiometer. All potentials were found to establish rather quickly (5–8 min after each peroxide addition) and were reproducible to better than ±20 mV. The following indicator electrode combinations were examined: O_2–Ag, O_2–Cu, O_2–Fe, O_2–W, O_2–Ni, Pt–Ag.

RESULTS AND DISCUSSION

The feasibility of silver, copper, iron, nickel and tungsten electrodes as indicator electrodes for potentiometric acid–base titrations in molten KNO_3 at 350° was established by titrating the acid $K_2Cr_2O_7$ with Na_2O_2[7]. Examples for the titration curves are depicted in Figs. 1 and 2 for the electrode combinations O_2–Ag and O_2–Fe. The curves with open circles are titration curves constructed by measuring the potential of the oxygen (Pt) electrode relative to that of the reference electrode. The curves with the black circles show the variation of the potential of either the silver or iron electrode during the progress of the neutralization reaction. It can be seen from the curves of Figs. 1 and 2, and from similar curves obtained with copper, nickel, and tungsten electrodes, that normal potentiometric titration curves characterized by distinct potential drops at the equivalence points were obtained. It is

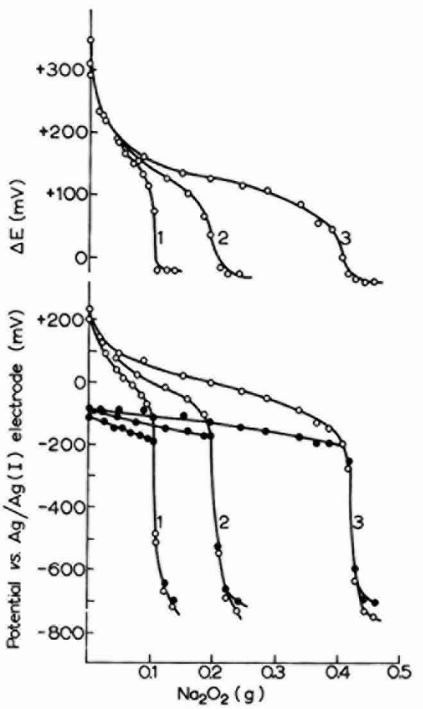

Fig. 1. Titration of the acid $K_2Cr_2O_7$ with Na_2O_2 in molten KNO_3 at 350° (1), 0.400; (2), 0.750; (3), 1.500 g acid. ○, O_2 electrode; ●, Ag electrode. Upper curves, O_2–Ag combination.

reasonable to assume that other metallic electrodes would behave similarly. The average error in the determination of known amounts of the acid was comparable to that obtained with the oxygen electrode[7]. Consideration of the potentials established by the different electrodes along the upper branch of the titration curves revealed that they were invariably more negative than those for the oxygen electrode. Similarly, the potential drops at the inflexion points of the titration curves depended upon the particular indicator electrode used. Average values were: O_2, 600; Ag, 500; Ni, 600; W, 700; Fe (fresh), 550; Fe (aged in the melt), 600; mV, respectively. Apparently both effects are related to the fact that the E^0 values of these electrodes (as oxygen electrodes) are different.

The various indicator electrodes were affected differently by fused KNO_3. Both the silver and the tungsten electrodes were polished by the melt. The iron, nickel and copper electrodes were covered, however, by dark oxides. The thickening of the brown oxide on the iron electrode upon prolonged exposure to the nitrate melt eliminated the difference in potentials between this electrode and the oxygen electrode (Fig. 2, curve B). The electrode could be reactivated by polishing with emery paper before immersion into the melt (Fig. 2, curves A).

The upper curves of Figs. 1 and 2 were obtained by measuring the potential difference, ΔE, between the oxygen electrode and the other indicator electrode. Here,

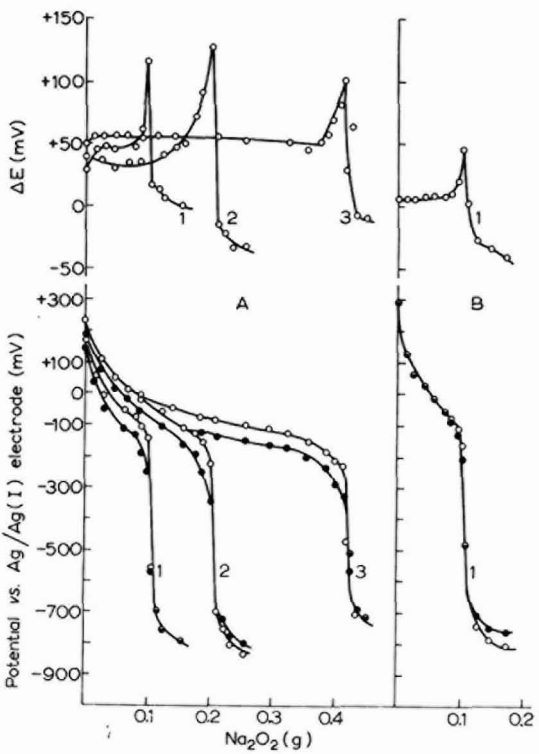

Fig. 2. Titration of the acid $K_2Cr_2O_7$ with Na_2O_2 in molten KNO_3 at 350°. (1), 0.400; (2), 0.750; (3), 1.500 g acid. ○, O_2 electrode; ●, Fe electrode. Upper curves, O_2–Fe combination. (A), fresh electrode; (B), aged electrode.

the equivalence point was reflected as a normal potential drop (Ag, Ni), as an upward maximum (Cu, Fe) or as a downward minimum (W) depending upon whether the particular indicator electrode established positive or negative potentials with respect to the oxygen electrode at the points of maximum inflexion of the titration curves, and also upon the magnitude of potential difference after the equivalence point. The inflexion in ΔE coincided with that measured with single indicator electrodes. The applicability of bimetallic electrodes to the determination of equivalence points in acid–base titrations is, therefore, established. As has been mentioned before, this technique offers the much appreciated advantage of overcoming the previously considered indispensable need for a reference electrode.

Attempts to apply a carbon rod for the determination of $K_2Cr_2O_7$ in KNO_3 melts were unsuccessful. Although sharp potential drops amounting to *ca.* 600 mV were measured, the inflexions occurred much earlier than had been theoretically calculated or measured with the oxygen electrode. The reason for this behaviour seems to be

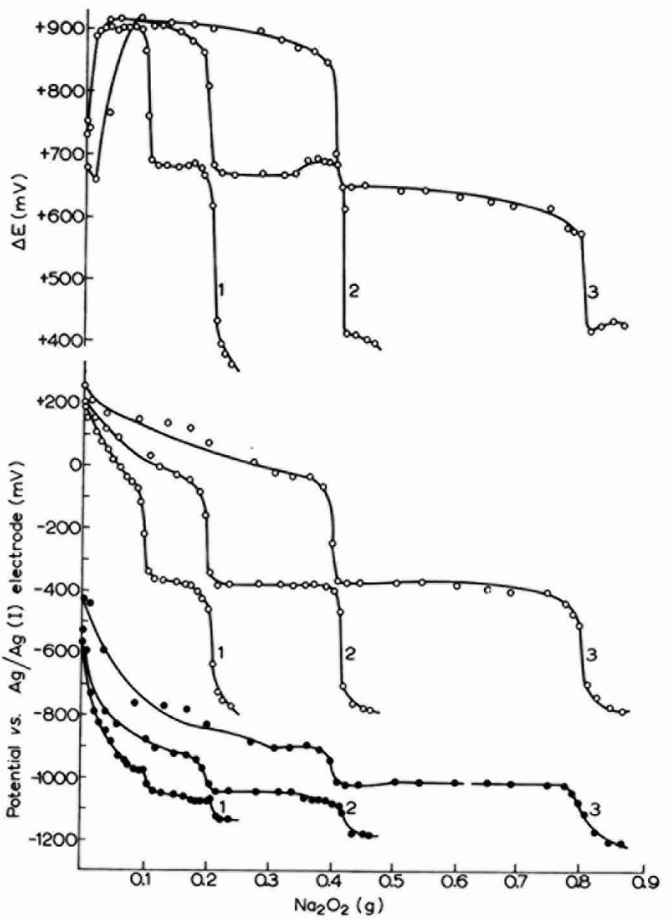

Fig. 3. Titration of the acid $NaPO_3$ with Na_2O_2 in molten KNO_3 at 350°. (1), 0.250; (2), 0.500; (3) 1.000 g acid. ○, O_2 electrode; ●, W electrode. Upper curves, O_2–W combination.

related to the oxidizing properties of both the nitrate and dichromate ions in the fused state.

We have recently found that the acids $NaPO_3$ and NaH_2PO_4 can be titrated potentiometrically with Na_2O_2 in fused KNO_3[11]. During the course of neutralization of these acids, two inflexions were registered. These were due, respectively, to the formation of $Na_4P_2O_7$ and Na_3PO_4 in the case of $NaPO_3$ and Na_2HPO_4 and Na_3PO_4 in the case of NaH_2PO_4. It was of interest to establish whether the neutralization of these 'dibasic' acids could also be followed potentiometrically with bimetallic electrodes.

The titration curves for the acid $NaPO_3$ in fused KNO_3 at 350° are shown in Fig. 3. The lower curves of this figure represent the variation of the potentials of both the oxygen and tungsten electrodes relative to the Ag/Ag(I) reference electrode. Contrary to its behaviour during the titration of the acid $K_2Cr_2O_7$, the tungsten electrode established limited potential drops at the equivalence points of the acid $NaPO_3$. This is, however, an apparent advantage. When these potentials were measured against those of the oxygen electrode, potential drops of *ca.* 200 and 300 mV were established at the two molar ratios acid : base, of 2 : 1 and 1 : 1, respectively (Fig. 3, upper curves).

The acid NaH_2PO_4 was titrated similarly using platinum (without bubbling oxygen)

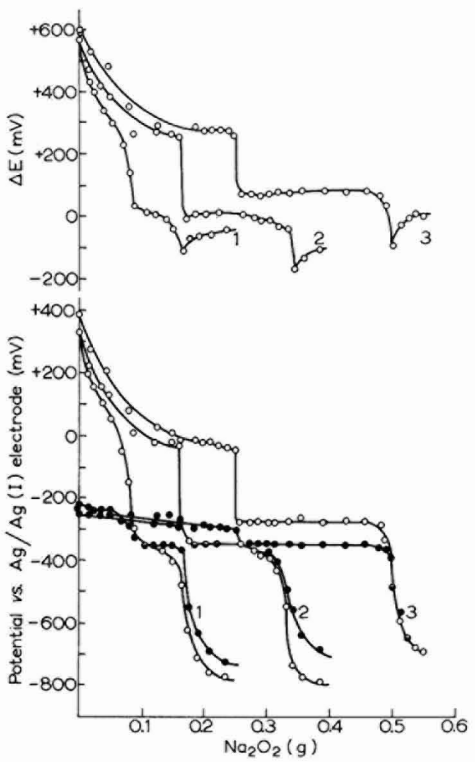

Fig. 4. Titration of the acid NaH_2PO_4 with Na_2O_2 in molten KNO_3 at 350°. (1), 0.250; (2), 0.500; (3), 0.750 g acid. ○, Pt electrode; ●, Ag electrode. Upper curves, Pt–Ag combination.

and silver as indicator electrodes (Fig. 4). At the molar ratio, acid : base, of 2 : 1 the platinum electrode registered inflexions of *ca.* 300 mV, while the silver electrode gave a drop of only 60–80 mV. The second neutralization step, occurring at the molar ratio, 1 : 1, was characterized by potential drops of *ca.* 400 and 350 mV for the two electrodes, respectively. The upper curves of Fig. 4 represent the variation of the potential of the silver electrode relative to that of the platinum during the progress of the neutralization reaction. The two neutralization stages of the acid NaH_2PO_4 were reflected as potential inflexions of *ca.* 200 and 100 mV respectively.

The results presented in Figs. 3 and 4 show that bimetallic electrodes can be applied successfully for the determination of equivalence points of acids neutralizing in more than one step. The applicability of bimetallic combinations for the study of reactions in silicate and borate melts is now being investigated.

SUMMARY

Silver, nickel, copper, iron and tungsten were successfully applied as indicator electrodes in the titration of the acid $K_2Cr_2O_7$ in molten KNO_3 at 350°. With all electrodes sharp potential drops were recorded at the theoretically calculated equivalence points. Because of differences in E^0 potentials (as oxygen electrodes), the measurement of potential differences between any two indicator electrodes allowed the determination of equivalence points. In this type of titration no reference electrode is needed.

Bimetallic combinations were equally suitable for the determination of equivalence points of acids neutralizing in more than one step, *e.g.*, $NaPO_3$ and NaH_2PO_4

REFERENCES

1 S. N. Flengas and E. K. Rideal, *Proc. Roy. Soc. (London), Ser. A*, 233 (1956) 442.
2 H. A. Laitinen and B. B. Bhatia, *Anal. Chem.*, 30 (1958) 1995.
3 D. L. Hill, J. Perano and R. A. Osteryoung, *J. Electrochem. Soc.*, 107 (1960) 698.
4 A. M. Shams El Din, *Electrochim. Acta*, 7 (1962) 285.
5 H. Tl. Tien and G. W. Harrington, *Inorg. Chem.*, 2 (1963) 369.
6 A. M. Shams El Din and A. A. A. Gerges, *Electrochim. Acta*, 9 (1964) 613.
7 A. M. Shams El Din and A. A. A. Gerges, *J. Electroanal. Chem.*, 4 (1962) 309.
8 A. M. Shams El Din, A. A. El Hosary and A. A. A. Gerges, *J. Electroanal. Chem.*, 6 (1963) 131.
9 A. M. Shams El Din and A. A. A. Gerges, paper presented before *The First Australian Conference on Electrochemistry, Sydney and Hobart, February 1963*, Pergamon Press, in press.
10 A. M. Shams El Din and A. A. El Hosary, *J. Electroanal. Chem.*, 7 (1964) 464.
11 A. M. Shams El Din and A. A. A. Gerges, *Electrochim. Acta*, 9 (1964) 133.

THE CHRONOPOTENTIOMETRIC OXIDATION OF OXALIC ACID AND OXALATE IONS AT PALLADIUM ANODES

THOMAS R. BLACKBURN* AND PETER C. CAMPBELL

Carleton College, Northfield, Minnesota (U.S.A.)

(Received April 3rd, 1964)

INTRODUCTION

The chronopotentiometric oxidation of oxalic acid at platinum and gold anodes has been the subject of several recent studies[1-4]. Early studies established that the presence of an oxide film on a platinum anode is inhibiting to the oxidation. Evidence for this is the fact that the chronopotentiogram is shorter and less reversible after the establishment of a partial oxide film in a previous anodization, and that after prolonged or repeated anodization, no oxalic acid chronopotentiogram precedes the oxidation of water. ANSON AND SCHULTZ[6] have shown that similar effects are produced by the presence in solution of chloride or thiocyanate ions, or amyl alcohol, presumably because these species are tightly adsorbed on the anode, and block access to it in the same way that an oxide layer might.

As part of a study of the properties of palladium as a material for electrochemical techniques, we have investigated the oxidation of oxalic acid and of oxalate ions at a palladium anode by the chronopotentiometric technique. The results indicate that oxalic acid and the hydrogen oxalate and oxalate ions are oxidizable at a palladium anode by a mechanism which is not inhibited by the presence of adsorbable species in solution, and which operates at an electrode which is covered with a film of palladium oxide.

EXPERIMENTAL

The circuit and cell for chronopotentiometry were of a common type described previously[6]. Chronopotentiograms were observed with a Tektronix Type 503 oscilloscope, and transition time measured by opening simultaneously the electrolysis circuit and the circuit powering an electric stopclock when the potential corresponding to the transition time was reached.

Oxalate solutions were prepared by weight from primary standard sodium oxalate, which was dissolved in the appropriate supporting electrolyte. Temperature was controlled at 25.0° by means of a thermostatted water bath. The cylindrical palladium anode, 99.99% pure, had a radius of 0.051 cm, and an exposed area of 0.220 cm^2, defined by a Tygon paint seal.

* Present address: Department of Chemistry, Wellesley College, Wellesley, Mass. U.S.A.

RESULTS

The mechanism of oxalic acid oxidation

Curve 1 of Fig. 1 is the anodic chronopotentiogram of 0.01 *M* oxalic acid in a 1.0 *M* perchloric acid solution. Before Curve 1 was photographed, the electrode was freed from oxide films by cathodization. Curve 2 of Fig. 1 was obtained by re-anodizing after the solution had been stirred, following the recording of Curve 1.

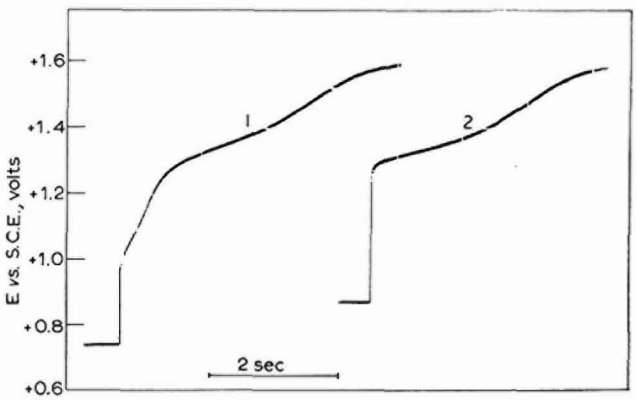

Fig. 1. Chronopotentiograms for the oxidation of 0.01 *M* oxalic acid in 1.0 *M* $HClO_4$. Curve 1 was obtained with an originally unfilmed palladium anode. After the solution was stirred and allowed to become quiet, curve 2 resulted on anodization.

Palladium forms, on anodization in non-electroactive solutions, an oxidized layer containing palladium in two oxidation states, the lower of which is definitely +2. The known properties of palladium suggest that the higher oxide is that of +4 palladium[6]. The first potential inflection of Curve 1 corresponds to the formation of the +2 oxide film; it is not affected by stirring, and reversal of the current before +1.3 V is reached results in a cathodic chronopotentiogram characteristic of the reduction of the +2 film[6]. In a stirred solution, anodization results in an indefinitely long potential halt at +1.3 V *vs.* S.C.E. Therefore the second wave of Curve 1 is the chronopotentiogram of the diffusing species, $H_2C_2O_4$.

Two important conclusions can be drawn from Fig. 1. The first is, that since the oxalic acid chronopotentiogram follows that for the formation of the +2 oxide, the presence of that film does not inhibit the oxidation of oxalic acid. This conclusion is borne out by Curve 2, the anodic chronopotentiogram of oxalic acid at a filmed electrode. That the +2 oxide film is still present after the time interval that followed Curve 1 is clear from the complete absence in Curve 2 of a potential halt for its re-formation. (Also, the presence of a film of PdO may be detected by the chronopotentiogram for its reduction if the electrode is cathodized.) This fact also makes it clear that oxalic acid does not react rapidly with the +2 oxide.

The second conclusion to be drawn from Fig. 1 is that, since it commences abruptly at +1.3 V *vs.* S.C.E., the oxidation of oxalic acid seems likely to proceed *via* a different mechanism from that which operates at gold and platinum electrodes, at both of which the oxalic acid wave begins at +0.9 V. We feel that the experimental evi-

dence outlined below points to a mechanism for the oxidation at palladium anodes which involves the higher (+4) oxide as an intermediate:

$$\left.\begin{array}{l} PdO + 2\,OH^- \rightarrow PdO_2 + H_2O + 2\,e \\ (\text{or } Pd + 4\,OH^- \rightarrow PdO_2 + 2\,H_2O + 4\,e) \end{array}\right\} \quad (1)^*$$

$$PdO_2 + H_2C_2O_4 \rightarrow 2\,CO_2 + H_2O + PdO \quad (2)$$

The experimental evidence for this mechanism is based largely on the observation that the +4 oxide film is rapidly reduced on contact with oxalic acid solutions. In strongly acid solutions, or neutral solutions of sodium sulfate, perchlorate, or nitrate, this reduction proceeds rapidly. In neutral or weakly acidic solutions of phosphate or tartrate salts, and in strongly basic solutions the +4 oxide is not reduced, or is reduced only very slowly, by oxalic acid or oxalate ions, and in these solutions the anodic oxidation of the oxalate species is inhibited. In short, oxalic acid or either of its anions is oxidizable at a palladium anode only if the direct chemical reaction between the oxalate species and the +4 palladium oxide is rapid.

Experimental observations which support but do not necessarily prove the above mechanisms are as follows:

1. Oxidation of the oxalate species never precedes the formation of the +4 oxide film. If, in the observation of the chronopotentiogram like that shown in Curve 1 of Fig. 1, the current is reversed before the beginning of the oxalate wave, and a cathodic chronopotentiogram observed, only the +2 oxide film is found to be present.

2. Since the oxidation of oxalic acid proceeds at an electrode that is covered by a film of palladium oxide, the mechanism of the oxidation cannot require direct access to the metal surface. Indeed, the fact that palladium is less noble than platinum or gold doubtless accounts for the fact that no oxalic acid wave is observed at the potential at which the oxidation takes place on the other metals.

3. Attempts to produce inhibition of the wave by introducing chloride or *n*-pentanol into the solution produced no effect on the reversibility or transition time of the oxalate wave. Inhibition by these species, according to ANSON AND SCHULTZ[5], is characteristic of an oxidation mechanism involving direct access to the metal surface.

Quantitative studies

In order to demonstrate that diffusion-controlled oxidation of oxalate species can take place at a palladium anode in the presence of a palladium oxide film, quantitative current–transition time studies of chronopotentiograms corresponding to Curve 2 of Fig. 1 were undertaken. It was found that such studies could not easily be applied to the oxidation of the species $H_2C_2O_4$, since the +2 oxide film is sufficiently soluble in strongly acid solutions to cause an appreciable positive error in the oxalic acid transition time observed, due to the current required to re-establish the oxide film, which had partly dissolved between trials. The data in Table 1 illustrate this effect

* The simplest formulae of the oxides are shown here, without any intended implications about their anionic compositions. The presence of an oxidized film, containing palladium in two oxidation states, was established in a previous study[6].

for a 1.0 *M* perchloric acid solution of oxalic acid (columns 1 and 2). Columns 3 and 4 show that this effect is negligible for moderate times of exposure to the solution when the pH is raised to 3.0.

TABLE 1

Transition times at a single current density for oxalic acid oxidation in 1 *M* $HClO_4$ and in 0.001 *M* $HClO_4$, as a function of time of exposure of the filmed electrode to the solution between trials. The gradual enhancement observed in the strongly acid solution results from the current required to re-form the oxide film, which is soluble in strongly acid solutions[6].

1.0 M $HClO_4$		*1.0 M $NaClO_4$ + 0.001 M $HClO_4$*	
Time of exposure to soln. (sec)	*τ*	*Time of exposure to soln. (sec)*	*τ*
30	5.40	30	5.30
60	5.51	60	5.32
100	5.73		
150	6.01		
250	6.28	300	5.41

The qualitative aspects of the chronopotentiograms observed in neutral or weakly acid solutions are very similar to those discussed above for strongly acid solution. Figure 2 shows chronopotentiograms corresponding to those of Fig. 1, for originally unfilmed (Curve 1) and filmed (Curve 2) palladium anodes in a 0.50 *M* $NaClO_4$ solution at pH 5.28. Apart from the fact that these chronopotentiograms are somewhat better developed than those in acid solutions, the same remarks apply to these curves as were given earlier for those of Fig. 1.

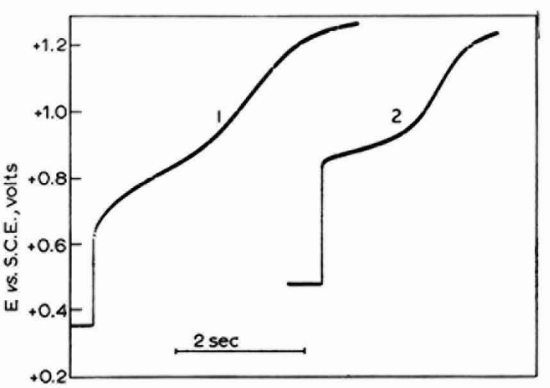

Fig. 2. Chronopotentiograms for the oxidation of 0.01 *M* oxalate ion in unbuffered 1.0 *M* $NaClO_4$, pH = 7.1. Curve 1 was obtained with an originally unfilmed palladium anode. After the solution was stirred and allowed to become quiet, curve 2 resulted on anodization.

Quantitative studies were carried out under two limiting conditions: pH 7.1, at which oxalic acid was quantitatively converted to $C_2O_4^{2-}$, and pH 2.45, at which 92% of the extant species was present as the ion $HC_2O_4^-$ [7]. The data for the two cases is given in Table 2.

TABLE 2

QUANTITATIVE CHRONOPOTENTIOMETRY OF OXALATE SPECIES

Total oxalate concn. is 9.85 × 10⁻³ M. Supporting electrolyte is 1.0 M $NaClO_4$ titrated to pH 2.45 with $HClO_4$			*$[C_2O_4^{2-}]$ = 1.043 × 10⁻² M. Supporting electrolyte is 1.0 M $NaClO_4$, pH = 7.1*		
i (μA)	τ (sec)	$i\tau^{\frac{1}{2}}/AC$ (A sec$^{\frac{1}{2}}$ cm^{2}mole^{-1})	i (μA)	τ (sec)	$i\tau^{\frac{1}{2}}/AC$ (A sec$^{\frac{1}{2}}$ cm^2 mole^{-1})
403	11.18 ±0.16	621	403	11.53 ±0.06	594
498	7.11 ±0.02	613	437	9.57 ±0.04	589
576	5.18 ±0.04	604	575	5.22 ±0.03	572
785	2.69 ±0.03	593	699	3.32 ±0.01	555
883	2.09 ±0.04	588	781	2.66 ±0.01	555
1004	1.60 ±0.02	586	783	2.63 ±0.01	554
			994	1.58 ±0.01	544

The data in Table 2 are plotted as a function of τ in Fig. 3. The solid curves are graphs of the function

$$\frac{i\tau^{\frac{1}{2}}}{AC} = \frac{\pi^{\frac{1}{2}}nFD^{\frac{1}{2}}}{2[1 - \pi^{\frac{1}{2}}D^{\frac{1}{2}}\tau^{\frac{1}{2}}/4r + D\tau/4r^2 - 3\pi^{\frac{1}{2}}D^{\frac{1}{2}}\tau^{\frac{1}{2}}/32r^3 + \ldots]},$$

where D is the diffusion coefficient of the electroactive species, r the radius of the electrode, and τ transition time, which was derived by PETERS AND LINGANE[3] for chronopotentiometry with cylindrical electrodes. Values of the bracketed polynomial were taken from the table computed by EVANS AND PRICE[8] for a six-term polynomial. Values of the diffusion coefficient were chosen to given a reasonable fit to the experimental data at long transition times.

In the case of the solution of pH 2.45 (upper curve and points in Fig. 3) a mixture

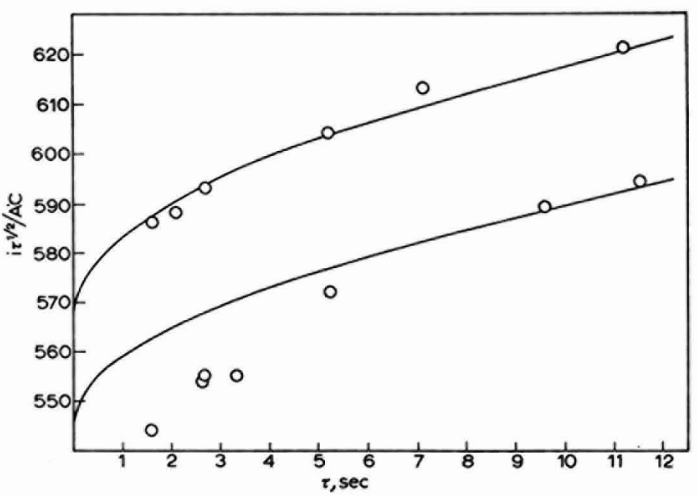

Fig. 3. $i\tau^{\frac{1}{2}}/AC$ (A sec$^{\frac{1}{2}}$ cm^{2}mole^{-1}) as a function of τ for the chronopotentiometric oxidation of oxalate species. Upper curve and points, pH 2.45. Lower curve and points, pH 7.1. Data in both cases were obtained with a palladium anode which bore a film of PdO.

of oxalate species, 92% $HC_2O_4^-$, and 4% each $H_2C_2O_4$ and $C_2O_4^{2-}$ was present, and presumably the diffusion coefficient is an effective value[9], of the form

$$D^{\frac{1}{2}}_{(\text{effective})} = \frac{C_{H_2Ox} D^{\frac{1}{2}}_{H_2Ox} + C_{HOx^-} D^{\frac{1}{2}}_{HOx^-} + C_{Ox^{2-}} D^{\frac{1}{2}}_{Ox^{2-}}}{C_{H_2Ox} + C_{HOx^-} + C_{Ox^{2-}}}$$

where C_{H_2Ox} and D_{H_2Ox}, etc., are the equilibrium bulk concentrations and diffusion coefficients of the respective species at the pH and ionic strength of the supporting electrolyte. However, since all diffusion coefficients are not known, no attempt was made to interpret the apparent diffusion coefficient of the mixture, 1.1×10^{-5} cm^2sec^{-1}, in terms of the individual diffusion coefficients. It is, however, evident from the close agreement of the slope of the experimental points with the Peters-Lingane equation that the oxidation is diffusion-controlled at pH 2.45 at a filmed palladium electrode.

The lower curve and set of points in Fig. 3 refer to the data taken at pH 7.1, again at an electrode filmed with PdO. The line is a graph of the Peters-Lingane relationship, using $D_{C_2O_4^{2-}} = 1.02 \times 10^{-5}$ cm^2sec^{-1}, chosen to fit the data at long transition times. Since the slope of the experimental points appears to approach the theoretical slope at long transition times, it is fair to conclude that diffusion control of the transition time is approached at low currents. However, the significant negative deviation of the points at high currents (short τ) is good evidence that the transition time in this region is under the control of a kinetically-hindered step in the overall oxidation mechanism. In view of our observation that the +4 oxide film is immune to reduction by oxalate ion in basic solutions (though thermodynamically the reaction should go to completion) it is reasonable to speculate that even at pH 7.1 it is the reaction of the oxalate ion with the higher palladium oxide film (reaction (1) in the proposed mechanism above) which is sufficiently slow to cause an appreciable kinetic effect on the transition time at larger current densities.

ACKNOWLEDGEMENT

This work was supported by an Undergraduate Research Participation Grant from the National Science Foundation.

SUMMARY

An investigation of the anodic chronopotentiometry of oxalic acid and the oxalate anions indicates that the oxidation of these species is not inhibited by coverage of the palladium anode surface with a film of PdO, in contrast to behavior reported elsewhere for platinum anodes. An oxidation mechanism which accounts for the observed behavior is suggested, and quantitative studies indicate that the oxidation is diffusion-controlled at pH 2.45, although subject to slight but significant kinetic hindrance at pH 7.1.

REFERENCES

1 F. C. ANSON AND J. J. LINGANE, *J. Am. Chem. Soc.*, 79 (1957) 4901.
2 J. J. LINGANE, *J. Electroanal. Chem.*, 1 (1960) 379.
3 D. G. PETERS AND J. J. LINGANE, *J. Electroanal. Chem.*, 2 (1961) 1.
4 J. GINER, *Electrochim. Acta*, 4 (1961) 42.
5 F. C. ANSON AND F. A. SCHULTZ, *Anal. Chem.*, 35 (1963) 1114.
6 T. R. BLACKBURN AND J. J. LINGANE, *J. Electroanal. Chem.*, 5 (1963) 216.
7 J. BJERRUM, G. SCHWARZENBACH AND L. G. SILLÉN, *Stability Constants*, The Chemical Society, London, 1958.
8 D. H. EVANS AND J. E. PRICE, *J. Electroanal. Chem.*, 5 (1963) 77.
9 T. R. BLACKBURN, Ph.D. thesis, Harvard University, 1962.

REVIEW

APPLICATION OF ELECTRON PARAMAGNETIC RESONANCE TECHNIQUES IN ELECTROCHEMISTRY

RALPH N. ADAMS

Department of Chemistry, The University of Kansas, Lawrence, Kansas (U.S.A.)

(Received April 3rd, 1964)

Scarcely five years ago the diverse areas of electron paramagnetic resonance and electrochemistry were mated and, in this short period, the union has provided considerable and significant contributions to both research fields. The title of this paper might be reversed to indicate the role of electrochemistry in electron paramagnetic resonance studies. In fact, the intent of this article is to discuss both viewpoints—the contributions of each technique to problems of the other.

No attempt is made to present the principles of electron paramagnetic resonance (EPR). Thorough and authoritative treatments are available[1-3]. Two recent reviews by CARRINGTON[4] and HORSFIELD[5] give an excellent picture of the applications. The technique can be viewed as a specific measurement in the broad area of absorption spectroscopy. (It should be noted that the terms electron spin resonance (ESR) and electron magnetic resonance (EMR) are synonymous with EPR).

EPR is concerned, among other things, with the detection and identification of free radicals and radical ions. The other diverse applications will not be discussed here. Free radicals and radical ions are unique in that they contain an unpaired electron and therefore an associated magnetic moment due to the spin of this unpaired electron. One can perturb the natural energy levels of such a system by applying a gross magnetic field to the sample. If one then irradiates the sample with energy of the correct wave length or frequency, transitions can be induced among the perturbed energy levels.

The magnetic moment of the unpaired electron not only experiences an orientation due to the large laboratory magnet, but it may also interact with various magnetic nuclei in the particular molecule involved. This results in sub-splitting of the energy levels and transitions among these levels provide the so-called hyperfine splittings. These electron-nuclear interactions are two-fold in nature. One results from the interaction of the two (nearby) magnetic dipoles. The magnitude of this influence depends on the distance and spatial orientation between the electron and nuclear dipoles and therefore produces an anisotropic effect. This anisotropic portion of the hyperfine interaction is effectively averaged to zero for a radical or radical ion which is in solution and therefore undergoing rapid tumbling motion. Only solution radicals are considered in this discussion and the anisotropic component of the hyperfine inter-

action can be neglected. The isotropic portion results when the wave function of the unpaired electron has a finite density at the magnetic nucleus in question. This contact or Fermi hyperfine interaction is of fundamental significance especially in organic radical systems. It can be used to map the unpaired electron distribution around the molecular framework.

The EPR spectra of paramagnetic species, then, are characterized by a series of absorption lines (due to instrument design most EPR spectra are presented in derivative form) resulting from the interaction of the unpaired electron with various magnetic nuclei in the molecule. The spacing between these lines is a measure of the magnitude of this interaction and is called the coupling or splitting constant. This is usually given the symbol a_Z where Z is the magnetic nucleus in question. Coupling constants are most often given in gauss and are converted approximately to frequency units of Mc/sec by multiplying by 2.8. Proton couplings are, of course, most frequent and interaction of an unpaired electron with a single proton gives rise to a doublet splitting. Interaction with n equivalent protons produces $(n + 1)$ lines in the EPR spectrum. The intensities of these lines will be in the ratio of the coefficients of a binomial expansion (*i.e.*, the intensities of the 5 lines arising from interaction with 4 equivalent protons will have the ratio 1:4:6:4:1, etc.). A ^{14}N nucleus with spin 1 gives rise to three lines of equal intensity. A thorough discussion of other hyperfine interactions and how they arise in aromatic radicals is contained in the review by CARRINGTON[4].

The details of the construction and operation of an EPR spectrometer are too involved to be treated in detail here. It is worthwhile considering a general description of a typical X-band, reflection type spectrometer for the purpose of examining the relationship of the electrochemical experiment to the instrument. Like any complex instrument the EPR spectrometer can be broken down into several general sections: (1) an input section; (2) a detector system; (3) the output section; and (4) associated power supplies.

The input section of the spectrometer consists of a klystron tube which generates microwave radiation in the general region of 9–9.5 kMc (this corresponds roughly to a wave length of *ca.* 3 cm and this spectral region is frequently called X-band, hence the name X-band spectrometer). The klystron is tunable over a small span but is normally operated at essentially fixed frequency. Also to be included in the input section is the large electromagnet which provides the initial conditions for the resonance experiment. The magnet provides a homogeneous field of *ca.* 3000–4000 gauss. (The magnet normally has a wider range of field strength but it is this region which is of interest in the present discussion.)Provision is made for automatic variation of the field in a slow, linear sweep through the region of the resonance absorption of microwave energy.

The output from the klystron source is fed through microwave plumbing (rectangular waveguides) to the microwave bridge which contains the cavity and a crystal diode detector. Strictly speaking the crystal is the detector but the classification given above is only for convenience. The assembly of microwave bridge, cavity and crystal may be thought of as the detector *system*. The microwave bridge is a device commonly called a magic or hybrid T and consists of four arms. Microwave power from the klystron enters through one arm and divides equally between two others, one of which terminates in the cavity containing the sample. The fourth arm holds

the crystal detector. The microwave bridge functions in a fashion analogous to a d.c. bridge network familiar in electrochemistry. Thus, in a classical potentiometer network for measuring redox potentials, if the bridge is balanced and a change of solution redox properties occurs, the electrodes provide an unbalance output signal to, say, a galvanometer. With a microwave bridge, balanced for no paramagnetic resonance absorption in the cavity, no signal appears at the crystal detector. When the magnetic field sweeps through the resonance condition, unbalance occurs and microwave power is fed to the crystal arm and appears as a crystal output signal. The microwave bridge is more subtle in appearance and operation than its d.c. counterpart due primarily to the frequency region in which it operates. Authoritative treatments of microwave bridges and their operation should be consulted for further details[1,2,6].

The microwave cavity consists of a length of wave guide closed at each end. Microwave power can be concentrated in the cavity in the form of standing waves and the paramagnetic sample, in a suitable holder, is positioned in the region of highest r.f. magnetic field strength (H_1). The entire cavity is held between the poles of the large magnet (H_0). An additional magnetic field is provided by a set of sweep coils built on the walls of the cavity. These are excited at 100 kc and provide a modulation of the microwave energy in the cavity. This small, oscillating magnetic field provides for the derivative output form of the EPR signal.

The output section of the spectrometer consists of an oscilloscope for adjusting the operating conditions and ordinarily a pen-and-ink recorder. Associated phase detector networks provide the final d.c. signal for the recorded EPR spectra. Various power supplies are obviously required and important additional components not mentioned above include an automatic frequency control to maintain the klystron frequency constant[6].

Assuming the spectrometer is operated properly, there remains the problem of obtaining a satisfactory EPR spectrum. This reduces to introducing a sufficient quantity of radicals or radical ions into the sample cell. Proper response may be limited by too low a radical concentration, insufficient lifetime of the radical, or improper utilization of the input microwave energy. The latter limitation is of considerable consequence in the electrochemical method wherein radical species are generated directly in the cavity. This problem is discussed in the next section.

ELECTROCHEMICAL GENERATION TECHNIQUES

Apparently GALKIN *et al.* first employed electrolysis in an EPR spectrometer but the experiment had little significance in electrochemistry[7]. AUSTEN *et al.* showed that aromatic radical ions were formed in electro-reductions. They carried out the electrolyses in non-aqueous media, froze the samples, and then introduced them into the EPR spectrometer[8]. But the elegant work of MAKI AND GESKE introduced the real potentialities of electrochemical generation to EPR spectroscopy. They carried out the electrolysis directly in the microwave cavity, *i.e*, by internal generation (IG) and produced a variety of radical ions in acetonitrile and other non-aqueous media[9-12]. The technique was extended to aqueous solutions by the writer and coworkers[13,14]. The electro-generations of a wide range of anion and cation radicals have been reported in the meantime by this technique. It is also possible to employ external generation

(EG) of the radical species and to pass them through the sample cell in the cavity by a variety of pumping methods. This technique has been used widely by FRAENKEL and coworkers[15]. The applicability and relative merits and disadvantages of each of these techniques are next discussed.

The technique of IG is probably to be preferred in studies where it is desired to detect and identify a radical ion intermediate in an electrode process. From the identification viewpoint the results are excellent—in many cases it is not difficult to obtain an EPR signal with excellent signal/noise ratio within a few seconds after initiating the electrolysis. The difficulties arise in the quantitative interpretations of the IG method. This does not mean the quantitative determination of the number of radical species produced—EPR spectroscopy has its own limitations in this respect. Rather, it is difficult to correlate relative amounts of radicals formed with electrochemical quantities or to discuss precisely those electrochemical parameters which involve the radical concentration as a function of time of electrolysis and distance from the electrode. The reasons for this can be understood by examining the properties of the microwave cavity and sample cell in more detail.

In a reflection type EPR spectrometer the cavity commonly used operates in the so-called TE_{102} mode. This description fits the Varian V-4500 series EPR spectrometers. This is the instrument with which the writer is familiar and is that used by many workers. In the discussions to follow similar considerations will apply to almost any instrument. With a TE_{102} cavity the H_1 field is a maximum at the front, back, and middle of the cavity (*i.e.*, there are two modes or a full wave in the length of the cavity). The electrical field is at right angles to H_1 and is also 90° out of phase. Its maxima appear at points 1/4 and 3/4 of the cavity length. A typical quartz sample cell has a center portion in the form of a thin, flat plate and is suitable for aqueous or nonaqueous solutions. Collets at the top and bottom of the cavity provide for hand adjustment of cell position. The flat is oriented in the middle of the cavity parallel to the ends. Figure 1 shows the cell placement and a schematic arrangement for IG. Figure 2 shows the cell position with regard to the H_1 distribution. Comparisons of radical concentrations in successive runs require the sample be exposed to identical H_1 fields. This is very difficult to attain with the hand adjustment of cell position.

Another problem develops during the course of a single electrolytic run. The H_1 field decreases from the center of the cavity toward each end in a cosine function with zero strength at points 1/4 and 3/4 along the length (*i.e.*, where the E field is maximal). In addition, H_1 falls off approximately as a cosine function from the middle of the sample toward the top and bottom of the cavity. Thus most of the EPR signal comes from radical species which are contained in a small volume near the center of the electrolytic cell. Now for short periods of electrolysis, the concentration profile of radical species can be calculated assuming linear diffusion mass transfer (a tenuous extrapolation with the electrode geometry normally used) and the relative interaction with the H_1 field estimated. However it is easy to show experimentally that such calculations are unsatisfactory. After electrolysis times of 60 sec or longer, a large amount of natural convection occurs in the thin electrolytic cells (thickness of *ca.* 0.5 mm for aqueous solutions[14]). One can demonstrate this effect by generating a highly colored radical ion (*i.e.*, tetracene anion radical in acetonitrile) in the cell but outside the cavity. The swirl and convection patterns are clearly visible. Thus it is difficult to make

valid assessments of radical concentration as a function of electrolysis time or other parameters. The problem is not quite so serious as this suggests. The convection processes in time reach a relatively steady state and the mixing is advantageous. Actually VISCO and coworkers have made some very succesful measurements of radi-

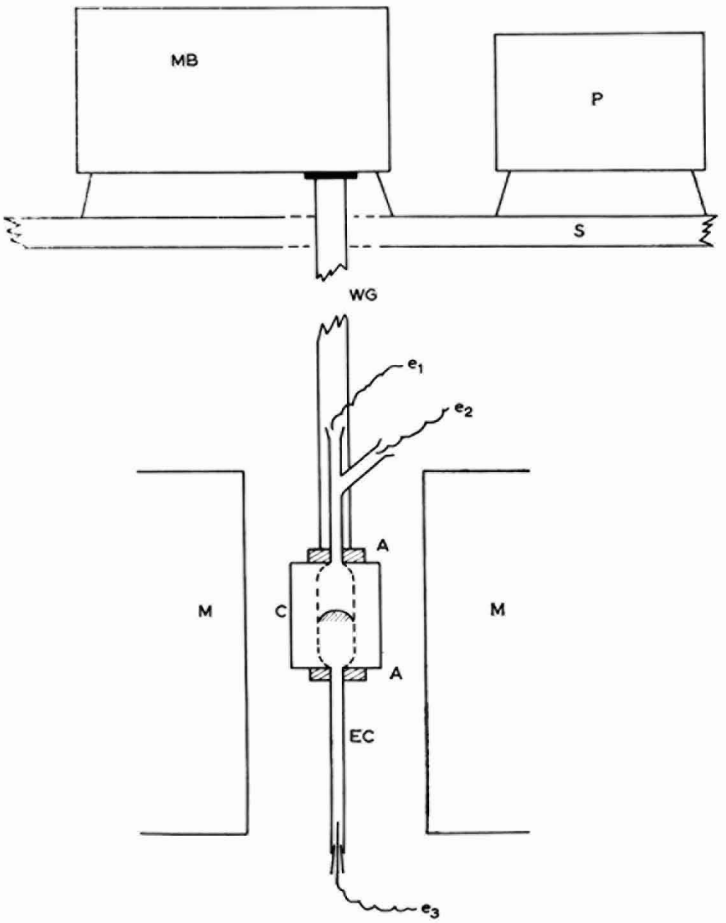

Fig. 1. Typical arrangement for EPR electrochemical experiment. MB, microwave bridge; P, potentiostat or other electrochemical equipment; S, shelf to support bridge, etc.; WG, wave guide connecting microwave bridge to cavity; M, magnet (H_0); C, microwave cavity; A, top and bottom adjusting collets; EC, electrochemical cell, flat portion parallel to front of cavity, shaded portion shows typical placement of mercury pool level; e_1, e_2, e_3, electrodes, for reduction e_3 connects to mercury pool, e_1 and e_2 are reference and auxiliary leads (other configurations as required). Dimensions not necessarily in scale.

cal concentrations with IG using advantageous electrode designs[16]. Some of the problems mentioned above also can be alleviated by using double cavities or internal references. Other cavity configurations such as a cylinder in the TE_{011} mode are very useful[43].

One might suspect the validity of the EG technique applied to electrode mechanism studies because the radical species have a relatively long time to undergo complex reactions before being seen in the EPR spectrometer. With relatively stable and long-lived radical ions this worry is of course unfounded. Even where follow-up chemical reactions predominate, excellent interpretations of organic reductions are possible as has been shown by FRAENKEL *et al*[15]. With short-lived species the EG must be used with fast transfer systems. The EG technique has, in fact, several significant advan-

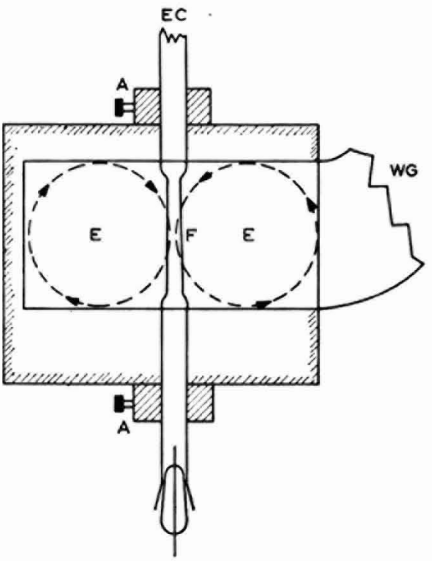

Fig. 2. Positioning of electrochemical cell in microwave cavity. – – –→, H_1 field distribution; EC, electrochemical cell; F, flat portion of cell in maximum H_1 field; A, top and bottom adjusting collets; WG, wave guide connection to microwave bridge; E, maximum electrical field. The general outside shape of the cavity portion is indicated by the shaded outline but the diagram is not intended to be accurate in any dimensions. Coupling devices, modulation coils, etc., are not depicted.

tages. First there is little doubt about the quantitative measurement of radical concentrations. Using controlled-potential coulometry, precisely known amounts of radicals can be generated and transferred to the EPR cell. The solution is homogeneous and positioning effects can be eliminated by leaving the sample cell undisturbed while the external electrochemical cell is varied as desired. In fact, controlled-potential coulometry techniques with stable radical ions could well be used for calibration purposes in EPR. There are problems concerned with oxygen contamination, contact of solution with flexible tubing, etc, in the transfer process but these are easily circumvented. Another point to be considered in the use of EG concerns the phenomenon of homogeneous electron exchange which is dealt with in the next sections.

APPLICATIONS OF EPR TO ELECTROCHEMISTRY

There are at least two areas in which EPR has contributed to electrochemistry. The

first, and most obvious of these, is in the detection and identification of radical intermediates in electrode reactions (predominantly organic electrode processes). The second, which has not been exploited fully yet, provides information about solution interactions of radical ions which contribute to a fuller understanding of these entities as oxidation–reduction intermediates.

When a well-defined spectrum is obtained, the EPR method is without peer in identifying radical intermediates in complex electrode processes. While all purely electrochemical methods reflect secondary properties (*i.e.*, redox potential, diffusion coefficient, etc.) EPR provides positive identification of radical species. This is so, because the hyperfine interaction can give a clear picture of the molecular structure. While EPR spectra are not absolutely unique (*e.g.*, the EPR spectra of nitrobenzene or nitrosobenzene anions contain the same number of lines and differ only slightly in a_N and a_H, etc) it is rare that a well-resolved spectrum cannot provide positive identification of the radical species in electrochemical studies.

The first work of MAKI AND GESKE showed the nitrobenzene anion radical ($NB^{\cdot-}$) as a definite intermediate in the reduction of nitrobenzene[9,10]. Later studies showed $NB^{\cdot-}$ had a definite lifetime even in aqueous media[13,14]. The nitrobenzene reduction had been studied, with innumerable publications, since the original work of HABER, but no radical ion intermediates had been identified prior to the EPR work. The reduction of substituted aromatic nitro compounds leads, in general, to the corresponding substituted anion radicals[11,13]. With certain halonitrobenzenes elimination of halogen occurs during electrolytic reduction. Thus the isomeric chloronitrobenzenes all yield the expected chloronitro anion radical upon reduction in dimethylformamide. With the ortho-bromo-and all three iodo-nitrobenzenes the halogen atom is ejected and one identifies the $NB^{\cdot-}$ in the EPR spectrometer. These eliminations are solvent dependent and by using mixtures of water-dimethylformamide, the halogens can be partially or fully retained. In the case of the iodo derivative it is possible to show, by a combination of cyclic voltammetry and the EPR, that the first reduction is a two-electron process to produce the ejected iodide ion followed by one-electron process to give the unsubstituted $NB^{\cdot-}$ Overlapping waves obscure the individual steps with the other compounds[17]. Some indications of such reactions existed in the polarography of the halonitrobenzenes. The EPR evidence is immediate and unequivocal since halonitrobenzene anion radicals give 27 or 36 lines but never 54 (as the unsubstituted $NB^{\cdot-}$) in their EPR spectra.

The anion radicals of aliphatic nitro compounds can also be identified as intermediates during electro-reduction[13]. An example of the use of cyclic voltammetry coupled with EPR to unravel complex reductions is given in the recent work by HOFFMAN *et al.* on the reduction of tertiary aliphatic nitro compounds in glyme[18].

Elimination reactions are not limited to the reduction of nitro compounds. FRAENKEL *et al.* using EG found very interesting results in the reduction of 4-aminobenzonitrile in dimethylformamide. The EPR spectrum of the reduction product showed without question the presence of two equivalent ^{14}N nuclei and two sets of four equivalent protons. (The EPR spectrum actually states that there are two equivalent nuclei of spin 1 and two sets of four nuclei with spin 1/2 but it is difficult to imagine any other than the assignment above). The electrochemistry (cyclic voltammetry) suggested a reversible charge transfer step followed by an irreversible chemical reaction. The reduction apparently proceeds in the following fashion[15]:

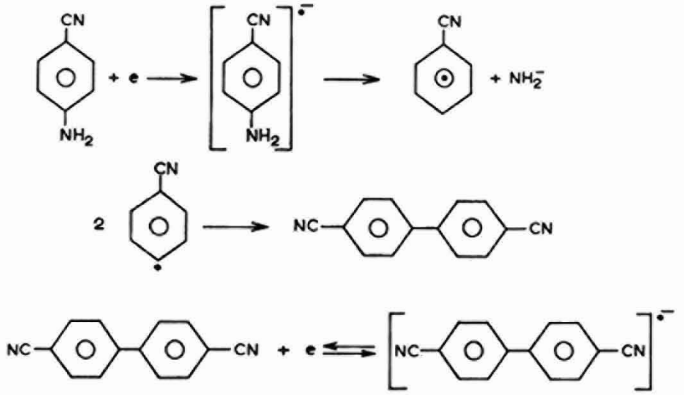

A similar reaction to form the 4,4'-dicyanobiphenyl anion radical was found in the reduction of the 4-fluorobenzonitrile.

These elimination reactions are apparently quite prevalent in the reduction of aromatic compounds. Thus electrolysis of *p*-dinitrobenzene at potentials corresponding to the second wave in dimethylformamide leads to elimination of a nitro function and unequivocal EPR identification of the product as the *p*-nitrophenol anion radical. Similarly the EPR spectrum of electrolytically reduced 9-nitroanthracene shows no ^{14}N couplings and hence elimination of the nitro group[19].

EPR has been very valuable in the study of anodic oxidations at solid electrodes. One can cite the positive identification of the N,N'-tetramethylbenzidine cation radical formed in the anodic oxidation of N,N-dimethylaniline[20] and triphenylmethane dyestuffs like crystal violet. In the latter case, the tetramethylbenzidine arises by a splitting out of the central "methane" carbon attached to its substituted phenyl nucleus, followed by *intra* molecular coupling of the remaining two N-dimethylanilino fragments[21]. The oxidation of *p*-phenylenediamine with the formation of the cation radical has been studied in both aqueous[14] and non-aqueous media[22]. Chemical reactions between *p*-phenylenediamine cation and materials like *m*-phenylenediamine have been investigated and their influence on the electro-oxidation of mixtures of these compounds determined[23].

The exclusive use of electrochemical techniques for studying processes like the above, which contain complicated follow-up reactions, involves measuring secondary properties of the species (*i.e.*, rates of the follow-up reactions in terms of transition times, potentials, etc.). These frequently are vague and, where factors like specific adsorption predominate, may be misleading or difficult to evaluate. Where EPR is applicable it gives clear evidence of the actual existence (not inferred) of intermediates from which a reaction scheme can often be devised. This reaction scheme can then be tested for correlation with the electrochemical information. When positive EPR signals are obtained, there is no question as to the existence of a paramagnetic intermediate. Conversely, the lack of an EPR signal does *not* eliminate the possibility of a radical species. The EPR signal may not be obtained for a variety of reasons. Furthermore EPR falls far short of providing all the answers to the nature of a complex electrode reaction. The proof that the $NB^{\cdot-}$ entity exists in the electro-reduction of nitrobenzene leaves much still to be known about this process.

As mentioned previously, EPR provides information of interest to electrochemists exclusive of the study of electrode mechanisms. Physical interactions (solvation, hydrogen bonding) of radical ions with the solvent and association with metal ions are of direct interest to electrochemists as well as EPR spectroscopists. These studies are treated in the next section.

Of specific interest to electrochemists is the study of homogeneous electron exchange reactions between a radical ion $X^{\cdot-}$ and its parent X. If a fixed concentration of $X^{\cdot-}$ is generated in the presence of increasing quantities of the parent X, then the increasing rate of the electron exchange is evidenced by a broadening of the hyperfine lines in the EPR spectrum. The theory of the exchange process is moderately involved but reasonably accurate values of the bimolecular rate constant, k_{exc}, can be obtained easily by measuring the line broadening as a function of concentration of parent compound as shown by WEISSMAN and coworkers[24,25]. The value of k_{exc} for the system benzonitrile anion/benzonitrile (in dimethylformamide as solvent) was estimated at *ca.* $2 \cdot 10^8$ mole^{-1} sec^{-1} using the IG electrochemical method[26]. Recent theories of electron transfer processes by MARCUS provide a direct correlation between k_{exc} and k_{el}, the heterogeneous electrochemical rate constant[27]. The EPR measurements can be used to calculate k_{el} values not accessible to electrochemical measurement and to test the theory further.

Recently it has been found that k_{exc} for certain systems is remarkably sensitive to solvent composition. The exchange rate for the system $NB^{\cdot-}$/NB (which is slow compared to the benzonitrile mentioned above, or to, say, naphthalene anion/naphthalene) in dimethylformamide, is slowed very considerably by the addition of 10% water. On the other hand, the benzonitrile system is hardly affected by a similar addition of water. It has been clearly established (*via* coupling constant changes as discussed in the next section) that the nitrobenzene anion is strongly solvated by water whereas the parent nitrobenzene seems to be less solvated than the anion. Hence, in the electron exchange reaction, with water present, conditions are such that there is a distinct solvent reorientation required and thus a lower exchange rate. Similar solvent effects on coupling constants are absent in the case of the benzonitrile anion and presumably the degree of *aquo* solvation is approximately the same in the anion and the parent benzonitrile. Consequently the presence of water has relatively little effect on the electron exchange rate. The exchange rate of the system benzophenone anion/benzophenone again decreases with the addition of small amounts of water in accord with the expected strong solvation of the benzophenone anion radical[28]. A thorough study of the effects of solvent, metal ions, and molecular geometry on exchange rates of these and similar aromatic systems is being carried out in the writer's laboratory.

APPLICATIONS OF ELECTROCHEMISTRY TO EPR

Although the work of most fundamental significance to EPR spectroscopy borders on physics (or chemical physics) it is safe to say that the electrochemical generation techniques have made significant contributions to EPR over the last few years. Especially in the generation of anion radicals, the electrochemical method provide a much wider range of experimental conditions than previously available. In the chemical production of radical ions, the metal reductants—sodium, potassium, etc—restricted the choice of solvents to a few like dimethoxyethane or tetrahydrofuran.

These chemical reductions involve special techniques and high purity solvents. Furthermore, the resulting metal ions tend to associate with the radical anions and complicate the EPR spectrum (although some studies are specifically directed toward such interactions). The electrochemical method allows a wide range of solvents including even aqueous media. Solvent purity is also not such a critical problem and the time involved in obtaining a satisfactory EPR spectrum is, of course, far less with the electrochemical method. A considerable amount of work was thus facilitated for EPR spectroscopists who were interested in such problems as correlating hyperfine coupling constants with molecular orbital calculations[15,22,29-31], line width variations[32,33], or investigating a new set of radical ions[29,36]. (The references throughout this manuscript are not all inclusive and are intended to be illustrative only.)

One of the consequences of the wide range of solvents usable in the electrochemical method was the discovery that the ^{14}N coupling constants in aromatic nitro anions were very dependent on small amounts of water[13]. Further studies showed this to be a general effect with solvents capable of solvating or hydrogen bonding with the anion radical. Solvent effects were noted for other systems[37] and a quantitative interpretation was given by GENDELL, *et al.*[38]. Extensive experimental studies have been made of this solvation effect, particularly on nitrobenzene and substituted nitrobenzene anions[39,40]. These studies show the importance of taking solvent effects into consideration in correlations of experimental hyperfine coupling constants with molecular orbital calculations. Further they provide physical insight into subtle interactions of these redox entities. Recent work has shown that ^{14}N coupling constants in aromatic nitro anions are also very dependent on metal ion concentrations (*i.e.*, Na^+, Li^+, K^+, Mg^{2+}) whereas large cations like the tetraethylammonium ion are almost without effect[41].

Another fruitful area which developed along with the electrochemical method involves the study of molecular geometry in radical ions. MAKI and coworkers examined rotational isomerism in various benzaldehyde radical ions[30,31]. GESKE AND RAGLE examined steric effects on ^{14}N coupling constants in substituted nitrobenzene anions[42]. Correlations of these effects with molecular orbital parameters have been accomplished[43].

PRACTICAL OBSERVATIONS ON ELECTROCHEMICAL GENERATION

The following comments result from several year's experience in the writer's laboratory and are included in the hope they may be of value to others.

For exploratory work or electrode mechanism studies the IG method appears most advantageous. A three-electrode, potentiostatic system should be used if possible. Even with potentiostatic control, the positioning of reference electrodes is far from ideal in the small sample cells. Much satisfactory work has been carried out with the rather crude arrangement in which the reference electrode (SCE with salt-bridge arm) and the auxiliary electrode (heavy-gauge platinum wire) were inserted more or less side by side through the top of the sample cell (for diagrams of the cells, see ref. 14, Fig. 1). (It can be mentioned that cells can be fashioned from ordinary pyrex glass and will function satisfactorily for non-aqueous work, These are, of course, far less expensive than their quartz counterparts.) Rather than the usual mercury pool for reductions, a platinum gauze, similar to that for oxidations, can be mercury-plated and used advantageously. Positioning of the electrode in the cell and cavity should be in accord with the geometry of the H_1 field discussed earlier.

Cells filled with aqueous solutions often require much adjustment to obtain a good coupling of the cavity. This is just a matter of trial and error and much patience. When working with dilute solutions and radical species which are short-lived, care must be taken not to exhaust the supply of parent compound in the thin cell section. When this occurs, signal intensity may begin to fall off during the course of several sweeps. It normally takes several sweeps of a spectrum before conditions are optimized for the best signal/noise ratio. It is best not to prolong electrolysis for several reasons. First, if the radical species are short-lived, their decomposition products may result in unexpected complications. Also, too high a concentration of radical species can lead to undesirable dipolar interactions. This normally requires higher concentrations than are reached in electrolytic methods.

Power saturation is rare with any of the solution radical ions mentioned herein but this should be routinely checked by increasing power input from the klystron and testing for a decrease in signal amplitude. Modulation broadening of lines (from too large a 100 kc modulation amplitude) is prevalent in all systems with narrow lines. The spectrometer settings must be repeatedly optimized to eliminate this false broadening. In the IG technique, the possibility of homogeneous electron exchange may broaden lines. This can be checked *via* IG by generating the same quantity of radicals (at controlled-potential the product of average current by time can be *approximately* adjusted to be equal in different runs) in a decreased parent concentration. Narrower line widths indicate this form of exchange broadening may be present. With exhaustive electrolysis externally (hence no parent compound left) this problem is eliminated. This point argues strongly in favor of EG when only the quality of the EPR signal is of interest.

There are no serious limitations to the use of aqueous solutions. Naturally many radical ion species are longer lived in aprotic media. Dimethylformamide is an excellent solvent system. Reagent-grade material can be used without further purification in most cases. The non-aqueous solvents now familiar in electrochemistry, acetonitrile, dimethylsulfoxide, benzonitrile, dioxane, etc., are all suitable. The supporting electrolyte should be *ca.* 0.1 *M* and preferably of the tetraalkylammonium type. Tetraethylammonium perchlorate is excellent and easy to prepare from the bromide which is inexpensive. Recrystallization until the sample is free of bromide is necessary, if it is to be used in anodic work, to eliminate the bromide oxidation wave. Lithium and sodium perchlorates are quite usable as supporting electrolytes but may have an effect on coupling constants. The latter is definitely true for aromatic nitro anions[41].

Since even the best purified of non-aqueous solvents ordinarily contain (or absorb through conventional polarographic handling techniques) *ca.* millimolar water, there will be some scatter to values of coupling constants for systems which show a strong solvent dependence. It is probably safe to say $\pm$ 0.08 g is the best reproducibility one can expect unless one takes extreme precautions to keep the water content extremely low (or very constant). The point here is that most electrochemists start with well-dried (*ca.* 1 m*M* or less in water) solutions but the usual exposure they receive during electrochemical operations plus indiscriminate amounts of water added through aqueous salt-bridges, etc., results in variable water content. A rough estimate of the water content under operating conditions may be from 1–3 m*M*. This is, of course, about equal to the usual concentration of electroactive material and hence is certainly not negligible with respect to radical concentrations.

ACKNOWLEDGEMENTS

The support of this work by the Atomic Energy Commission through contract AT-(11-1)-686-38 and by the Air Force through AFOSR is gratefully acknowledged. This work was partially completed while the writer was a Guggenheim Fellow at the Varian AG Research Laboratories and the E.T.H. in Zürich, Switzerland.

REFERENCES

1 D. J. E. INGRAM, *Free Radicals as Studied by Electron Spin Resonance*, Academic Press, New York, 1958.
2 G. K. FRAENKEL, in *Techniques of Organic Chemistry*, Vol. I, part IV, edited by A. WEISSBERGER, Interscience Publishers Inc., New York, 1960.
3 R. BERSOHN, in *Determination of Organic Structures by Physical Methods*, Vol. 2, edited by F. C. NACHOD AND W. D. PHILLIPS, Academic Press, New York, 1962, Chap. 9.
4 A. CARRINGTON, *Quart. Rev. (London)*, 17 (1963) 67.
5 A. HORSFIELD, *Chimia (Aarau)*, 17 (1963) 42.
6 F. A. NELSON, in *NMR and EPR Spectroscopy*, Chap. 16, 3rd. Varian NMR–EPR Workshop, Palo Alto, 1959, Pergamon Press, New York, 1960; see also Chap. 5 by W. C. LOCKHART AND R. C. JONES.
7 A. A. GALKIN, I. L. SHAMFAROV AND A. V. STEFANISHINA, *J. Exptl. Theoret. Phys. (U.S.S.R.)*, 32 (1957) 1581.
8 D. E. G. AUSTEN, P. H. GIVEN, D. J. E. INGRAM AND M. E. PEOVER, *Nature*, 182 (1958) 1784.
9 A. H. MAKI AND D. H. GESKE, *J. Chem. Phys.*, 30 (1959) 1356.
10 D. H. GESKE AND A. H. MAKI, *J. Am. Chem. Soc.*, 82 (1960) 2617.
11 A. H. MAKI AND D. H. GESKE, *J. Am. Chem. Soc.*, 83 (1961) 1852.
12 A. H. MAKI AND D. H. GESKE, *J. Chem. Phys.*, 33 (1960) 825.
13 L. H. PIETTE, P. LUDWIG AND R. N. ADAMS, *J. Am. Chem. Soc.*, 83 (1960) 2671; 84 (1962) 4212.
14 L. H. PIETTE, P. LUDWIG AND R. N. ADAMS, *Anal. Chem.*, 34 (1962) 916.
15 P. H. RIEGER, I. BERNAL, W. H. REINMUTH AND G. K. FRAENKEL, *J. Am. Chem. Soc.*, 85 (1963) 683.
16 R. E. VISCO, Ph.D. thesis, University of Illinois, 1963.
17 T. KITAGAWA, T. LAYHOFF AND R. N. ADAMS, *Anal. Chem.*, 35 (1963) 1086.
18 A. K. HOFFMANN, W. G. HODGSON, D. L. MARICLE AND W. H. JURA, *J. Am. Chem. Soc.*, 86, (1964) 631.
19 J. CHAMBERS AND R. N. ADAMS, unpublished data.
20 Z. GALUS AND R. N. ADAMS, *J. Am. Chem. Soc.*, 84 (1962) 2061.
21 Z. GALUS AND R. N. ADAMS, *J. Am. Chem. Soc.*, 86 (1964) 1666.
22 M. T. MELCHIOR AND A. H. MAKI, *J. Chem. Phys.*, 34 (1961) 471.
23 H. Y. LEE AND R. N. ADAMS, *Anal. Chem.*, 34 (1962) 1587.
24 F. C. ADAM AND S. I. WEISSMAN, *J. Am. Chem. Soc.*, 80 (1958) 1518.
25 S. I. WEISSMAN, *Z. Elektrochem.*, 64 (1960) 47.
26 P. LUDWIG AND R. N. ADAMS, *J. Chem. Phys.*, 37 (1962) 828.
27 R. A. MARCUS, *J. Phys. Chem.*, 67 (1953) 853.
28 T. LAYLOFF AND R. N. ADAMS, unpublished data.
29 P. H. RIEGER AND G. K. FRAENKEL, *J. Chem. Phys.*, 37 (1962) 2795; 37 (1962) 2811; 39 (1963) 609.
30 A. H. MAKI, *J. Chem. Phys.*, 35 (1961) 761.
31 E. W. STONE AND A. H. MAKI, *J. Chem. Phys.*, 37 (1962) 1326; 38 (1963) 1999.
32 J. H. FREED AND G. K. FRAENKEL, *J. Chem. Phys.*, 37 (1962) 1156.
33 J. H. FREED, P. H. RIEGER AND G. K. FRAENKEL, *J. Chem. Phys.*, 37 (1962) 1881.
34 P. H. RIEGER, I. BERNAL AND G. K. FRAENKEL, *J. Am. Chem. Soc.*, 83 (1961) 3918.
35 I. BERNAL, P. H. RIEGER AND G. K. FRAENKEL, *J. Chem. Phys.*, 37 (1962) 1489.
36 P. B. ASCOUGH AND R. WILSON, *J. Chem. Soc.*, (1963) 5412.
37 E. W. STONE AND A. H. MAKI, *J. Chem. Phys.*, 36 (1962) 1944.
38 J. GENDELL, J. H. FREED AND G. K. FRAENKEL, *J. Chem. Phys.*, 37 (1962) 2832.
39 P. LUDWIG, T. LAYLOFF AND R. N. ADAMS, *J. Am. Chem. Soc.*, accepted for publication.
40 J. CHAMBERS, T. LAYLOFF AND R. N. ADAMS, *J. Phys. Chem.*, 68 (1964) 661.
41 T. KITAGAWA, T. LAYLOFF AND R. N. ADAMS, *Anal. Chem.*, 36 (1964) 925.
42 D. H. GESKE AND J. L. RAGLE, *J. Am. Chem. Soc.*, 83 (1961) 3532.
43 D. H. GESKE, J. L. RAGLE, M. A. BAMBENEK AND A. L. BALCH, *J. Am. Chem. Soc.*, 86 (1964) 987.

Short Communications

Anodic oxidation of *p*-methoxyphenol

The electrode reactions of aromatic amines and phenols have been studied extensively in recent years. The chemical and electrochemical oxidation of these compounds often results in the formation of intermediates which undergo subsequent chemical reactions. The detection and identification of these intermediates and their reaction products are of fundamental importance in the elucidation of the overall electrochemical oxidation mechanism. Reverse current chronopotentiometry (RCC)[1,2], cyclic voltammetry (CV)[3-5], and electron spin resonance (ESR)[6,7] are among several of the techniques ideally suited to the detection and identification of these intermediates and their resulting products. The application of these three techniques to the study of the electrochemical oxidation of *p*-methoxyphenol is reported in this short paper.

EXPERIMENTAL

A carbon paste electrode (CE-NjP) having a geometrical area of 0.238 cm^2 was used. Details of the construction of this electrode have been given previously[8]. The *p*-methoxyphenol was Eastman White Label and was used without further purification. Solutions were prepared immediately before use by dissolving a weighed amount of sample in de-aerated 2.037 *M* sulfuric acid. Doubly-distilled water was used in the preparation of all solutions. All measurements were made at 25.0% $\pm 0.1°$ and all potentials are reported *vs.* S.C.E.

A modification of the chronopotentiometric circuit described by MACERO AND

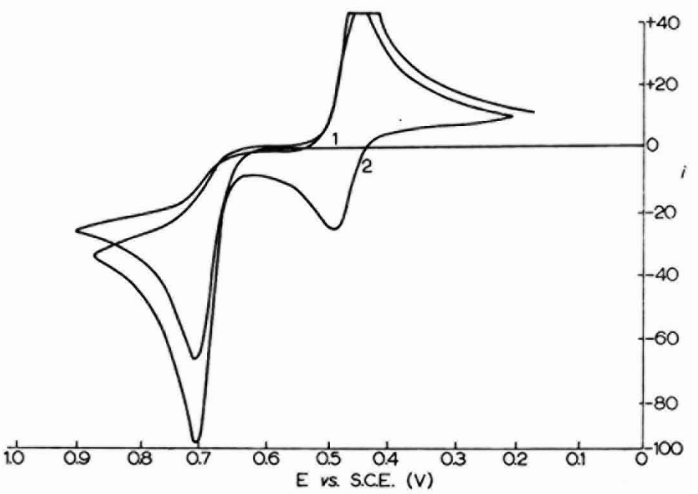

Fig. 1. Cyclic voltammetry of PMP. 1.13×10^{-3} *M* *p*-methoxyphenol in 2.037 *M* H_2SO_4 at 25.0°. Electrode area, 0.238 cm^2; scan rate, 2.0 V/min.

ANDERSON[9] was used. Details on the CV instrumentation have been previously reported[10].

Figure 1 shows the cyclic voltammetry of *p*-methoxyphenol (PMP) at the CE-NjP electrode. Only the oxidation of PMP to PMPox is observed on the first anodic scan. On the reverse sweep (cathodic going) the reduction of PMPox is not observed, but a cathodic wave with E_p *ca.* 0.45 V does appear. In addition to the primary oxidation wave observed on the first scan, the second, and all subsequent anodic sweeps, show the development of another anodic wave with an E_p *ca.* 0.49 V. This new redox system can be readily identified as that of the *p*-benzoquinone–hydroquinone couple.

Figure 2 shows a typical chronopotentiogram of PMP with current reversal.

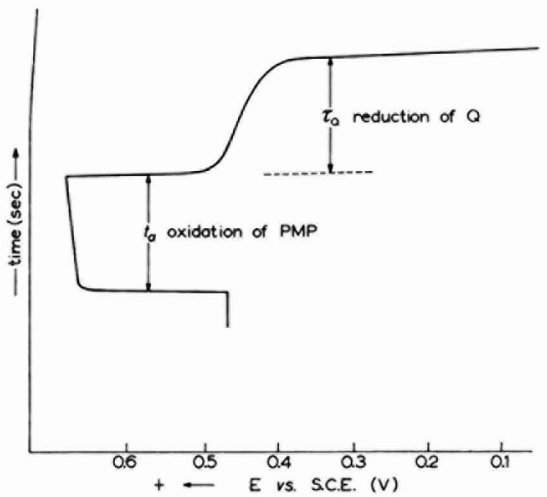

Fig. 2. Chronopotentiogram of PMP with current reversal. 1.13×10^{-3} *M* *p*-methoxyphenol in 2.037 *M* H_2SO_4 at 25.0°. Electrode area, 0.238 cm²; $i_a = -25$ μA; $i_c = 10.35$ μA; $t_a = 7.77$ sec.

Since the first wave involves only the oxidation of PMP to PMPox, the observed potential rises rapidly to *ca.* 0.68 V. Upon reversal of the current at time t_a ($t_a \leq \tau_{PMP}$), the potential drops rapidly to *ca.* 0.47 V, and a transition wave for the reduction of *p*-benzoquinone is observed. As was observed qualitatively with CV, the electrochemically generated PMPox is short-lived, since a transition time for its reduction cannot be detected. If, (i) the decomposition of PMPox is rapid; (ii) $i_{cathodic} = -0.414\, i_{anodic}$, and (iii) the same number of electrons is involved in the reduction step as in the oxidation step, then the ratio of the forward time, t_a, to the reverse transition time, t_Q, should be 1:1, as is observed. A linear plot of E *vs.* $-\ln [1-(t/\tau)^{\frac{1}{2}}]$ is also predicted[11]. The value of βn_a is readily determined from the slope of that plot, while the value of the anodic heterogeneous rate constant, $k_{a,h}{}^0$, is determined from the intercept at $t=0$. The average values determined from 12 such measurements, each on a new electrode surface, are: $\beta n_a = 1.38 \pm 0.05$; $-\ln k_{a,h}{}^0, = 43.7 \pm 1.3$; and $i\tau_{PMP}{}^{\frac{1}{2}} = 194.9 \pm 0.8$ μA sec$^{\frac{1}{2}}$.

ESR further substantiates that quinone arises from the oxidation of PMP. When

the pH of an electrolyzed PMP solution is raised to pH 8, the five-line ESR spectrum of *p*-benzosemiquinone ion is immediately obtained. This spectrum is identical with that from an authentic sample of *p*-benzosemiquinone.

The electrochemical oxidation mechanism suggested by the data is in accord with that proposed by ADLER AND MAGNUSON[12,13], who studied the chemical oxidation of *p*-alkoxyphenols with sodium metaperiodate. Since the reduction of *p*-benzoquinone to hydroquinone is a two-electron process, the chronopotentiometric data shows the oxidation of PMP is also a two-electron process:

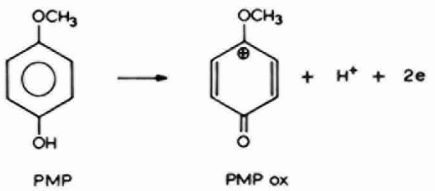

The PMPox is then rapidly hydrolyzed to yield the reaction products, *p*-benzoquinone and methanol:

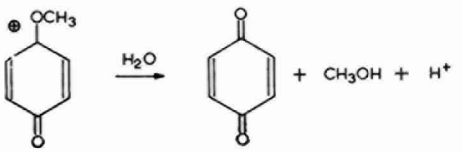

Although the results given above may not be unusual we wish to point out the data obtained with regard to the overall process is unequivocal. There are very few anodic oxidations of aromatic amines or phenols at solid electrodes about which such a statement can be made and we wish to cite this electrode reaction as a model system against which more complex ones may be compared and evaluated. This does not mean that the evaluation of various electrochemical parameters for this system are highly accurate (*i.e.*, βn_a, $k_{a,h}{}^0$, etc.). There is always the difficulty in reproducing such data on *different* electrode surfaces. On the same electrode surface (carbon paste in this case) the correlation of various electroanalytical techniques is good, however. Thus for a particular solution of PMP (1.13 m*M* in PMP and 2.037 *M* in H_2SO_4), a diffusion coefficient of $0.70_1 \times 10^{-5}$ cm²/sec was calculated from Cottrell measurements. The value obtained *via* chronopotentiometry was $0.69_1 \times 10^{-5}$ cm²/sec. Using the value of βn_a from chronopotentiometry and substituting into the equation for peak current *via* linear potential scan voltammetry gives a *D* value of $0.69_1 \times 10^{-5}$ cm²/sec. It would appear that a mean value of 0.69×10^{-5} cm²/sec is a reliable value for the diffusion coefficient of PMP in this medium.

Examination of other amine and aminophenol oxidations in the light of this model reaction are in progress.

ACKNOWLEDGEMENTS

This work was supported in part by the General Research Fund of the University

of Kansas and by the Atomic Energy Commission through contract AT(11-1)-686-39 and this support is gratefully acknowledged.

Department of Chemistry,
The University of Kansas,
Lawrence, Kansas (U.S.A.)

DALE HAWLEY
RALPH N. ADAMS

1 C. FURLANI AND G. MORPURGO, *J. Electroanal. Chem.*, 1 (1959) 351.
2 A. C. TESTA AND W. H. REINMUTH, *Anal. Chem.*, 32 (1960) 1512.
3 Z. GALUS, H. Y. LEE AND R. N. ADAMS, *J. Electroanal. Chem.*, 5 (1963) 17.
4 T. MIZOGUCHI AND R. N. ADAMS, *J. Am. Chem. Soc.*, 84 (1962) 2058.
5 Z. GALUS AND R. N. ADAMS, *J. Am. Chem. Soc.*, 84 (1962) 2061.
6 L. H. PIETTE, P. LUDWIG AND R. N. ADAMS, *Anal. Chem.*, 34 (1962) 916.
7 D. H. GESKE AND A. H. MAKI, *J. Am. Chem. Soc.*, 82 (1960) 2671.
8 C. OLSEN AND R. N. ADAMS, *Anal. Chim. Acta*, 22 (1960) 582.
9 D. J. MACERO AND C. B. ANDERSON, *J. Electroanal. Chem.*, 6 (1963) 221.
10 J. R. ALDEN, J. Q. CHAMBERS AND R. N. ADAMS, *J. Electroanal. Chem.*, 5 (1963) 152.
11 W. H. REINMUTH, *Anal. Chem.*, 32 (1960) 1514.
12 E. ADLER AND R. MAGNUSON, *Acta Chem. Scand.*, 13 (1959) 505.
13 E. ADLER, I. FALKEHAG AND B. SMITH, *Acta Chem. Scand.*, 16 (1962) 529.

Received April 25th, 1964

J. Electroanal. Chem., 8 (1964) 163–166

The effectiveness of *iR* compensation in controlled-potential polarography

The purpose of a potentiostat is to keep the potential of an investigated electrode independent of the current flowing through the solution. Principles of potentiostat design have been the subject of many articles; the most recent reviews were published in 1963[3,9]. Potentiostatic circuitry is used also in polarography and instruments incorporating this device have been developed by ARTHUR AND VANDERKAM[1] and by KELLEY *et al.*[5,6] and are commercially available (Hungarian polarograph OH-102 and the products of two American firms[8]).

A critical review of the effectiveness of ohmic potential drop compensation was published by BARNARTT[2]. He pointed out the significance of the location of the Luggin capillary connecting the reference electrode with the nearest possible vicinity of the stationary electrode under investigation. For distant reference electrodes (more than 0.04 mm) the *iR* compensation is quite inefficient; even at the relatively low current density of 30 mA/cm^2 the *iR* potential drop in 1 *N* KCl solution exceeds 10 mV.

For the dropping mercury electrode the situation is rather complicated. The distance between the reference electrode and the electrode surface is changed during the drop time as a result of which the value of *iR* between the tip of the Luggin capillary and the surface of the electrode is changed.

In the present paper a simple theoretical treatment of iR potential drop compensation effectiveness in controlled potential polarography is presented assuming the spherical symmetry of the D.M.E. and of the working electrode.

The real D.M.E. and working electrode arrangement is not spherically symmetrical; KELLEY *et al.*[5] tried to increase the efficiency of a controlled potential arrangement by locating the reference electrode above the D.M.E., *i.e.*, in the region of lower current density. It can be easily shown that this position of the reference electrode improves the iR compensation only negligibly. The electrical field in vicinity of the D.M.E. is rather complicated and two effects should be considered, (i) unsymmetrical location of the working electrode and (ii) shielding the drop by the end of the capillary. Both effects were accounted for by MATYÁŠ[7] using the method of electrical images. The system of the D.M.E. and of the large plane working electrode is equivalent to a system of two identical spherical electrodes located symmetrically on both sides of the plane of the working electrode (Fig. 1). If the effect of shielding is neglected, the potential difference between the points A and B of Fig. 1 can be approximately evaluated.

$$U_1' - U_2' = \frac{i}{4\pi\varkappa d} \frac{2}{(2n+1)(2n-1)} \qquad (1)$$

where $n = l/d$, i denotes the current and $\varkappa$ the specific conductance of the solution.

In a practical electrode arrangement, n normally exceeds a value of 10. Thus the difference between the potentials U_1' and U_2' is equal approximately 0.5% of their

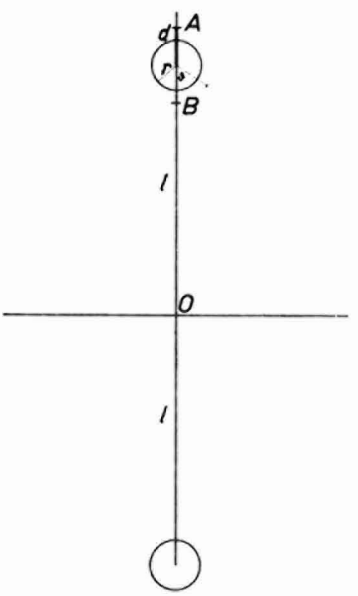

Fig. 1. The system of the D.M.E. and of the large plane working electrode is equivalent to a system of two identical spherical electrodes located symmetrically on both sides of the plane of the working electrode.

value and can be entirely neglected. Neglecting then the spherical asymmetry of electrical field in the vicinity of the D.M.E., the potential difference, ΔU, between the surface of D.M.E. and any point at a distance d' is given by

$$\Delta U = \frac{i}{4\pi\varkappa r}\left(1 - \frac{r}{d'}\right) \tag{2}$$

where r is radius of the D.M.E. An approximate value for the distance d' is obtained from the following expression.

$$d' = d\sqrt{1 - 4n\cos\vartheta + 4n^2}/\sqrt{1 - 4n\cos\vartheta + 4n^2} - 1 \tag{3}$$

where ϑ is the angle between d and l. In most cases d' is not more than 5% greater than d. Therefore we shall ignore this difference and use only the symbol d.

For a very distant reference electrode, the term r/d is negligible compared with unity and for the potential drop in the polarographic cell without iR compensation one has[4]

$$\Delta U_1 = \frac{i}{4\pi\varkappa r} \tag{4}$$

For an estimate of i–E-curve distortion it is useful to evaluate the mean iR potential drop $\overline{\Delta U}$ during the drop life:

$$\overline{\Delta U} = \overline{\Delta U_1} - \frac{\bar{i}}{4\pi\varkappa b r_m} \tag{5}$$

where $b = d/r_m$ and r_m is the maximum D.M.E. radius.

$\overline{\Delta U}$ can be easily calculated assuming the i–t curve in the form $i = kt^a$. Then

$$\overline{\Delta U_1} = \frac{\bar{i}p}{4\pi\varkappa r_m} \tag{6}$$

where p is a numerical coefficient depending on a

$$p = \frac{3a + 3}{3a + 2} \tag{7}$$

This coefficient is equal to 1.4 for the diffusion current (without correction for spherical diffusion), 2 for the capacitive current, 1.25 for the kinetic current ($a = 2/3$) and 1.18 for the autocatalytic current ($a = 7/6$).

It is of importance to compare the value of the uncompensated mean iR drop, $\overline{\Delta U_1}$, with the mean iR drop, $\overline{\Delta U}$, in controlled-potential polarography:

$$\overline{\Delta U} = \overline{\Delta U_1}\left(1 - \frac{1}{pb}\right) \tag{8}$$

It is evident that the iR compensation is relatively ineffective for the D.M.E. Taking 0.1 mm as an optimal distance of the reference electrode from the D.M.E. (*i.e.*, $b = 1.2$ for a typical D.M.E. with maximum radius 0.5 mm at $m = 2$ mg/sec and $t_1 = 3.54$ sec), the value of $1/pb$ for the diffusion current is 0.6. Thus the optimal iR compensation results in lowering of iR only to 40% of its uncompensated value. The

minimum distance between the D.M.E. and reference electrode can be reached only at the end of drop life; without mechanical drop time control the compensation effectiveness is reduced because of the lowering of the surface tension of mercury with potential. If the drop time is decreased twice, the potentiostat compensation drops to 47% of the uncompensated value of iR. SCHAAP AND MCKIMNEY also arrived at the same conclusion that practically it was impossible to obtain perfect iR compensation and they suggested a method for evaluation of R from derivative polarograms.

Thus, controlled-potential polarography is of importance only in a limited range of currents and conductances of solution where the compensation for iR to approximately one half of the initial value enhances the precision of measurement. However, it seems that this improvement cannot compensate for the complications involved with the precise location of the reference electrode towards the D.M.E. The same conclusion holds also for the half wave potential measurement using the so called three electrode system. This method has the one advantage that it prevents the current from flowing through the reference electrode, but its influence on iR compensation is negligible.

The mean iR potential drop for various values of $\bar{i}/\varkappa$ in an uncompensated electrode arrangement for the D.M.E. using the constants of the polarographic capillary as above, is given by the expression

$$\overline{\Delta U_1} = 2.2 \times 10^3 \frac{\bar{i}}{\varkappa} \quad (\mathrm{mV\,A\,\Omega^{-1}cm^{-1}}) \tag{9}$$

The compensation of solution resistance in a.c. and pulse techniques is somewhat better. In these methods instantaneous and not average values are frequently used. For maximum D.M.E. radius the optimal compensation of iR is reached:

$$R_{ett} = \frac{1}{4\pi\varkappa r}\left(1 - \frac{1}{b}\right) \tag{10}$$

For $b = 1.2$ and $r = r_m$, the effective solution resistance is lowered approximately six times, *i.e.*, equal precision can be reached for frequencies six times higher compared with a two-electrode measurement without iR compensation. The rise time of square pulse given on the D.M.E. is shortened in the same proportion using the controlled-potential circuitry.

From the view point of modern potentiostatic technique it can be concluded that the D.M.E. is not a very suitable object for d.c. ohmic potential drop elimination. For polarography in highly resistive solutions it is probably better to use the familiar method for extrapolation of potentials to zero limiting current. In a.c. and pulse techniques the situation is more favourable, but even so the location of the reference electrode to the nearest vicinity of the D.M.E. must be carried out with great care.

Polarographic Institute,
Czechoslovak Academy of Sciences,
Prague (Czechoslovakia)

L. NĚMEC

1 P. ARTHUR AND R. K. VANDERKAM, *Anal. Chem.*, 33 (1961) 765.
2 S. BARNARTT, *J. Electrochem. Soc.*, 108 (1961) 102.
3 G. L. BOOMAN AND W. B. HOLBROOK, *Anal. Chem.*, 35 (1963) 1793.

4 J. HEYROVSKÝ AND J. KŮTA, *Základy Polarografie*, Praha, 1962.
5 M. T. KELLEY, H. C. JONES AND D. J. FISHER, *Anal. Chem.*, 31 (1959) 1475.
6 M. T. KELLEY, D. J. FISHER AND H. C. JONES, *Anal. Chem.*, 32 (1960) 1262.
7 Z. MATYÁŠ, *Mém. Soc. Roy. Lettres Sci. Bohême, Classe des Sciences*, 1944, XXX.
8 W. B. SCHAAP AND P. S. MCKIMNEY, *Anal. Chem.*, 36 (1964) 29.
9 W. M. SCHWARZ AND I. SHAIN, *Anal. Chem.*, 35 (1963) 1779.

Received April 6th, 1964

Book Reviews

Elucidation of Structures by Physical and Chemical Methods, edited by K. W. BENTLEY, Part I and II. (*Techniques of Organic Chemistry*, edited by A. WEISSBERGER, Vol. XI). Interscience Publishers, J. Wiley, New York, 1963, x + 23 + x + 1181 pages, Part I, 147s; Part II, 125s.

Correlations between physico-chemical quantities and the structure of organic compounds can be used for two purposes. On one hand the effects of structure on changes of physico-chemical properties can contribute to better understanding of the physico-chemical process used. On the other hand observed changes of the magnitude of the measured quantity can be attributed to certain changes in structure and hence these quantities can be applied (usually together with chemical methods) for the elucidation of the structure of unknown organic compounds. This book deals with this second aspect in detail. The greater part of these volumes is devoted to spectroscopic and chemical methods for structural studies. It is somewhat surprising to find electron and X-ray diffraction studies omitted. Chapter VI (pp. 318–365) written by J. F. KING describes the application of dissociation constants and it is to this part of the book that the present review is restricted.

After a condensed but lucid introduction, describing theoretical principles, principles of measurement, and effect of external factors, structural effects on the dissociation of carboxylic acids, amines and hydroxyl-bearing compounds are discussed. The tables of pK-values included clearly indicate that extensive and easily consulted tables of this kind are urgently needed. These not too extensive tables are arranged in order of magnitude of pK-values. This type of arrangement is very useful when the possible structure for an acid with a known pK-value is required. When, however, the pK-value of a particular compound, or structural effects on the pK-values are needed, the arrangement used by H. C. BROWN, D. H. MCDANIEL AND O. HÄFLIGER (*Determination of Organic Structures by Physical Methods*, Vol. I, edited by E. A. BRAUDE AND F. C. NACHOD) seems to be preferable. Very little data is given for heterocyclics and recent tables by A. ALBERT (*Physical Methods in Heterocyclic Chemistry*, Vol. I, edited by A. R. KATRITZKY,) should be consulted for information in this field. What is really surprising that with an exception of a note on p. 342, the principle of quantitive correlations between pK and structure of the Hammett and Taft type and its applications in structural studies, is not mentioned. Although it is not mentioned explicitly by the editor of these volumes in the Preface, applications of particular methods are more or less restricted to structures of natural products and in accordance with this, pK-values for several examples of this type are quoted. The effects of steric hindrance of coplanarity and steric shielding of

solvation (which can have opposing effects on pK-values) are discussed. Several effects of adjacent hydroxy- or amino-groups are explained by intramolecular hydrogen bridges; the basis for such discussions is usually by comparison with *para*- (or analogous) derivatives. It can be taken for granted that an *ortho* effect is also operative in these cases but a comparison with other *ortho*-substituents (*e.g.*, *o*-methoxy, *o*-methyl or *o*-halogeno) would have made for a better understanding.

It is a great pity that the possibilities offered by measurements of oxidation–reduction potentials and polarographic half-wave potentials for the elucidation of special structural problems, are not discussed; especially when several examples of their application in the chemistry of natural products can be quoted. For future editions there is definitely room for improvement and for extension of this Chapter to make better use of the opportunities that electrochemical methods offer for structural studies.

P. ZUMAN, Polarographic Institute, Prague

J. Electroanal. Chem., 8 (1964) 170–171

Treatise on Analytical Chemistry, Part I, Vol. 4, *Theory and Practice*, edited by I. M. KOLTHOFF, P. J. ELVING and E. B. SANDELL, John Wiley and Sons Ltd., London and New York, 1963, xxv + 955 pages, £ 9.9.0.

This is the fourth volume of a comprehensive treatise which will eventually comprise more than 25 volumes. It consists of two parts: the smaller on Magnetic Field Methods occupies 358 pages, and the larger on Electrical Methods occupies 564 pages. There is also an excellent index to this volume only.

The second part on Electrical Methods will be of greater interest to the readers of this Journal since it covers the classical field of Electroanalytical Chemistry. The first two chapters (by C. N. REILLEY and by C. N. REILLEY AND R. W. MURRAY) provide a combined general introduction and "bird's eye view" of the subject. The second of these chapters should prove particularly useful to the novice. Apart from the definition of overpotential on page 2178, this account is clear and helpful. The final section on Operational Aspects of Electrochemistry is a stimulating attempt at an overall classification of electroanalytical methods.

P. DELAHAY on Chronoamperometry and Chronopotentiometry will need no recommendation to the many users of his classic *New Instrumental Methods in Electrochemistry*. N. H. FURMAN's chapter on Potentiometry is more satisfactory on the more established techniques; the section on automatic titration is rather short. The discussion on the use of polarised electrodes is not particularly clear; for example Fig. 43.12 on page 2185 seems to clarify the situation more than does Fig. 45.10 on page 2298.

There are now many books on polarography, but the admirably clear chapter by L. MEITES may be recommended as one of the best available introductions to this subject. R. N. ADAMS extends this to "Electrodes with Fixed Surfaces"—a rather odd title—but one which has to do duty for all electrodes except the dropping electrode—even the streaming mercury electrode! N. TANAKA's chapter on Electrodeposition inevitably departs somewhat from the purely analytical aspects in considering the mechanism of the process and the structure of deposits. The chapters

on Coulometric Analysis (D. D. DE FORD AND J. W. MILLER) and Stripping Analysis (I. SHAIN) return to more directly analytical procedures with clear practical accounts.

The last two chapters of this section stand somewhat apart from the remainder since they do not deal with electrode reactions. Conductometry and Oscillometry by J. W. LOVELAND includes a discussion on the theory of conductance which is probably too brief to be much help, but the rest of the chapter will be of great help to beginners. This chapter mentions one or two commercial instruments while the last, on Dielectric Constants (by B. W. THOMAS AND R. PERTEL), refers to many more but only those manufactured in the U.S.A. and Germany! Parts of this chapter might be more appropriate to Part III of the Treatise (Analysis of Industrial Products).

The shorter half of the present volume has four chapters: Analytical Application of Magnetic Susceptibility by L. N. MULAY, N.M.R. and E.P.R. (only 7 pages on the latter) by N. F. CHAMBERLAIN, Mass Spectrometry by F. W. MELPOLDER AND R. A. BROWN and Ion Scattering Methods by S. RUBIN. The last of these, in particular, emphasizes the vast range of modern analytical chemistry. The electrochemist may perhaps be permitted a chuckle at the picture on page 2089 which is said to show a 2 mV(!) Van de Graaff generator.

ROGER PARSONS, University of Bristol

J. Electroanal. Chem., 8 (1964) 171–172

Ionic Equilibrium: A Mathematical Approach, by J. N. BUTLER, Addison Wesley Publishing Co. Inc., Reading (Mass.), Palo Alto, London, 1964, xi + 547 pages, $8.75.

This is a useful book with a rather misleading sub-title. Two brief introductory chapters on types of ionic equilibria and their determination, are followed by the illustration in great detail of the calculation from tabulated equilibrium constants of the concentrations of species present in solutions in which protolytic, solubility, complex ion, or redox equilibria have been established, and the application of the results of these calculations to analytical procedures. The effects of changes of ionic activity coefficients are ignored until the last chapter. This apart, the treatment is very thorough and the author either avoids or justifies approximations which are often not fully explained in the treatment of such topics as overlapping step equilibria, multiple buffer systems, mixed ligand systems, and polynuclear complex ions. Some will find the algebraic detail tedious, but the extended treatment together with the numerous problems to which answers are provided will be useful to many, especially students who are working largely on their own. Each chapter has a useful bibliography. There are numerous examples of the uses of logarithmic concentration diagrams and predominance -area diagrams.

Statements made about a few general topics such as ion pairs (p. 94), chelate stability (p. 374), and the Debye-Hückel theory (pp. 432 and 433) are to say the least, liable to confuse. On p. 433 a Debye-Hückel equation which incorporates an ion size is said to be derived from a model in which ions are treated as point charges. Equilibrium constants are taken from standard sources but a sceptical word would have been appropriate about some of the values, such as those for the stability constant of mononuclear hydroxy complexes of transition-metal cations.

J. E. PRUE, Chemistry Department, University of Reading

CONTENTS

ELSEVIER PUBLISHING COMPANY, AMSTERDAM

Printed in The Netherlands by

NEDERLANDSE BOEKDRUK INRICHTING N.V., 'S-HERTOGENBOSCH

RODD'S CHEMISTRY OF CARBON COMPOUNDS

Second Edition

edited by S. COFFEY, M.Sc. (London), D.Sc. (Leyden). Formerly of I.C.I. Dyestuffs Division, Blackley, Manchester. Assisted by an Advisory Board of prominent scientists.

More than 12 years have passed since the appearance of the first volume of CHEMISTRY OF CARBON COMPOUNDS. During this period great advances have been made in both theoretical and experimental organic chemistry, and these are being recorded in a completely new and revised edition.

In all important respects the second edition will be the same as the first, although some minor changes will be made. The large volume of new material will certainly cause an increase in total size and thus make it necessary to produce a greater number of sub-volumes. However, to reduce the delay between the appearance of these sub-volumes, each will be of smaller size than was the case for the first edition.

VOLUME IA - GENERAL INTRODUCTION, HYDROCARBONS, HALOGEN DERIVATIVES

General Introduction

1. The saturated or paraffin hydrocarbons. Alkanes. 2. Unsaturated acyclic hydrocarbons. 3. Halogen derivatives of the aliphatic hydrocarbons.

6 × 9″ xx + 569 pages subscription price £7.0.0.
non-subscription price £8.0.0.

VOLUME IB - MONOHYDRIC ALCOHOLS, THEIR ETHERS AND ESTERS, SULPHUR ANALOGUES; NITROGEN DERIVATIVES; ORGANOMETALLIC COMPOUNDS

4. Monohydric alcohols, their ethers and esters. 5. Sulphur analogues of the alcohols and their derivatives. 6. Nitrogen derivatives of the aliphatic hydrocarbons. 7. Aliphatic organometallic and organometalloidal compounds.

6 × 9″ xx + 277 pages + index, 16 tables; to appear late in 1964

VOLUME IC - ACYCLIC ALDEHYDES, KETONES AND MONOCARBOXYLIC ACIDS; CARBON MONOXIDE, ISOCYANIDES AND FULMINIC ACID; CARBONIC ACID AND ITS DERIVATIVES

VOLUME ID - DIHYDRIC ALCOHOLS, THEIR OXIDATION PRODUCTS AND DERIVATIVES

VOLUME IE - TRIHYDRIC ALCOHOLS, THEIR OXIDATION PRODUCTS AND DERIVATIVES

VOLUME IF - TETRA-, PENTA- AND HIGHER POLYHYDRIC ALCOHOLS, THEIR OXIDATION PRODUCTS AND DERIVATIVES; SACCHARIDES

VOLUME IG - ENZYMES; MACROMOLECULES; CUMULATIVE INDEX TO VOLUME I

To follow

Volume II Alicyclic Compounds
Volume III Aromatic Compounds
Volume IV Heterocyclic Compounds
Volume V Miscellaneous; General Index

Multi-volume works such as Rodd's Chemistry of Carbon Compounds represent a considerable outlay for the purchaser. In order to alleviate this to a certain extent, the publishers offer a discount of 15% on the publication price. Subscribers to the complete series will thus be able to acquire the work for only 26s. (approx.) per 100 pages.

ELSEVIER PUBLISHING COMPANY
AMSTERDAM LONDON NEW YORK

380 E